

**University of Nevada Reno**

**Strategies for Targeting and Isolating Cryptic Natural Products from Plants:  
Isolation and Structural Determination of piperholdripine and  
raduladioxanolide**

A dissertation submitted in partial fulfillment of the requirements for the degree of  
Doctor of Philosophy in Chemistry

By

Megan J Burroughs

Dr. Christopher S. Jeffrey/Dissertation Advisor

August 2024



THE GRADUATE SCHOOL

We recommend that the dissertation  
prepared under our supervision by

entitled

be accepted in partial fulfillment of the  
requirements for the degree of

*Advisor*

*Committee Member*

*Committee Member*

*Committee Member*

*Graduate School Representative*

Markus Kemmelmeier, Ph.D., Dean  
*Graduate School*

## Abstract

Archives of empirical data of medicinal herb usage can be found in ancient civilizations, but the start of the 19<sup>th</sup> century brought about the beginning of rational drug discovery from plants with Friedrich Sertürne's 1817 publication on the isolation, structure, and pharmaceutical effects of morphine. The so-called "waste" products of plants were sought after in the fields of medicine, agriculture, materials science, and ecological studies. This paper focuses on the strategies of isolation of "cryptic" natural products.

Cryptic natural products represent a treasure trove of untapped potential. A cryptic natural product may be a minor component, only exist in certain individuals in a species, or require specific conditions to be generated. These specialized metabolites are often observed through their function or are hypothesized to exist based on the biosynthetic gene clusters. However, mining the genome of a multi-cellular organism, often on a cell-to-cell level, is an extremely difficult process. While other experiments focus on function, the actual isolation of a cryptic natural product, especially one that exists as a minor component or only functions in a synergistic system, can be difficult and time consuming.

Chapter 2 focuses on the isolation of cryptic natural products through their function. Using <sup>1</sup>H NMR resonance networking in correlation with bioactivity allows for the targeted isolation of bioactive metabolites. The structural information provided by the <sup>1</sup>H NMR resonances allow for separations to be completed without a bioassay study at each step. This chapter describes using this method to isolate a novel cryptic natural product that shows high growth inhibition against *S. cerevisiae*.

Chapter 3 demonstrates using untargeted metabolomic analysis to explore chemical heritability in *Piper scintillans*. A chemical heritability experiment requires the comparison of the chemical profiles of wild-type species. This chapter focuses on the annotation of the chemotype-defining masses. Chapter 4 offers proof that this untargeted/targeted method can lead to the isolation of a novel cryptic natural product.

While these methods prove observing cryptic natural products can be accomplished, the isolation and full characterization can be difficult. Chapter 5 explores the potential of using single crystal x-ray diffraction to increase the rate of structure elucidation. The crystal sponge method and co-crystallization have potential to determine the absolute structure of hard to crystallize or liquid natural products. This chapter explores the methods, as well as future work to improve the chance of guest intake.

Changing isolation strategies to increase the chance of isolated cryptic natural products is a common endeavor. These strategies use multivariate analysis to target compounds of interest, decreasing the amount of time and material necessary for isolation.

## **Dedication**

To my mom, Paula, for the strength she always gave, for being the person I can count on for anything, for supporting my dreams, for boosting me in my struggles and celebrating my successes.

To the rest of my family, who love and support me even when we're far apart.

## Acknowledgements

Graduate school isn't a sprint, but a marathon. There is no doing this alone, and I have had amazing people behind me and beside me every step of the way. Thank you to Dr. Vincent Catalano, who accepted me as a masters student and convinced me I should really consider a Ph.D. His sage advice reminded me that it's called "*re*-search", and I knew I could always count on him to point me in the right direction. Thank you to Dr. Christopher Jeffrey, who adopted me into his group so smoothly it was like I was always a part of them. His enthusiasm drove me to love the research I was a part of and to make it mine. His passion for mentoring awoke my own, and through him I have been able to guide others. His support for my love of teaching allowed me to determine what I truly want to do with my life, and to grow past what I saw as my limits.

I would like to thank Dr. Lyndsay Munro and Dr. Janell Mahoney, who supported my teaching goals and were always answering my questions. They gave me the confidence to grow and improve, and I can only hope my teaching style will reflect the passion they show.

Thank you to my committee, Dr. Lora Richards, Dr. Elizabeth Pringle, and Dr. Matthew Tucker for your time and effort throughout my graduate career. I'd like to thank Dr. Casey Philbin, who brought me onto this project that has become such a part of my life.

I want to thank Jennifer McCracken, who could have an entire page dedicated to her. She was the first person to teach me how to use HPLC instrumentation and has been

working beside me ever since. Her help and support, both in the labor and bouncing ideas off of, made this dissertation possible.

To Katherine Chacon-Godoy, who dove headfirst into a summer research position and worked with me for a year on all my projects. I am so proud of what you have accomplished and am so thankful for the help you gave me.

I would like to thank my family, who supported and loved me. To taking the middle of the night phone calls and making sure I stayed connected. They supported my dreams and listened to my gushing (or venting) about research, even if they didn't understand why I would spend all day moving samples from one container to another.

I'd like to thank my friends from UNR. Hannah Anderson, who supported me and kept me sane. Katie Graham, who kept me laughing and my phone full of cat pictures. Alex English, who motivated me and welcomed me into a new research group.

To the rest of my research group, Garret, Zach, Tanzil, Brittney, Jordan, Tugba, Chris and Nayeli. I've loved being a part of this group and will miss you all. Thank you for accepting me, even when I'm more comfortable with physical chemistry than organic.

## Table of Contents

Abstract.....	i
Dedication.....	iii
Acknowledgements.....	iv
Table of Contents .....	vi
List of Tables.....	ix
List of Figures.....	xi
List of Schemes.....	xiii
Chapter 1: Introduction.....	1
1.1: A Short History of Natural Product Chemistry.....	1
1.2: Cryptic natural products.....	1
1.3: Limitations of classic methods of isolation .....	3
1.4: Changing the isolation workflow.....	4
1.4.1: Isolation based on compound function .....	4
1.4.2: Isolations based on chemical heritability .....	4
1.4.3: Isolation based on increasing annotation rate .....	5
Chapter 2: Piperholdripine.....	7
2.1: <sup>1</sup> H-NMR network-based isolation of antifungal compounds of the genus <i>Piper</i> .....	7

2.2:	Methods.....	8	
2.2.1:	Sample Preparation .....	8	
2.2.2:	General Isolation Procedures .....	8	
2.3:	Compound Isolation: piperholdripine .....	8	
2.4:	Structure elucidation: piperholdripine .....	14	
2.5:	Synthesis of piperholdripine .....	17	
2.6:	Confirmation of the bioactivity of piperholdripine.....	20	
2.7:	Conclusions.....	20	
Chapter 3: Chemical Heritability: Annotation of metabolomic chemical heritability			
experiment of <i>Piper scintillans</i> .....			23
3.1:	Chemical Heritability .....	23	
3.2:	Metabolomics and Chemotypes .....	24	
3.2.1:	Classes of Compounds .....	26	
3.3:	General Procedures .....	27	
3.4:	Chemotype 1 .....	29	
3.5:	Chemotype 2 .....	35	
3.5.1:	Mass Lists and Initial Isolation Procedures .....	36	
3.5.2:	Characterization and Annotation.....	39	
3.5.3:	SCXRD analysis of compounds isolated .....	42	
3.6:	Chemotype 3 .....	45	

3.7: Conclusions and future work .....	49
Chapter 4: A metabolomics guided discovery of cryptic flavanone sesquiterpene conjugate raduladioxanolide .....	51
4.1: A highly heritable cryptic compound.....	51
4.2: Sample Preparation .....	52
4.3: Compound Isolation: raduladioxanolide.....	52
4.4: Structure determination: raduladioxanolide.....	54
4.5: Proposed biosynthetic pathway of raduladioxanolide .....	60
4.6: Conclusions.....	61
Chapter 5: Using single crystal x-ray diffraction in natural product chemistry .....	63
5.1: The struggle of absolute configuration .....	63
5.2: Crystalline Sponge Method.....	64
5.3: Co-crystallization Method .....	67
5.4: Conclusions.....	70
References.....	71

**List of Tables**

Table 2.3-1: Prep-HPLC method of pilot run of <i>P. holdrigeanum</i> .....	9
Table 2.3-2: Prep-HPLC method of isolation of <i>P. holdrigeanum</i> .....	9
Table 2.3-3: Prep-HPLC method of fraction containing 344.4 m/z.....	14
Table 2.4-1: NMR spectroscopic assignments for isolated compound 1 .....	16
Table 2.5-1: NMR spectroscopic assignments of compound 1a.....	19
Table 3.4-1. Annotation of chemotype-defining masses for Chemotype 1.....	29
Table 3.4-2: Prep-LCMS method used for initial separation of Chemotype 1 .....	31
Table 3.4-3: Annotation of compounds isolated from Chemotype 1 .....	33
Table 3.4-4: NMR spectroscopic assignments of isolated compound 9 .....	33
Table 3.5-1: Annotation of chemotype-defining masses for Chemotype 2.....	36
Table 3.5-2. Annotation of chemotype-defining masses for CT2-sCT3 .....	37
Table 3.5-3. Annotation of chemotype-defining masses for CT2-sCT5 .....	37
Table 3.5-4: Prep-HPLC method of initial separation for CT2 .....	39
Table 3.5-5: Annotation of compounds isolated from CT2 and sCT3/5.....	40
Table 3.5-6: Crystallographic data of compounds .....	45
Table 3.6-1: Annotation of chemotype-defining masses for Chemotype 3.....	46
Table 3.6-2: Prep-HPLC method of initial isolations of Chemotype 3.....	47
Table 3.6-3: Annotation of isolated compounds from CT3 .....	48
Table 4.1-1: Cryptic compounds in Chemotype 2 .....	51
Table 4.3-1. HPLC method of Brown Module Sibling Yamazan Run 1 .....	53
Table 4.3-2. HPLC method of Brown Module Sibling Yamazan Run 5-26 .....	53
Table 4.3-3. Prep-HPLC of BrMo_Sib_Yz_8/9_Inf_Run1-6.....	54

Table 4.4-1: NMR assignments for isolated compound 18.....	57
--	----

## List of Figures

Figure 1.2-1: General isolation process of natural products from plants.....	3
Figure 2.3-1. Comparison of prep-HPLC chromatographs of crude extract of <i>P. holdrigeanum</i> from Aglient Infinity prep-HPLC+MS.....	10
Figure 2.3-2: Comparison of <sup>1</sup> H NMR spectra of fractions containing cryptic compound. .....	10
Figure 2.3-3: Antifungal activity analysis of <i>P. holdrigeanum</i> . ....	11
Figure 2.3-4: Comparison of HPLC chromatography between Run 2 and Run 3 .....	11
Figure 2.3-5: Comparison of MS spectra of Run 2 and 3, focusing on 344 m/z (EIC). ...	13
Figure 2.4-1: Steps of structure determination. ....	15
Figure 2.4-2: UV-Vis of isolated compound 1 in methanol. ....	17
Figure 2.5-1: Previously isolated compounds with similar moiety to compound 1. ....	18
Figure 2.6-1: Growth inhibition analysis of isolated compound 1 and synthesized compound 1a. ....	20
Figure 3.2-1: PCA plots of phytochemical diversity of LC-MS entities .....	24
Figure 3.2-2: PCA plot of phytochemical variation by <sup>1</sup> H NMR spectroscopic entities ..	25
Figure 3.2-3: Correlation of LC-MS data with <sup>1</sup> H NMR structural data .....	25
Figure 3.2-4: General structure and numbering of flavanones and chalcones.....	26
Figure 3.2-5: Example structure and numbering of a sesquiterpene lactone .....	27
Figure 3.4-1: Comparison of Chemotype 1 compounds retention times using m/z and RT from tandem MS/MS data.....	31
Figure 3.4-2: Structure of compound 272.1 with variable substituents on A ring .....	34
Figure 3.5-1: PCA plot of LC-MS entities showing separation into 5 sub-Chemotypes..	35

Figure 3.5-2: Comparison of Chemotype 2 compounds retention times using m/z and RT from tandem MS/MS data.....	37
Figure 3.5-3: Comparison of CT2-sCT3 compounds retention times using m/z and RT from tandem MS/MS data.....	38
Figure 3.5-4: Comparison of CT2-sCT5 compounds retention times using m/z and RT from tandem MS/MS data.....	38
Figure 3.5-5: Tandem MS/MS of mixture containing 231.1380 m/z.....	41
Figure 3.5-6: Tandem MS/MS spectrum of mixture containing 433.1127 m/z.....	42
Figure 3.5-7: Crystal structure of Compound 13.....	43
Figure 3.5-8: Crystal structure of compound 14.....	44
Figure 3.6-1: Comparison of CT3 compounds retention times using m/z and RT from tandem MS/MS data.....	47
Figure 4.1-1: Heat map of correlation between <sup>1</sup> H NMR resonance variation and LC-MS/MS variation.....	52
Figure 4.4-1: Circular Dichroism Spectrum of Raduladioxanolide 0.625 mmol/mL.....	59
Figure 4.4-2: UV-Vis absorbance spectrum of compound 18 in acetonitrile.....	59
Figure 5.1-1: GMCS of metabolites in crude extract of <i>P. scintillans</i> .....	63
Figure 5.2-1: Unit cell of MOF [(ZnI <sub>2</sub> ) <sub>3</sub> -(tpt) <sub>2</sub> ·x(cyclohexane)] <sub>n</sub> .....	65
Figure 5.2-2: Crystal structure of the unit cell of Eu MOF.....	67
Figure 5.3-1: Crystal structure of TBro with pinene guest.....	69

## List of Schemes

Scheme 2.5-1: Synthesis of compound 1a piperholdripine. ....	19
Scheme 3.4-1: Isolated compounds from Chemotype 1 .....	32
Scheme 3.5-1: Isolated compounds from CT2, CT2-sCT3 and CT2-sCT5 .....	40
Scheme 3.6-1: Isolated compounds from Chemotype 3 .....	48
Scheme 4.5-1: Proposed biosynthetic pathway of isolated compound 18.....	60
Scheme 5.1-1: Isolated compounds from <i>P. scintillans</i> .....	64
Scheme 5.3-1: Synthesis of compound 25 .....	68
Scheme 5.3-2: Synthesis of TIodoA and TPA .....	70

## **Chapter 1: Introduction**

### **1.1: A Short History of Natural Product Chemistry**

For millennia, the diversity of molecules and their bioactivities from plants (phytochemicals) have profoundly influenced the field of natural products chemistry and driven advancements in medicinal and biotechnological applications. One major driver of the immense structural and compositional diversity of these phytochemicals is the co-evolutionary arms race between plants and herbivores.<sup>1</sup> Today, the field of chemical ecology focuses on specialized metabolites functioning through chemically mediated interactions between organisms and their environments.

The oldest record of human use of natural products dates back to Mesopotamia, with documentation of over a thousand plant based medicines.<sup>2</sup> While humans found uses for these “waste” products, the concept of these biological processes being purposefully sought after by plants was not universally accepted by the scientific community until the late 1950s.<sup>3,4</sup> The persistent generation of specialized metabolites suggests that they play a vital role in species survival and evolution. In particular, the heritability and variation of a species or individuals’ chemical profile could lead to insights into the function of natural products, both within a plant and how it interacts with its environment.

### **1.2: Cryptic natural products**

The drive to discover new compounds with therapeutic relevance remains as one of the main motivations for research focused on natural products variation and function. The diverse biochemistry of plants correlates to the large variety of bioactive compounds.

A review of the source of new drugs from the past forty years has shown that almost a quarter of all new drugs have roots in natural products, while over half of the anti-bacterial drugs are natural product derived.<sup>5</sup>

Of particular interest are the “cryptic” natural products: compounds that are minor or not expressed in every individual of the same species yet are highly influential in the chemical profile. A cryptic natural product may be condition dependent, such as requiring the presence of an antagonistic microbe or certain abiotic environments. A genetic variation could lead to the generation of a cryptic natural product but not all individuals in a species will have identical chemical profiles. The biosynthetic pathways of specialized metabolites allow for a high degree of variation, which can allow for the chemical adaptation against stresses present in an environment even when the metabolites are in small concentration.<sup>6,7</sup> The isolation of cryptic natural products can involve focusing on the expression of function, or by triggering biosynthetic gene clusters (BCG) in an organism.<sup>8,9</sup> However, the isolation of such minor components can be difficult and time-consuming.

### 1.3: Limitations of classic methods of isolation



**Figure 1.2-1:** General isolation process of natural products from plants

The workflow of isolation generally contains the following: plant collection, extraction, separation, purification and analysis. The collection of plant material can take months. It is necessary to obtain kilograms of material, although the compounds of interest could be less than 0.0001% of the biomass.<sup>10</sup> The composition of compounds within a crude extraction determine which method of separation is required, as the methods rely on solubility, viscosity, and stability of individual compounds;<sup>11</sup> this requires individualized methods usually determined through trial and error.

Often, the initial search for novel compounds, especially bioactive compounds, is based on the major components of an extract, and the isolates that are easier to isolate and detect, such as volatile pheromones or alkaloids. To prevent the loss of possible bioactive specialized metabolites existing as minor components, methods such as bioassays of individual fractions are required at each stage of isolation. This starts a cycle of bioassay studies, further separation and analysis, only to repeat the process (Figure 1.2-1). In addition, it is common to isolate compounds that are known in scientific literature.

Methods of dereplication include the comparison of mass spectrometry (MS) data and <sup>1</sup>H

nuclear magnetic resonance spectroscopy ( $^1\text{H}$  NMR) data to known compounds, which in turn requires a database of spectroscopic analysis.<sup>12,13</sup>

#### **1.4: Changing the isolation workflow**

##### ***1.4.1: Isolation based on compound function***

Multivariate analysis paired with several analytical techniques can provide pathways to discovering novel specialized metabolites in a more efficient manner than traditional isolation methods.<sup>14–16</sup> Richards and coworkers applied weighted network analysis with  $^1\text{H}$ NMR spectroscopic structural information against bioassays of crude plant extracts.<sup>17</sup> Of the many analytical techniques available, NMR spectroscopy and LC-MS analysis are two of the most used to provide quantitative datasets. NMR spectroscopy is a non-destructive technique, readily detects organic compounds, and provides structural information of the compounds within a sample. Liquid chromatography – mass spectrometry requires a small amount of material, has highly sensitive detection, and can provide quantitative information of a crude sample. Chapter 2 validates this work by demonstrating that structural information provided by the proton resonances in  $^1\text{H}$ NMR spectra can be correlated to the bioactivity of compounds in the crude extracts to guide the isolation of target compounds, even those that are expressed in low concentrations, but have high potency.

##### ***1.4.2: Isolations based on chemical heritability***

Chemical heritability of specialized metabolites in plants refers to the degree to which the variation in the concentration and composition of specialized metabolites is genetically determined and can be passed from one generation to the next. Though

heritability should be a foundation of the evolution of new structural types within an organism, however very few studies of chemical heritability of natural products have been completed, especially in wild type populations and in multi-cellular organisms. The requirement for extensive genetic and metabolomic analyses conducted over multiple generations makes this study particularly challenging. Of particular importance is that variation in metabolomic profile must be annotated to gain a clear picture of probable biosynthetic relationships. While detailed mass spectrometry provides tentative structures, full structural annotation still requires isolation and characterization using methods such as NMR spectroscopy and XRD analysis. Chapter 3 provides detailed annotation of the 3 major chemotypes identified through our chemical heritability study. The comprehensive detail of the heritability experiment coupled with the thorough chemical annotation that was described in Chapter 3, laid the foundation for identifying some of the most heritable metabolites found in only a few individual families, in low concentrations, and were structurally unique via tandem MS techniques. Chapter 4 demonstrates how guidance by the details of the chemical heritability experiment led to the discovery of novel compounds with the elucidation of a novel and highly heritable natural product of unknown and unique biosynthetic origins.

#### ***1.4.3: Isolation based on increasing annotation rate***

One of the most challenging limitations in natural product structure elucidation is the amount of purified material necessary for comprehensive spectroscopic analysis. X-ray diffraction (XRD) allows for reliable structure analysis using a very small amount of material. In recent years, two methods of structure elucidation using single crystal x-ray

diffraction (SC-XRD) have been applied to difficult to crystalize natural products: the crystalline sponge method and the co-crystallization method.<sup>18,19</sup> Chapter 5 discusses the work previously done with the crystalline sponge method and co-crystallization, as well as work completed to use these methods to determine the structure of novel natural products.

## Chapter 2: Piperholdripine

### 2.1: <sup>1</sup>H-NMR network-based isolation of antifungal compounds of the genus *Piper*

As discussed in the introduction, Richards and co-workers reported the development of a <sup>1</sup>H NMR-based network analysis (WCGNA) approach to identify collections of <sup>1</sup>H NMR resonances (modules) that can give insights into structural features in complex mixtures of compounds.<sup>17</sup> This approach severely reduces the bottleneck of bioassay repetition by allowing for targeted isolation based on <sup>1</sup>H NMR resonances.

Previous work completed in the Jeffrey research group screened methanolic extracts from 30 different *Piper* species for their ability to inhibit growth of *S. cerevisiae*. While most extracts displayed less than 20% inhibition, metabolite extracts from two species—*P. holdrigeanum* and *P. peracuminatum*—presented nearly total growth inhibition, followed by *P. pseudobumbratum* with 63% inhibition. This chapter focuses on the isolation and structure determination of a novel and minor bioactive compound found in *P. holdrigeanum* that had previously eluded isolation and structure determination despite being clearly identified by our <sup>1</sup>H NMR network analysis.

*P. holdrigeanum* was diagnostically associated with a unique set of resonances at the narrow range of  $\delta_{\text{H}}$  8.53-8.62. The singlet did not associate with any known compound structural features, which leads to the conclusion that this could be a structurally distinct compound from the reference material, and therefore a novel compound.

## **2.2: Methods**

### ***2.2.1: Sample Preparation***

The plant material was collected May 2016 from La Selva Biological Station in Costa Rica, Heredia Province (10°25' N, 84°00' W, 50 m). Two grams of ground leaf material were extracted with methanol, filtered, and dried under vacuum.

### ***2.2.2: General Isolation Procedures***

Crude material was initially separated with Agilent Infinity Prep-HPLC/MS. Pilot runs were used to determine the most efficient method. The solvent system used was optima acetonitrile with 0.1% formic acid and optima water with 0.1% formic acid. The initial separation was done on a C18 column (21.2 mm x 150 mm). Fractionation was based on UV absorbance using wavelength 254 nm with secondary wavelength 280 nm. These wavelengths were chosen as they would include most of the compounds. Data from the MS analysis was used to pool fractions in addition to UV absorption peaks.

Further purification of compounds was based on <sup>1</sup>H NMR spectroscopy and LC-MS/MS data. Based on the compound, the sample would be run on Agilent Infinity using a new method and column or separated by prep TLC. This would be repeated until a purified compound was acquired.

## **2.3: Compound Isolation: piperholdripine**

The initial isolation attempts completed by the Jeffrey research group resulted in the isolation of the main component, a prenylated benzoic acid derivative, which did not contain the targeted <sup>1</sup>H NMR resonances and showed no antifungal activity.

Further attempts to isolate the bioactive component(s) focused initially on the remaining 1 g of crude methanolic extract. 500 mg of the crude extract was dissolved in methanol to a concentration of 53.3 mg/mL. A pilot run of 106.7 mg was used to analyze the separation (Table 2.3-1) on Agilent Infinity Prep-HPLC/MS. Following the separation, the method was adjusted (Table 2.3-2) to extend the separation between the UV-Vis peaks. The chromatographs of runs 2 and 3 (133.3 mg and 159.9 mg respectively) were identical based on UV-Vis absorption (Figure 2.3-1).

**Table 2.3-1:** Prep-HPLC method of pilot run of *P. holdridgeanum*

<b>Time (min)</b>	<b>A (%)</b>	<b>B (%)</b>
<b>Start. Cond.</b>	70.00	30.00
<b>20.00</b>	00.00	100.00
<b>26.00</b>	0.00	100.00
<b>27.00</b>	70.00	30.00

**Table 2.3-2:** Prep-HPLC method of isolation of *P. holdridgeanum*

<b>Time (min)</b>	<b>A (%)</b>	<b>B (%)</b>
<b>Start. Cond.</b>	70.00	30.00
<b>20.00</b>	17.00	83.00
<b>21.00</b>	0.00	100.00
<b>29.00</b>	0.00	100.00
<b>30.00</b>	70.00	30.00

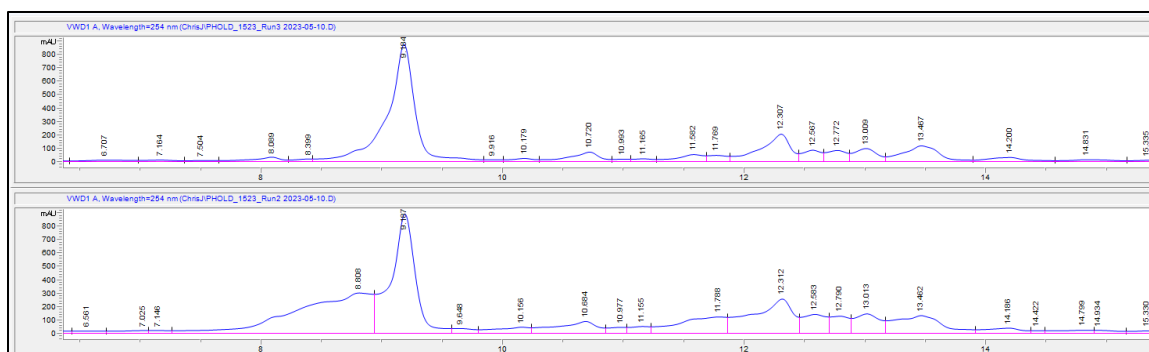


**Figure 2.3-1.** Comparison of prep-HPLC chromatographs of crude extract of *P. holdrigeanum* from Agilent Infinity prep-HPLC+MS.

Preliminary  $^1\text{H}$  NMR analysis of pools from Run 3 in the 10 min to 15 min retention frame showed the presence of the singlet of interest ( $\delta_{\text{H}}$  8.62) in 6 fractions. These fractions were sent to Dr. Ian Wallace for growth inhibition analysis.

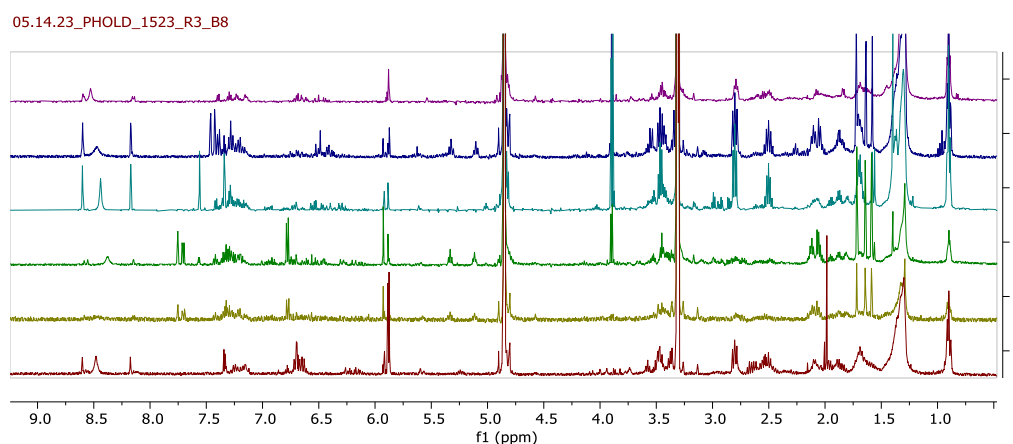


**Figure 2.3-2:** Comparison of  $^1\text{H}$  NMR spectra of fractions containing cryptic compound.  $^1\text{H}$  NMR spectra of fractions were analyzed to determine if the desired peak at  $\delta_{\text{H}}$  8.62 was present to determine which fractions would be sent for growth inhibition analysis.

The growth inhibition analysis of the samples against *S. cerevisiae* displayed high inhibition in three of the six fractions, designated fractions 4-6, with the most growth inhibition shown in Fraction 4 (Figure 2.3-3).

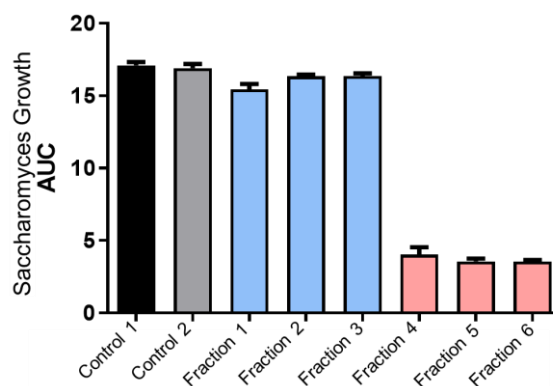


**Figure 2.3-3:** Antifungal activity analysis of *P. holdrieanum*. Fractions of extracted metabolites from Agilent Infinity prep-HPLC were assayed for antifungal activity against *S. cerevisiae*. The Area Under Curve (AUC) values for each fraction were quantified as a metric of total *S. cerevisiae* growth in the assay.

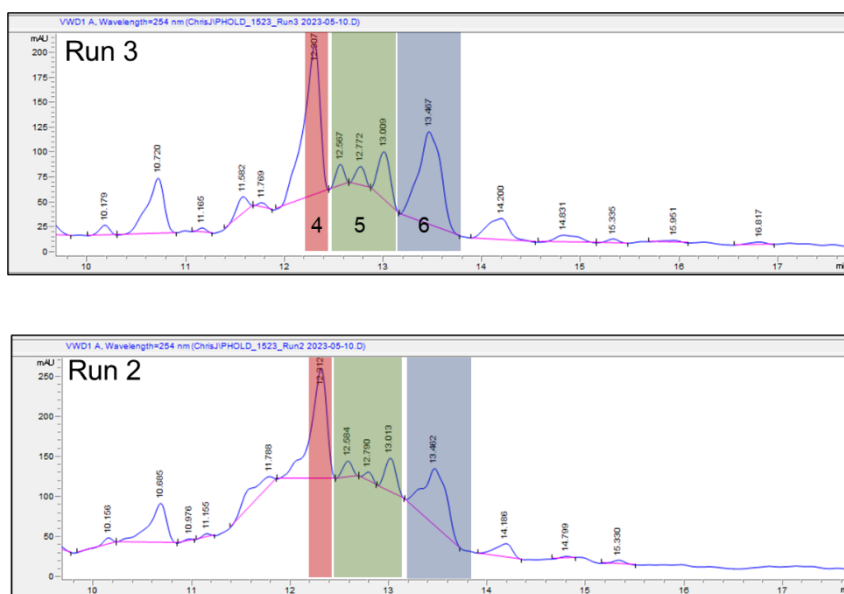


**Figure 2.3-4:** Comparison of HPLC chromatography between Run 2 and Run 3. The zoomed in view shows the fractions designated 4-6 which contained the compound of interest based on growth inhibition analysis. The same fractions (based on UV-Vis peaks) can be found in both runs.

The comparison of the UV-Vis peaks between Runs 2 and 3 (Figure 2.3-4) shows the same separation of the peaks. However, the review of the  $^1\text{H}$  NMR spectra of the same

pools in Run 2 showed less abundance of the compound of interest based on the presence of the desired singlet.

A pool with retention time 11.4 min to 11.8 min had a much higher concentration based on the intensity of the singlet in the  $^1\text{H}$  NMR spectrum compared to the other compounds in the mixture. From this data, the variation in the desired  $^1\text{H}$  NMR resonances that were affiliated with the bioactivity of the fractions was cross-referenced with the LC-MS data leading to the identification of a unique mass that co-varied with fractions demonstrating high growth inhibition in the bioassay. A review of the tandem LC-MS/MS data showed that the unique mass found in these fractions was 344.4 m/z. Returning to the HPLC chromatograph, the fractions containing 344.4 m/z contain the highest abundance of the singlet at  $\delta_{\text{H}}$  8.60.

Figure 2.3-5 shows the difference in retention time between the two runs, resulting in the pooling of future runs being based on MS data and not UV-Vis absorbance peaks.

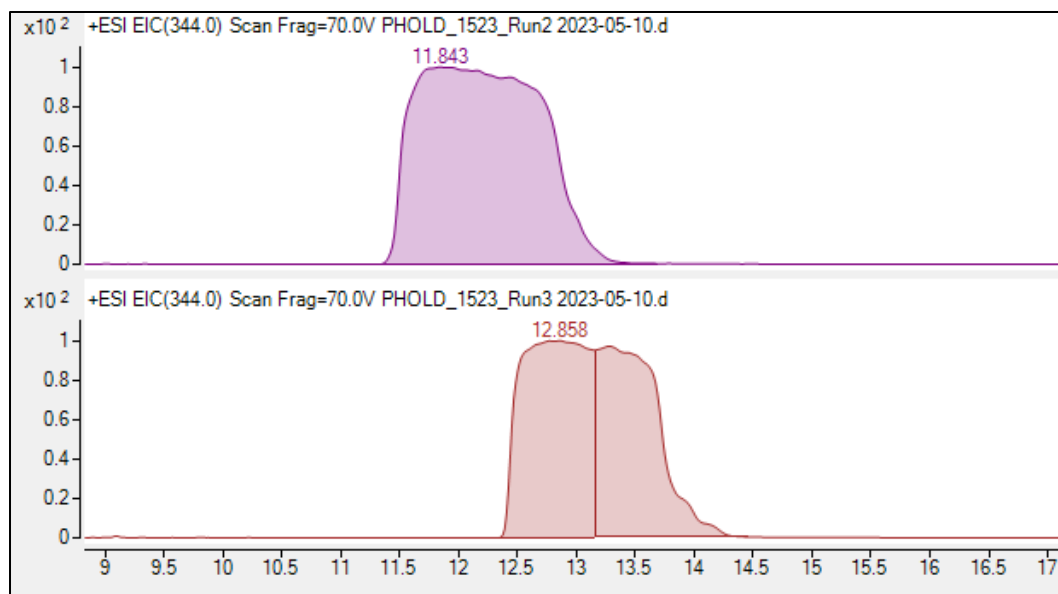


**Figure 2.3-5:** Comparison of MS spectra of Run 2 and 3, focusing on 344 m/z (EIC).

The 344.4 m/z pool from Run 2 (9.6 mg) was further purified using silica gel preparatory thin plate chromatography (prep-TLC) (500-micron, 80% ethyl acetate/20% hexanes + 0.5% methanol). However, it quickly became apparent with  $^1\text{H}$  NMR analysis that the silica gel degraded the sample, and this method could not be used in further isolation.

A second sample of 491 mg of crude material was purified on Infinity prep-HPLC, resulting in 7.9 mg of a mixture containing 344.4 m/z. An attempt was made to purify by acetone extraction; however, the desired compound (based on the singlets at  $\delta_{\text{H}}$  8.53-8.62) and an unknown impurity were both soluble in the acetone. The resulting material was too low in mass to allow for further separation without risking further material loss.

A new batch of plant material (*P. holdrigeanum*, Costa Rica, 2023) was provided, and a methanol extraction resulted in 5.1 g of crude extract. Using the previous method, 17 runs were performed on Infinity prep-HPLC, using the MSD detection to pool all partitions

with 344.4 m/z, which resulted in 105 mg of a partially purified fraction. The new sample was further separated with a column of a smaller diameter and longer length (C18 10mm x 250mm) that allowed for a longer gradient and more precise fractionation, using the method as described in Table 2.3-2. This separation resulted in an enriched sample of 344.4 m/z (0.8mg).

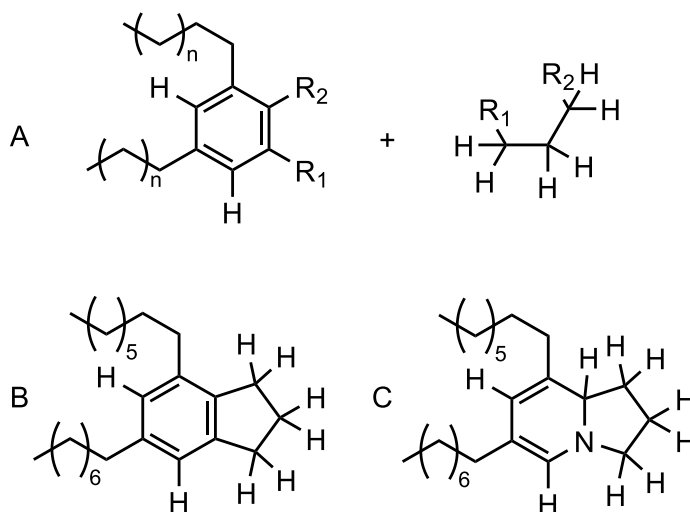
**Table 2.3-3:** Prep-HPLC method of fraction containing 344.4 m/z

<b>Time (min)</b>	<b>%H<sub>2</sub>O + 0.1%FA</b>	<b>%ACN +0.1%FA</b>
<b>Start. Cond.</b>	70.00	30.00
<b>2.00</b>	60.00	40.00
<b>20.00</b>	30.00	70.00
<b>24.00</b>	0.00	100.00
<b>25.00</b>	70.00	30.00

#### **2.4: Structure elucidation: piperholdripine**

Using Shigemi NMR tube (CD<sub>3</sub>OD), it was possible to perform 1D and 2D NMR analysis (SI S3.1) and elucidate the structure. The <sup>1</sup>H NMR spectrum showed several overlapping peaks in the alkane region, suggesting at least two aliphatic chains. The two singlets ( $\delta_{\text{H}}$  8.17 and 8.60) represent aromatic hydrogens near a hetero atom. The <sup>1</sup>H-<sup>1</sup>H COSY spectra showed a spin-isolated propyl system [ $\delta_{\text{H}}$  4.81 (t), 2.48 (pent), and 3.44 (t)]. Figure 2.4-1A represents the two fractions determined through the <sup>1</sup>H NMR spectrum. The fragments can be resolved into one compound (B) through the HMBC

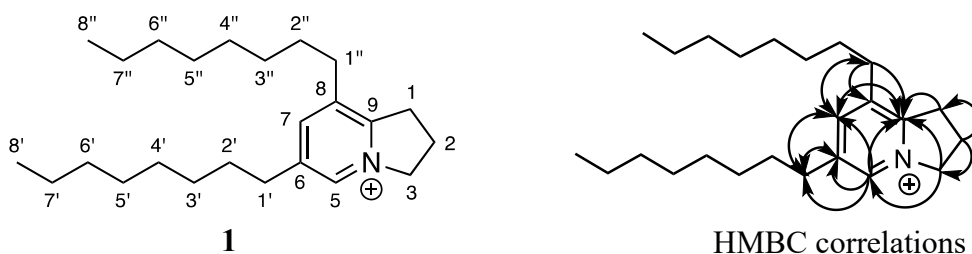
correlations between the propyl unit and aromatic carbons [ $\delta_{\text{H}}$  4.81 (t), 2.48 (pent), and 3.44 (t),  $\delta_{\text{C}}$  140.7, 156.6].



**Figure 2.4-1:** Steps of structure determination. A: Fragments of possible structure based on NMR analysis. B: Putting fragments together to create a single structure. C: Updating the structure to include hetero atoms.

When determining the chemical formula, the expected mass was 343.3 g/mol; the MS/MS data showed primarily the loss of  $\text{CH}_3$  or  $\text{CH}_2$  groups and therefore was not immediately helpful for structure determination. Using the monoisotopic mass, the chemical formula was determined to be  $\text{C}_{24}\text{H}_{41}\text{N}$  (Figure 2.4-1C). However, this structure requires the presence of a methine that is not observed in the  $^1\text{H}$  NMR spectrum. Subsequent literature searches eventually suggested that the desired compound contained a positive charge, corresponding to  $\text{C}_{24}\text{H}_{42}\text{N}^+$  and 344.3320 g/mol.

The HMBC spectrum reinforced the connection of the aliphatic substituents to the aromatic ring, through the correlation between C-1'/1'' and H-7 [ $\delta_{\text{C}}$  33.0,  $\delta_{\text{H}}$  8.17]; this supported the assignment of the novel C6,C8-*bis*-octyl substituted 2,3-dihydro-1*H*-indolizidinium alkaloid, piperholdripine (**1**), as the principal bioactive compound of the crude mixture of *Piper holdrigeanum* (Table 2.4-1).

**Table 2.4-1:** NMR spectroscopic assignments for isolated compound **1**

Position	$\delta_C$ , type	$\delta_H$	HMBC
1	31.6, CH <sub>2</sub>	3.47 t	8, 9
2	22.1, CH <sub>2</sub>	2.50 p	1,3,9
3	60.5, CH <sub>2</sub>	4.83 t	1,2,5,9
4	N		
5	138.8, CH	8.60 br s	6,7,9
6	142.9, C		
7	145.9, C	8.17 br s	5,9
8	140.7, C		
9	156.6, C		
1'/1''	33.0, CH <sub>2</sub>	2.80 t (7.3 Hz)	2'/2'', 5, 6, 7, 8, 9
2'/2''	31.7, CH <sub>2</sub>	1.69, 1.70 m	8, 6, 1'/1'', 3'/3''-7'/7''
3'/3''-4'/4''	30.2, 30.1, CH <sub>2</sub>	1.34-1.44 m	
5'/5''-7'/7''	32.7, 33.2, 23.6, CH <sub>2</sub>	1.26-1.36 m	
8'/8''	14.3 CH <sub>3</sub>	0.90 m	

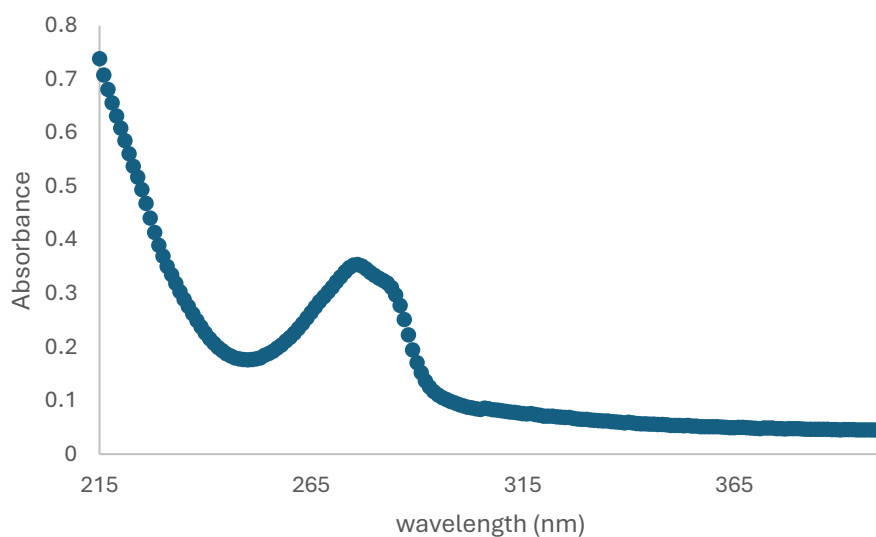


**Figure 2.4-2:** UV-Vis of isolated compound 1 in methanol.

Figure 2.4-2 shows the UV-Vis spectrum of piperholdripine in methanol from 400 nm to 215 nm, with a  $\lambda_{\text{max}}$  at 276 nm. The HPLC fractionation was collected at 254 nm, which shows a sudden decrease in absorption. This corresponds to the HPLC chromatograph, which does not show any absorption at retention times of the piperholdripine fractions. While a spectrum at a secondary wavelength during the HPLC run was collected at 280 nm, the absorption of the major component, a prenylated benzoic acid, is orders of magnitude greater than piperholdripine, a very minor component.

## 2.5: Synthesis of piperholdripine

A review of literature using the indolizidinium moiety revealed three similar natural products previously isolated from *Prosopis juliflora* and *Ficus septica*, as shown in Figure 2.5-1.<sup>20,21</sup>

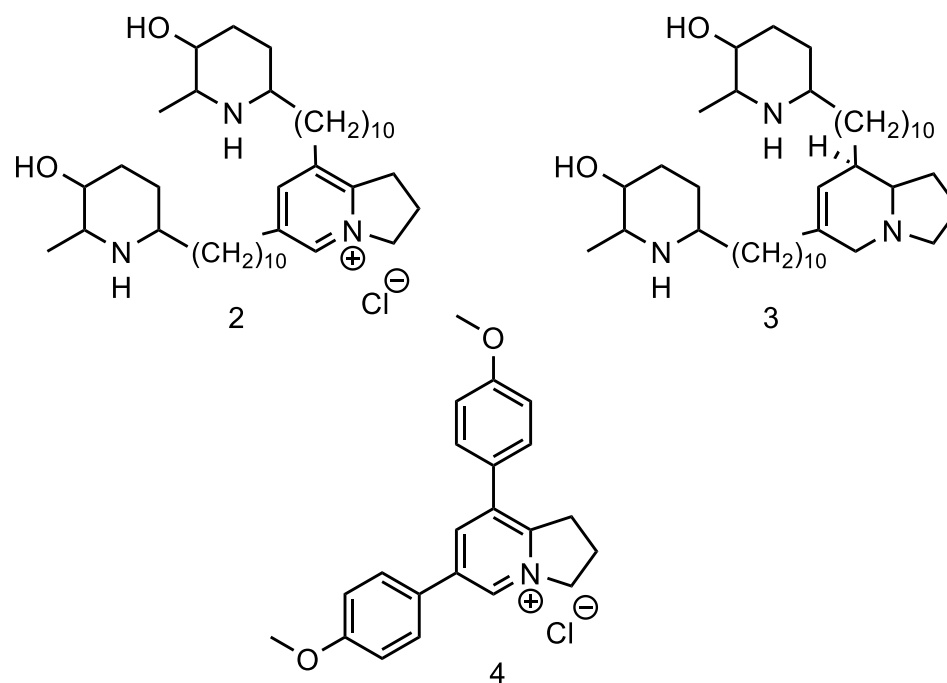
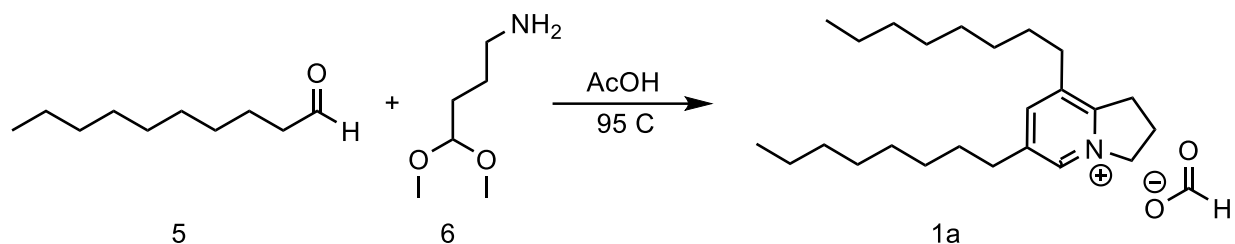


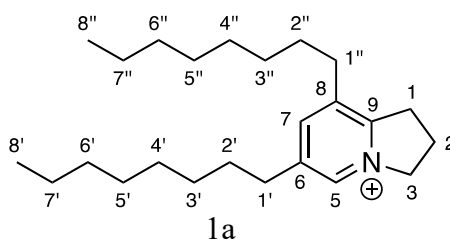
**Figure 2.5-1:** Previously isolated compounds with similar moiety to compound 1. Juliprosine (2) and juliprosopine (3) were isolated from *Prosopis juliflora*. Ficuseptine (4) was isolated from *Ficus septica*.

Following the method of Snider and Neubert<sup>22</sup> as seen in Scheme 2.5-1, (5) decanal (1.24 mL, 6.6 mmol) was added to a solution of (6) 4-aminobutyraldehyde dimethyl acetal (0.46 mL, 3.3 mmol) in 35 mL of glacial acetic acid. The solution was stirred at 95°C for 2 days, cooled to 25°C, and basified with 10 M NaOH. The solution was washed with hexanes, saturated with NaCl and extracted with CHCl<sub>3</sub>. The extract was concentrated under vacuum and separated on Yamazan C18 HPLC in 9% yield (gradient 10%MeOH/90%H<sub>2</sub>O to 100%MeOH over 20 mins) This yielded a product spectroscopically identical to the isolated compound **1a** (Table 2.5-1).



**Scheme 2.5-1:** Synthesis of compound 1a piperholdripine.

**Table 2.5-1:** NMR spectroscopic assignments of compound 1a



Position	$\delta_C$ , type	$\delta_H$	HMBC
1	31.6, CH <sub>2</sub>	3.47 t	8, 9
2	22.1, CH <sub>2</sub>	2.49 p	1,3,9
3	61.9, CH <sub>2</sub>	4.86 t	1,2,5,9
4	N		
5	140.20, CH	8.62 br s	6,7,9
6	144.1, C		
7	147.2, C	8.16 br s	5,9
8	141.9, C		
9	157.9, C		
1'/1''	33.1, CH <sub>2</sub>	2.81 td	2'/2'', 5, 6, 7, 8, 9
2'/2''	31.7, CH <sub>2</sub>	1.68, 1.71 m	8, 6, 1'/1'', 3'/3''-7'/7''
3'/3''-4'/4''	30.3, 30.2, CH <sub>2</sub>	1.32-1.44	
5'/5''-7'/7''	32.7, 33.1, 23.6, CH <sub>2</sub>	1.23-1.36	
8'/8''	14.5 CH <sub>3</sub>	0.90 m	

## 2.6: Confirmation of the bioactivity of piperholdripine

Samples of the isolated piperholdripine and the synthesized piperholdripine were assayed with *S. cerevisiae* to determine the extent of bioactivity. The antifungal activity of *P. holdrigeanum* compounds (Figure 2.6-1) demonstrated strong antifungal activity, inhibiting *S. cerevisiae* growth by greater than 80% compared to untreated and solvent controls (YPD and MeOH respectively). Based on the network analysis, the novel compound was present in the crude material at a considerably lower concentration, yet still displayed a significant inhibitory effect. Dose-response analysis of piperholdripine growth inhibition activity indicated an  $IC_{50}$  of 4.9  $\mu$ M.

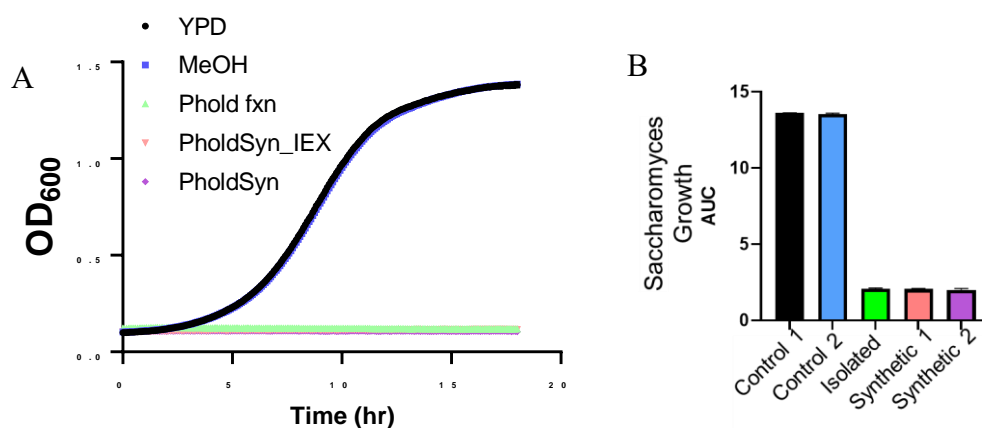


**Figure 2.6-1:** Growth inhibition analysis of isolated compound 1 and synthesized compound 1a.

## 2.7: Conclusions

From the previous work completed by the Jeffrey research group and my isolation of the elusive bioactive component of a mixture, three novel bioactive compounds were isolated using the presented approach. Piperholdripine represents a class of natural products that

could potentially be isolated in various *Piper* species but have not been previously isolated or described in this genus. In a traditional isolation method, a growth inhibition study would be necessary after every new purification step, adding weeks or months to the process. Additionally, it is easy to see that this minor and chemically challenging component would be easily overlooked. However, using the  $^1\text{H}$  NMR resonance targeted method, a 3 minute  $^1\text{H}$  NMR experiment determines if the desired peak is present in the sample. This severely decreases the amount of time spent on the isolation process and identifies the likely peaks that should be targeted during the isolation process, allowing the researcher to adjust and revise their isolation strategy accordingly.

The original isolation method used reverse phase chromatography, with separation based on UV-Vis absorbance at 254 nm. It was originally expected that the major compound would be the desired metabolite, which was proven untrue as the  $^1\text{H}$  NMR spectrum did not contain the singlet at  $\delta_{\text{H}}$  8.63. This method allowed for an analytical analysis that took minutes and was non-destructive to the small amount of material necessary. Compared to the usual workflow of necessary bioassays at each step of isolation, this method allows for the targeted isolation in a much faster timeline. The synthesis of piperholdripine (**1**) confirms the structure of the natural product, as well as its bioactivity. The adjustment to the method of Snider and Neubert shows that analogs of this compound could be generated. Similar compounds with the indolizidinium moiety have been isolated in other plant species. One such compound, Ficuseptine (**4**) from *Ficus septica* presented significant antifungal and antibacterial activity against microbes such as *E. coli*.<sup>20</sup> The function of this class of compound as a defense against microbes

speaks to the hypothesis that the biological origins are related to an environmental stress on the individuals. The presence of this class of compound in *P. holdrigeanum* could indicate the necessity of a defense that other *Piper* species do not face.

## Chapter 3: Chemical Heritability: Annotation of metabolomic chemical heritability experiment of *Piper scintillans*

### 3.1: Chemical Heritability

The degree of variation in the concentration and composition of specialized metabolites in plants can differ at the individual level in a species. A chemical heritability experiment explores this degree of variation through generations of a species. Such an experiment requires comprehensive genetic and metabolomic analysis of individuals across generations in a wild-type population. While high resolution mass spectrometry can provide insight into the compound class or structure, isolation and full characterization requires using multiple analytical methods such as NMR spectroscopy and XRD analysis. With specifically annotated compounds, collaborators are enabled to make biosynthetic inferences to understand heritability and rule out coincidental or artifactual features that can mislead this type of study. This chapter focuses on the isolation process to provide confirmatory annotation of the three major chemotypes that were identified through a metabolomics study, using chemotype-defining compounds as determined by untargeted metabolomic analysis.

This project uses leaf and seed samples of *Piper scintillans* (formerly *Piper sancti-felicis*) collected in Costa Rica to be grown in a common shade garden. Samples were collected from the parent individuals (100 individuals) and the third sexual adult generation (4 siblings, 332 individuals) for LC-MS/MS and <sup>1</sup>H NMR spectroscopy analysis. The purpose of this analysis was to observe the chemical variation between individuals and to group the individuals (parent and offspring) based on that variation.

### 3.2: Metabolomics and Chemotypes

Metabolomics is generally defined as the broad study of all metabolites in a biological system, but most plant metabolomic studies focus on the identification and quantification of small molecules. Due to the high chemical composition diversity of specialized metabolites, no single analytical tool covers an entire metabolomic profile and therefore must be combined for a comprehensive analysis based on the goals of the project.<sup>23,24,25</sup> There are three main types of approaches in metabolomic studies: targeted metabolomics, untargeted metabolomics, and semi-targeted metabolomics. In an untargeted metabolomic analysis, the goal is to survey the entire phytochemical profile to ensure the retention of minor components that may be of interest.<sup>26,27</sup>

The metabolomic analysis used LC-MS/MS data, as well as <sup>1</sup>H NMR data to group the parent and offspring samples based on the variation in their chemical profile. The PCA plot (Figure 3.2-1) summarizes the phytochemical variation used to determine chemotype-defining LC-MS/MS entries.

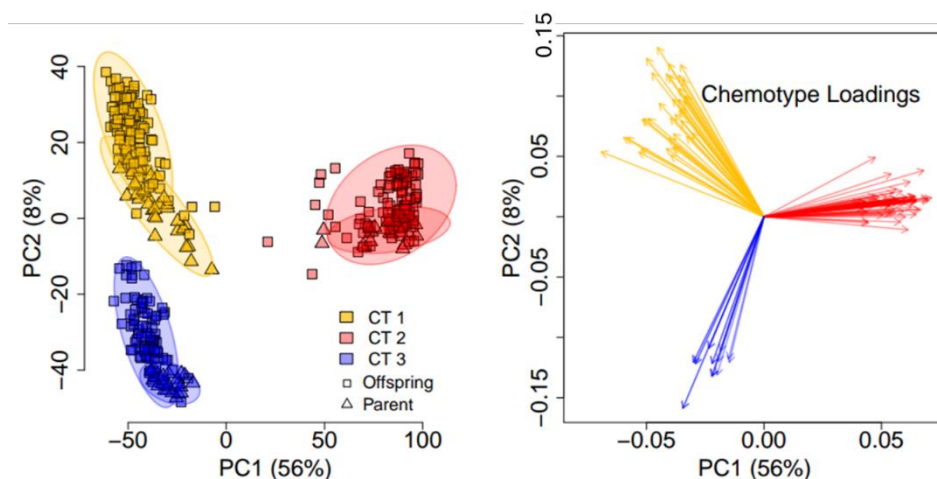


**Figure 3.2-1:** PCA plots of phytochemical diversity of LC-MS entities

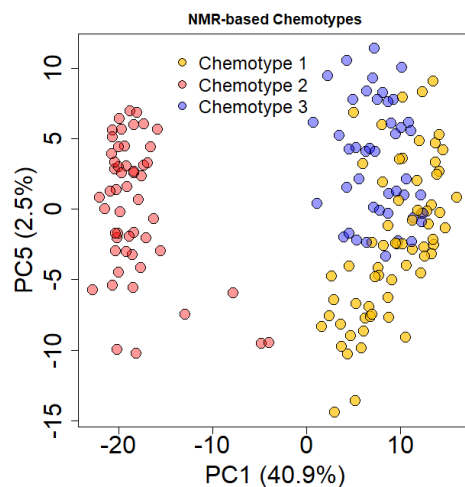


**Figure 3.2-2:** PCA plot of phytochemical variation by  $^1\text{H}$  NMR spectroscopic entities

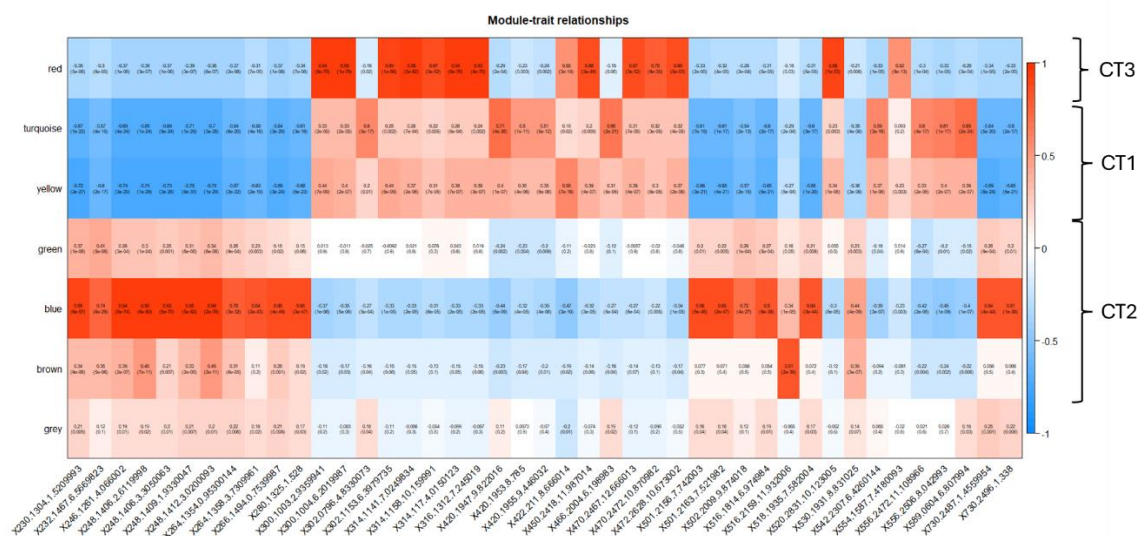


**Figure 3.2-3:** Correlation of LC-MS data with  $^1\text{H}$  NMR structural data

Concurrently, the phytochemical variation directed analysis to chemotype defining entities based on  $^1\text{H}$  NMR resonances, as seen in Figure 3.2-2. The PCA plots of Figures 3.2-1 and 3.2-2 describe the chemical variation across the populations. Figure 3.2-3 uses the cross section between the  $^1\text{H}$  NMR structural information and LC-MS/MS molecular ion and retention time information, allowing for the compounds and their features to be separated into discrete entities. The correlation between entities grouped them into “chemotypes”. The red color of the heat map represents the positive correlation

of that entity (or compound) with each other, while the blue represents a negative correlation. This chapter focuses on the methods of isolation and annotation of those compounds.

### 3.2.1: Classes of Compounds

Some of the most prominent classes of compounds found in *Piper scintillans* are flavonoids and terpenoids. Flavonoids are generated through the phenylpropanoids pathway (Shikimate acid). There are six major subcategories within the flavonoid group.

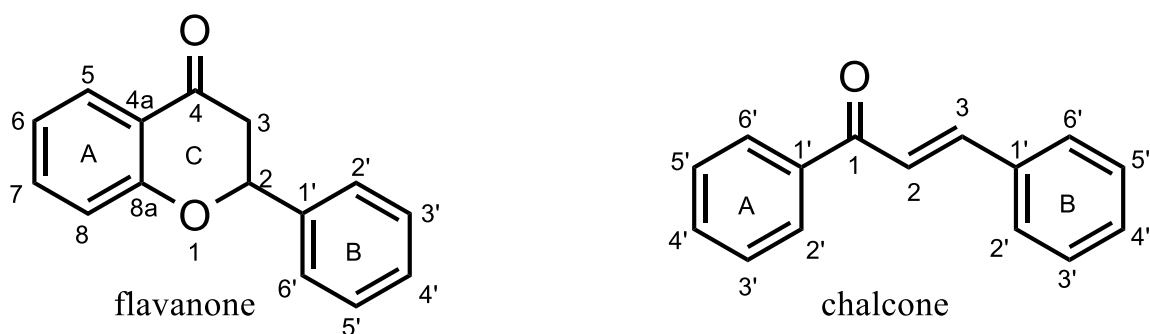


**Figure 3.2-4:** General structure and numbering of flavanones and chalcones

Figure 3.2-4 shows the general structure of flavanones and chalcones, which were two of the most commonly isolated classes of compounds in this project. Chalcones are the biosynthetic precursor of flavanones. Biological functions have been linked to plant defense through responses against pathogens and attracting pollinators through the pigmentation of pollen.<sup>28</sup> Sesquiterpene lactones were the most prevalent terpenoid isolated in this project.

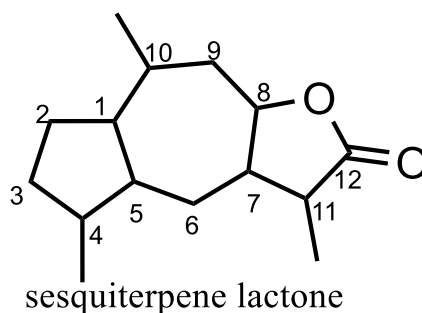


**Figure 3.2-5:** Example structure and numbering of a sesquiterpene lactone

Figure 3.2-5 shows a common structure of a sesquiterpene lactone, named for the fifteen-carbon backbone. The biological function of sesquiterpene lactones has been linked to plant defense, such as in natural latex, or as herbivore feeder deterrents.<sup>29</sup>

### 3.3: General Procedures

The parent samples were grouped based on their chemotype, ground, and three overnight methanol extractions were performed. To decrease the amount of choline in the crude extract, the crude extractions were washed with 100% water, 95% water/5% methanol, and 100% methanol in three phases. The 100% methanol fraction was used for all isolations.

A pilot run was used to determine the most effective separation method on Agilent Infinity prep-HPLC + MS. The pools of each chemotype are based on the UV-Vis absorption peak and m/z, targeting the compounds listed in the mass list.

	Chemotype 1	Chemotype 2	Chemotype 3
<b># of individuals</b>	32	27	22
<b>Crude extract</b>	2.50 g	1.83 g	1.64 g
<b>Prep-LCMS runs</b>	13	9	8
<b>Pools</b>	16	19	33

These pools were then further isolated using either the same column with a new method, a column of a smaller diameter and longer length, or prep-TLC. The compounds from the mass list would be targeted in each step of the isolation, using the MS detector of the Infinity or GC/MS and LC/MS to identify the masses in each fraction. This cycle would continue until a fraction containing a purified compound was achieved or the mass of the sample was too low abundance for analysis and further separation. While each step of the isolation was targeted, the process still resulted in hundreds of fractions, many of which were dead ends in the isolation process as the result of material loss through the partitioning process.

Typically, a pool was chosen for isolation based on the  $^1\text{H}$  NMR spectrum and LC-MS/MS data. If there appeared to be a high concentration of a compound from the desired mass list, that pool was prioritized. For example, if the  $^1\text{H}$  NMR spectrum of a pool showed a major component, such as the intensity of peaks that typically belong to a flavanone, over other compounds, that separation would be started first as the isolation would be more straightforward. This also prevented the re-isolation of known compounds, based on the mass and similar  $^1\text{H}$  NMR peaks. These fractions were saved for the future isolation of material, if needed for another experiment.

Samples containing majority flavanones could be determined by defining resonances in the  $^1\text{H}$  NMR spectra, such as a doublet of doublets around  $\delta_{\text{H}}$  5.3-5.5 and diastereotopic protons (doublet of doublets) in an a/b formation around  $\delta_{\text{H}}$  2.7 and 3.0. The most efficient separation technique is using reverse phase chromatography, with a method based on the previous isolation step. The defining  $^1\text{H}$  NMR resonances for

chalcones include doublets in an a/b pattern around  $\delta_{\text{H}}$  7.80 and 7.90, which represents the alkenyl protons of the chalcone. A similar method can be used as flavanones, using a wavelength of 380 nm.

Sesquiterpenes typically have multiple diastereotopic methylenes that can be confirmed with HSQC analysis. In a  $^1\text{H}$  NMR spectrum, the number of peaks below 3 ppm will be much higher than that of a flavanone and chalcone. The most efficient method of separation is normal phase chromatography, particularly prep-TLC. A series of TLC tests can provide insight into the best solvent system.

### 3.4: Chemotype 1

Chemotype 1 consists of 32 parent samples and their offspring (SI Table S2-1). Based on tandem MS/MS annotation, it was hypothesized that this chemotype would primarily include oxygenated flavanones and chalcones, which correlates to the profile of isolated compounds. The isolation process began with a mass list that consisted of the compounds that are considered “chemotype-defining” (Table 3.4-1). Through the isolation process, 4 of the 12 compounds from the mass list were fully characterized, while several others were isolated but not able to be fully characterized. Additionally, other major compounds were isolated and purified.

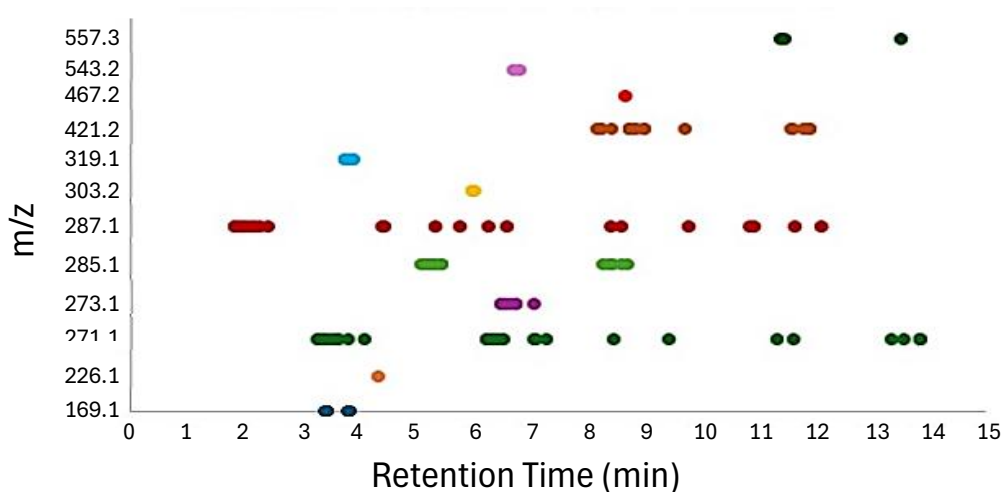
**Table 3.4-1.** Annotation of chemotype-defining masses for Chemotype 1

<b>Mass</b>	<b>m/z</b>	<b>RT (min)*</b>	<b>Annotation</b>
<b>168.05</b>	169.05	3.84	Fatty acid, not isolated
<b>226.15</b>	227.07	4.33	Terpenoid, not isolated
<b>270.1</b>	271.09, 271.10	6.23, 3.31	Flavanone, fully characterized
<b>272.1</b>	273.11	6.47	Dihydrochalcone, partially isolated
<b>284.1</b>	285.11	5.16, 8.41	Flavanone, fully characterized

<b>286.1</b>	287.09	1.80, 4.42, 11.63	Flavanone, fully characterized
<b>302.1</b>	303.16	5.92	Not isolated
<b>318.1</b>	319.12	3.77	Not isolated
<b>420.2</b>	421.20	8.16, 11.7	Partially isolated, flavanone
<b>466.2</b>	--	--	Not found
<b>542.23</b>	543.23	6.68	Not isolated, conjugate
<b>556.25</b>	557.25	11.37	Not isolated, conjugate

\*average retention times of ions from tandem MS/MS data

The LC-MS/MS analysis on the pools from the initial separation highlighted the abundance of the desired compounds, as well as the existence of isomers. The LC-MS/MS entities grouped together based on their  $m/z$  and then graphed against their retention times in the LC-MS/MS experiment. Each data point represents an ion that fractionated in tandem MS/MS and the pool that they can be found in is identified. This information can be used to focus the separation methods onto pools with higher potential of isolation. The breaks in retention times point to the presence of isomers, which was confirmed in later isolations. The pools with a shorter retention time typically contain flavanones, while the pools with a longer retention time contain chalcones. There were



multiple isomers of the desired compounds, as highlighted in Figure 3.4-1. For example, the row containing  $m/z$  285.1 displays two groups of different retention times. The group at retention time 5 min to 6 min represents flavanones while the group at retention time 8 min to 9 min represents chalcones. It was important to target both groups since the structure was different, even if the mass was the same.

The general isolation procedure began with the separation of the methanol partition of the crude material. The extract was separated using Agilent Infinity, using the method described in Table 3.4-2. Thirteen runs were completed, then pooled together into

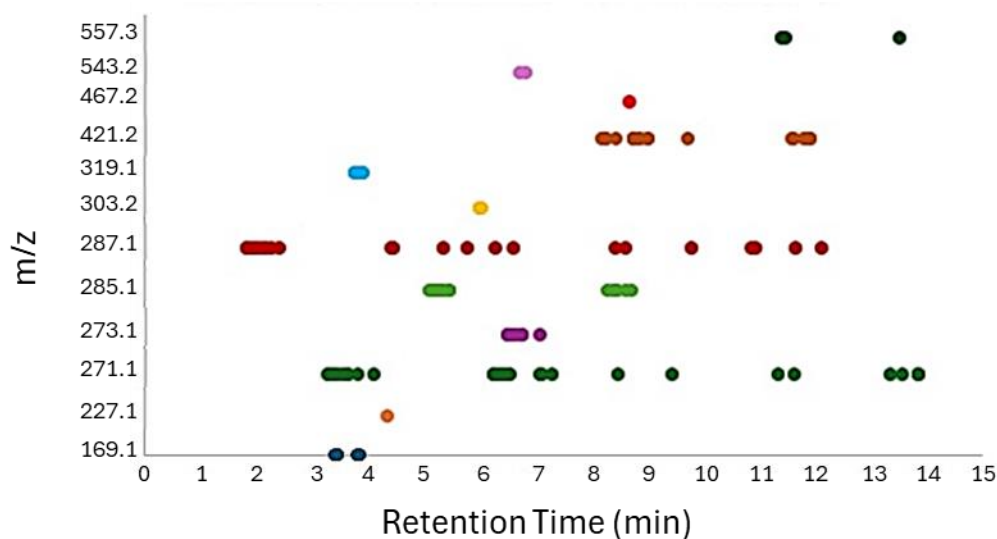


**Figure 3.4-1:** Comparison of Chemotype 1 compounds retention times using  $m/z$  and RT from tandem MS/MS data

16 fractions based on UV-Vis absorbance peak and  $m/z$ . The fractionation focused on major components and the compounds matching the desired mass list.

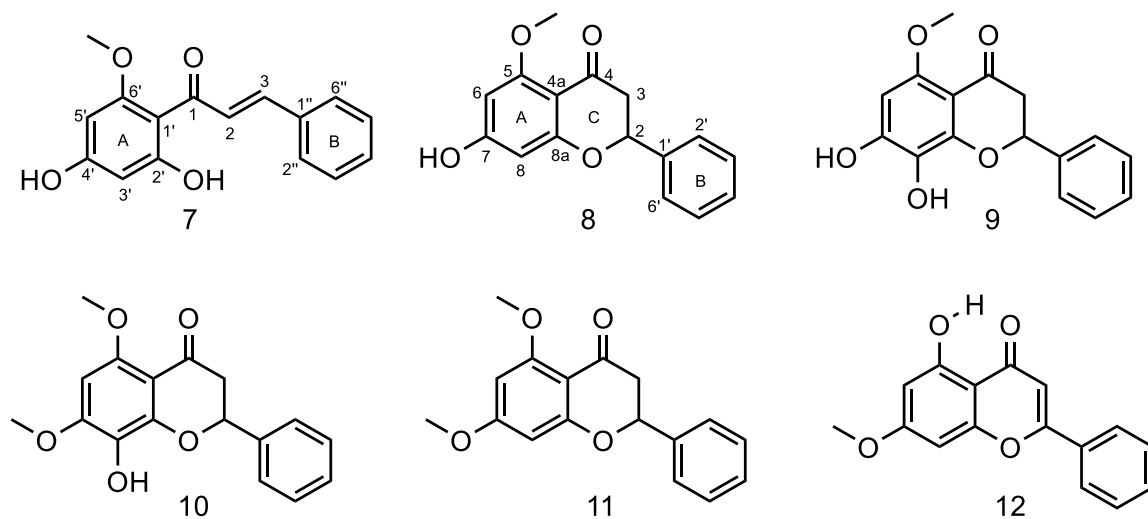
**Table 3.4-2:** Prep-LCMS method used for initial separation of Chemotype 1

Time (min)	%H <sub>2</sub> O + 0.1%FA	%MeOH + 0.1%FA
0	95	5
2	75	25
20	0	100

<b>30</b>	0	100
<b>31</b>	95	5

Further isolation on the samples was completed either through additional fractionation on the Infinity, by changing the column and method, or by normal phase prep-TLC. This was chosen based on the amount of material available, the purity as determined by  $^1\text{H}$  NMR spectroscopic analysis or LC-MS analysis, and the behavior of the crude sample on TLC plates, as outlined in section 3.2.2.

Two major components, 271 m/z and 287 m/z, consist of both flavanone and chalcone compounds. Within those masses are additional isomers, typically in terms of substitution on the A ring of the flavanone. The fully characterized compounds are shown in Scheme 3.4-1, with their m/z and retention time given in Table 3.4-3.



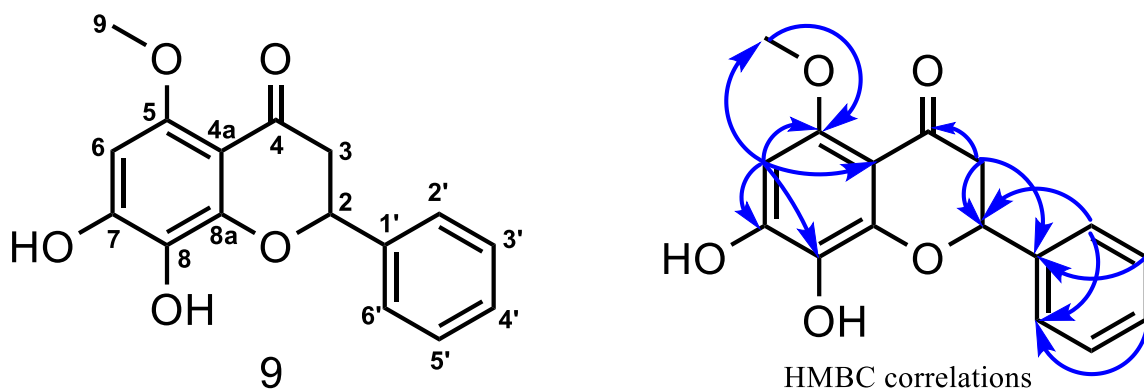
**Scheme 3.4-1:** Isolated compounds from Chemotype 1

**Table 3.4-3:** Annotation of compounds isolated from Chemotype 1

Compound	m/z	RT (min)*	Pool	Name
7	271.09	15.4-16.5	09	2',4'-Dihydroxy-6'-methoxychalcone <sup>30</sup>
8	271.09	10.7-11.1	03	5-Methoxy-7-hydroxyflavanone <sup>30</sup>
9	287.09	9.1-10.4	02	5-Methoxy-7,8-dihydroxyflavanone
10	301.10	10.7-11.1	03	8-Hydroxy-5,7-dimethoxyflavanone <sup>31</sup>
11	285.11	14.7-15.4	08	5,7-Dimethoxyflavanone <sup>32</sup>
12	269.08	16.9-17.5	10	5-Hydroxy-7-methoxyflavone <sup>33</sup>

\*Average retention time based on method POR\_100MeOH\_Inf\_Run4

Compound 9 (m/z = 287.09) is a flavanone not currently found in literature. It shares the same substituents as 5,6-dihydroxy-7-methoxy-flavanone, however the 2D NMR spectroscopic analysis showed different connection points on the A ring (Table 3.4-4). H-6, a methine singlet [ $\delta_{\text{H}}$  6.17] has HMBC correlations with C-5 and methoxy C-9 [ $\delta_{\text{C}}$  156.80 and 56.17 respectively] which places the methine adjacent to the methoxy on the A ring of the flavanone.

**Table 3.4-4:** NMR spectroscopic assignments of isolated compound 9

Position	$\delta_{\text{C}}$ , type	$\delta_{\text{H}}$	HMBC
1	O		
2	80.60, CH	5.48, dd	

<b>3</b>	46.45, CH	2.76 (dd), 3.03 (dd)	2, 4, 1'
<b>4</b>	192.31, C		
<b>4a</b>	105.94, C		
<b>5</b>	156.80, C		
<b>6</b>	93.83, CH	6.17, s	4a, 5, 7, 8, 9
<b>7</b>	155.28, C		
<b>8</b>	127.90, C		
<b>8a</b>	153.09, C		
<b>9</b>	56.17, CH <sub>3</sub>	3.78, s 3H	5
<b>1'</b>	140.63, C		
<b>2'/6'</b>	127.57, CH	7.54, m	2, 2', 6'
<b>3'/5'</b>	129.70, CH	7.41, m	1'
<b>4'</b>	129.58, CH	7.36, m	2', 6'

Several of the desired masses, such as 168.05 g/mol, 226.15 g/mol, 318.1 g/mol, and 542.23 g/mol, were in very low concentrations and could not be successfully isolated. However, some compounds such as 542.23 g/mol were partially isolated in other chemotypes. Compound 420.2 ( $m/z = 421.20$ ) was isolated in part but was not fully purified. Preliminary  $^1\text{H}$  NMR resonances and tandem MS/MS data suggest that it may be a prenylated flavanone due to the abundance of methylenes in the  $^1\text{H}$  NMR.

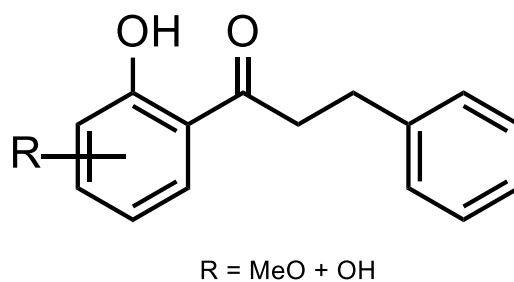


**Figure 3.4-2:** Structure of compound 272.1 with variable substituents on A ring

While the substitution on the A ring could not be fully determined due to impurities in the sample, Compound 272.1 ( $m/z = 273.11$ ) was partially isolated and assigned as a dihydrochalcone with two hydroxyls and a methoxy (Figure 3.4-2).

### 3.5: Chemotype 2

Chemotype 2 consists of 27 parent samples (SI Table S2-1), which could then be further separated into five sub-chemotypes (Figure 3.5-1) based on the variation in compounds within the chemotype. Tandem MS/MS annotation predicted that this chemotype would consist of sesquiterpenes and flavanones, which was supported by the isolation process. Sub-chemotypes 3 and 5 had individual mass lists, and the offspring samples were used for the targeted isolation. Sub-chemotype 4, originally labeled as the Brown Module, was used to isolate a cryptic compound of high interest, which is described in Chapter 4.

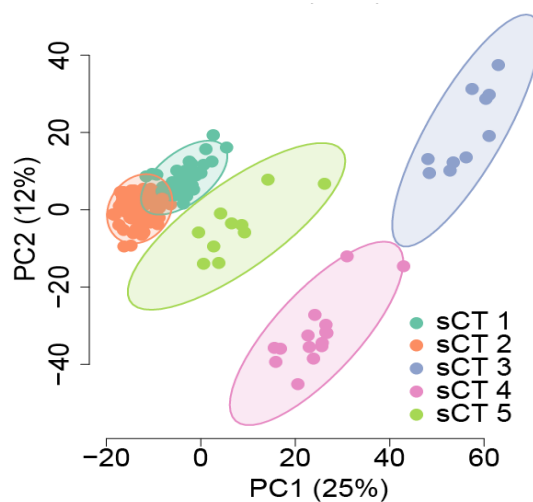


**Figure 3.5-1:** PCA plot of LC-MS entities showing separation into 5 sub-Chemotypes

### 3.5.1: Mass Lists and Initial Isolation Procedures

The desired mass list for Chemotype 2 (Table 3.5-1) differed greatly from the other chemotypes. The mass lists for sub-Chemotype 3 and sub-Chemotype 5 (Tables 3.5-2 and 3.5-3) were much smaller and shared some desired masses in common with the main chemotype. Further, some of the compounds with the desired masses listed in Chemotype 2 were found during the sub-chemotype isolations, most likely due to the excess amount of material.

**Table 3.5-1:** Annotation of chemotype-defining masses for Chemotype 2

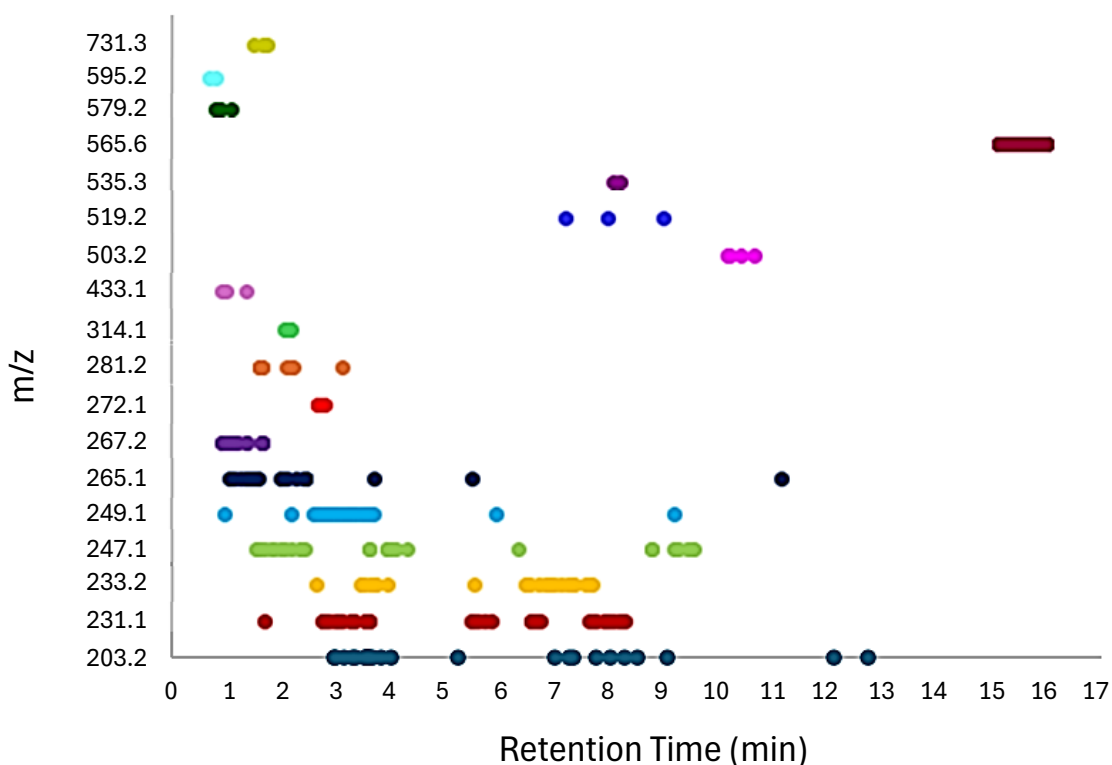
<b>Mass</b>	<b>m/z</b>	<b>RT (min)</b>	<b>Annotation</b>
<b>202.2</b>	203.14	3.48, 7.90	Not isolated, possible fragment of 249 or 231
<b>230.1</b>	231.14	3.22, 5.62, 6.63, 7.97	Partially isolated, sesquiterpene
<b>232.2</b>	233.15	3.62, 7.04	Fully characterized, sesquiterpene (sCT3)
<b>246.1</b>	247.13	1.95, 3.92, 9.20	Not isolated, sesquiterpene
<b>248.1</b>	249.15	3.08	Fully characterized, sesquiterpene (sCT5)
<b>264.1</b>	265.14	1.34, 2.37	Not isolated, sesquiterpene
<b>266.2</b>	267.16	1.23	Not isolated, sesquiterpene
<b>271.2</b>	272.13	2.71	Not isolated
<b>280.1</b>	281.17	1.97	Not isolated, sesquiterpene
<b>313.1</b>	314.14	2.12	Not isolated
<b>432.1</b>	433.11	1.09	Not isolated, flavonoid glycoside
<b>501.2</b>	502.22	8.08	Not isolated
<b>502.2</b>	503.20	10.34	Not isolated, possible conjugate
<b>518.2</b>	519.20	8.04	Partially isolated, conjugate
<b>534.1</b>	535.26	8.14	Not isolated, possible conjugate
<b>564.2</b>	565.56	15.51	Not isolated
<b>576.2</b>	--	--	Not found
<b>578.2</b>	579.17	0.89	Not isolated, flavonoid glycoside
<b>594.2</b>	595.16	0.73	Not isolated, flavonoid glycoside
<b>730.3</b>	731.25	1.63	Not isolated

**Table 3.5-2.** Annotation of chemotype-defining masses for CT2-sCT3

Mass	m/z	RT (min)	Annotation
<b>270.1</b>	271.10	3.39, 6.35, 7.14, 13.68	Fully isolated, flavanone
<b>272.1</b>	273.11	1.73, 6.52	Partially isolated, dihydrochalcone (same as CT1)
<b>297.1</b>	297.11	9.46	Not isolated
<b>542.2</b>	543.27	6.41, 9.50	Partially isolated, conjugate

**Table 3.5-3.** Annotation of chemotype-defining masses for CT2-sCT5

Mass	m/z	RT (min)	Annotation
<b>262.1</b>	263.11	1.45	Not isolated
<b>280.1</b>	281.12	1.41	Not isolated
<b>516.2</b>	517.38	--	Partially isolated, conjugate
<b>530.2</b>	531.27	--	Fully characterized from sCT4, conjugate
<b>550.2</b>	551.21	5.55	Partially isolated, conjugate
<b>730.2</b>	731.22	1.56	Not isolated

**Figure 3.5-2:** Comparison of Chemotype 2 compounds retention times using m/z and RT from tandem MS/MS data

Figures 3.5-2, 3, and 4 show the relationship between the masses and retention times, based on the MS/MS data. Compared to Chemotypes 1 and 3, the retention times of the desired compounds are much shorter. This was determined to correspond to sesquiterpenes, while flavanones and chalcones eluted at a longer retention time.

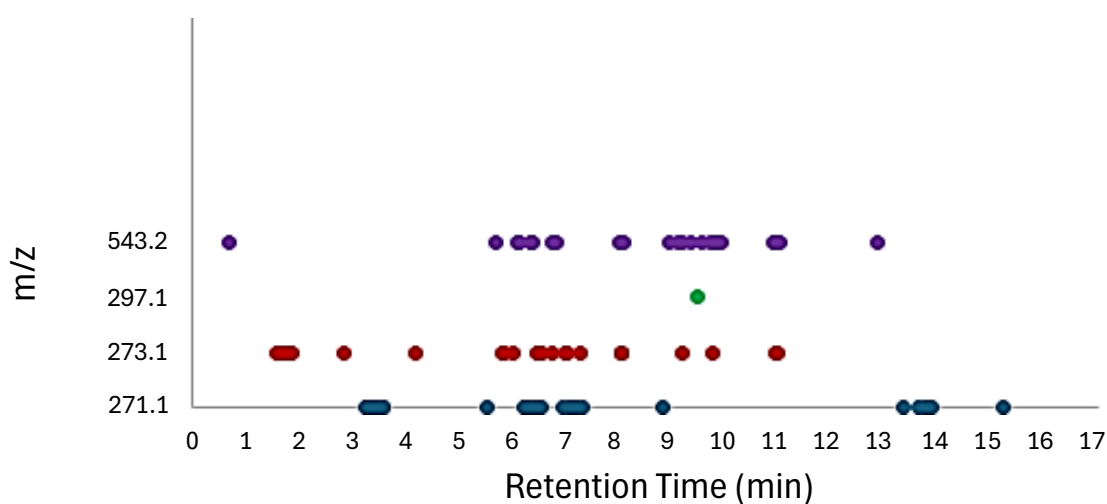


**Figure 3.5-3:** Comparison of CT2-sCT3 compounds retention times using m/z and RT from tandem MS/MS data

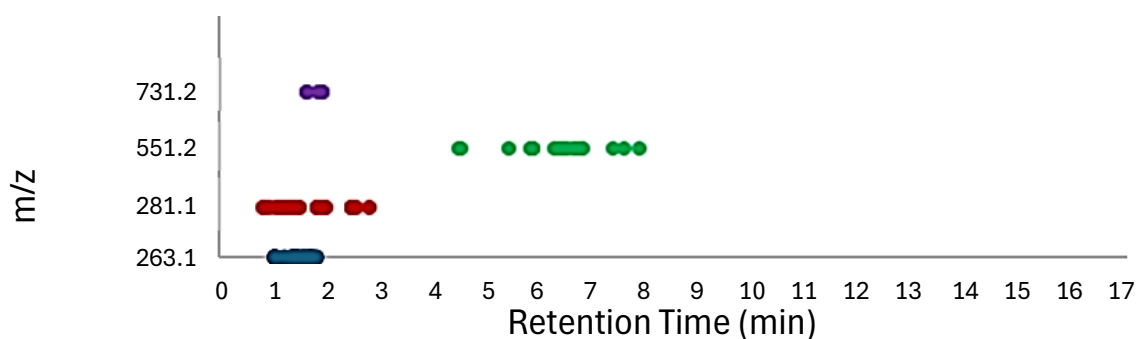


**Figure 3.5-4:** Comparison of CT2-sCT5 compounds retention times using m/z and RT from tandem MS/MS data

For Chemotype 2, the methanol partition of the original extraction (1.83g) was run on Agilent Infinity in 9 runs of 150-225 mg, as described in Table 3.5-4. The 19 pools were based on UV-Vis peaks (254 nm) and MS data.

**Table 3.5-4:** Prep-HPLC method of initial separation for CT2

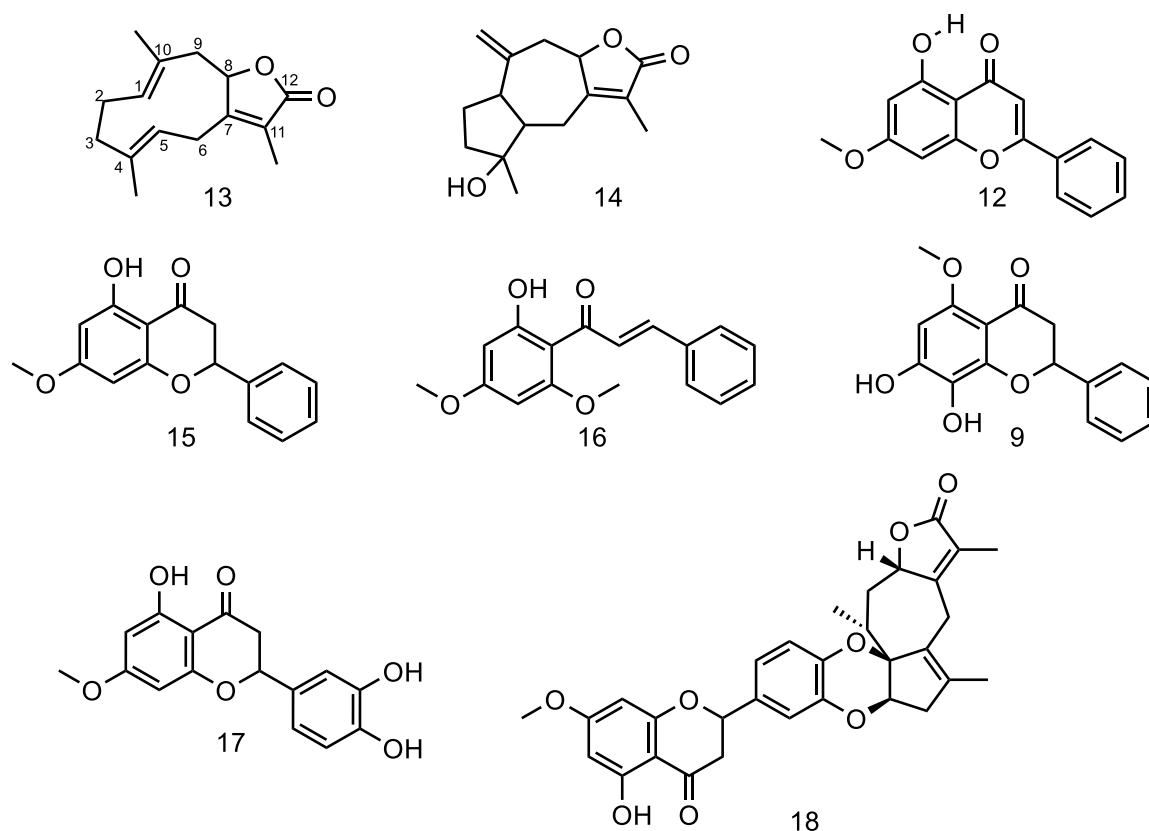
<b>Time (min)</b>	<b>%H<sub>2</sub>O + 0.1%FA</b>	<b>%MeOH +0.1%FA</b>
<b>0</b>	95	5
<b>2</b>	75	25
<b>20</b>	0	100
<b>30</b>	0	100
<b>31</b>	95	5

Chemotype 2-sub-Chemotype 3 consisted of sibling samples POR 35 and 63. The methanol extractions of the plant material resulted in 5.37 g of crude extract. The material was run on Agilent Infinity HPLC in 21 runs of 250-300 mg, using the same method as Chemotype 2. The 24 pools were based on UV-Vis peaks (280 nm) and MS data.

Chemotype 2-sub-Chemotype 5 consisted of sibling samples POR 55 and 97. The methanol extractions resulted in 7.64 g of crude extract. There were 27 runs of Agilent Infinity HPLC of 300 mg, using the same method as Chemotype 2. The 22 pools were based on UV-Vis peaks (280 nm) and MS analysis. Further purification on fractions of interested were completed using a new method and column size, or prep TLC, as outlined in Section 3.3.2.

### ***3.5.2: Characterization and Annotation***

The compounds isolated with full characterization from within Chemotype 2 and the sub-chemotypes are given in Scheme 3.5-1 with annotations given in Table 3.5-5.



**Scheme 3.5-1:** Isolated compounds from CT2, CT2-sCT3 and CT2-sCT5

**Table 3.5-5:** Annotation of compounds isolated from CT2 and sCT3/5

Compound	m/z	RT (min)*	Pool	Name
<b>13</b>	233.15	16.7-17.1	sCT3-P14	7,8,11,11a-Tetrahydro-3,6,10-trimethylcyclodeca[b]furan-2(4H)-one <sup>34</sup>
<b>14</b>	249.15	11.8-12.4	sCT5-P10	(1R,4S,5R,8S)-4-hydroxyguaia-7(11),10(15)-dien-12,8-olide <sup>35</sup>
<b>12</b>	269.08	17.1-17.6	sCT3-P15	5-Hydroxy-7-methoxyflavone
<b>15</b>	271.10	11.4-13.2	sCT3-P09/10	5-Hydroxy-7-methoxyflavanone <sup>33</sup>
<b>16</b>	285.10	17.7-18.2	sCT3-P16	2'-hydroxy-4',6'-dimethoxy chalcone <sup>36</sup>

<b>9</b>	287.11	9.8-10.2	sCT3-P07	5-Methoxy-7,8-dihydroxyflavanone
<b>17</b>	303.2	--	sCT4	5,3',4'-trihydroxy-7-methoxy-flavanone <sup>37</sup>
<b>18</b>	531.2	--	sCT4	Novel compound, conjugate

Compounds **13** and **14** were determined to be sesquiterpenes by SCXRD analysis (Section 3.5.3).

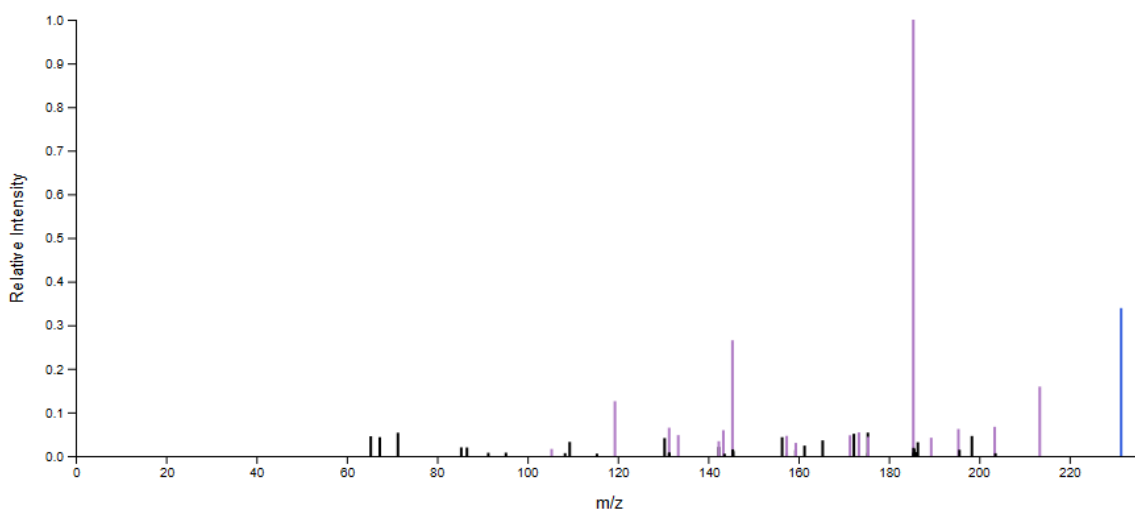
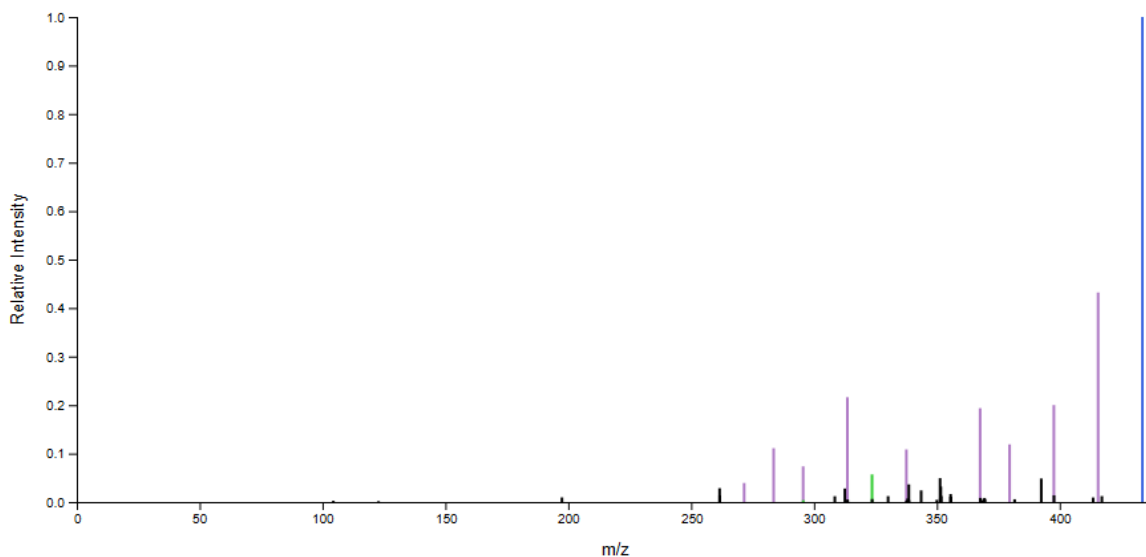


**Figure 3.5-5:** Tandem MS/MS of mixture containing 231.1380 m/z

Figure 3.5-5 shows an example of the MS/MS fractionation of 231.1380 m/z; the fractionation pathway suggests a sesquiterpene, which is supported by the crude <sup>1</sup>H NMR spectrum. Further, a possible fractionation loss of CO would lead to a m/z of 203.1421, a desired mass that was not isolated.

While not able to be fully characterized due to lack of material purity, compounds related to masses 502.2 and 518.2 are hypothesized to be flavanone/sesquiterpene

conjugates based on the similarity of the  $^1\text{H}$  NMR data to the fully characterized conjugate **18** described in Chapter 4.



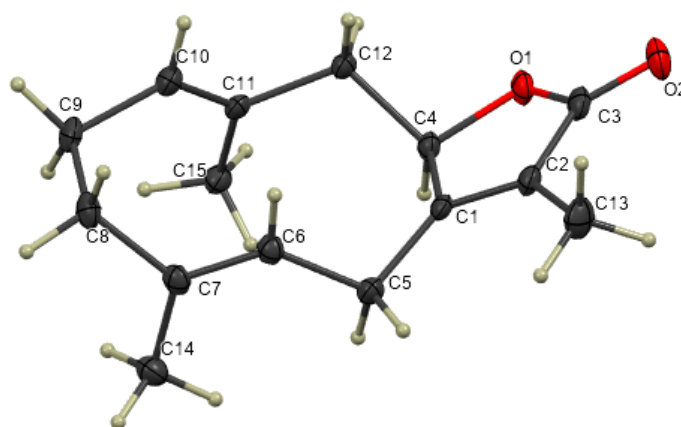
**Figure 3.5-6:** Tandem MS/MS spectrum of mixture containing 433.1127 m/z

Figure 3.5-6 shows an example MS/MS spectra of 433.1127 m/z and is hypothesized to be flavonoid C-glycoside based on the tandem MS/MS data. Other compounds such as 579.1676 m/z and 595.1628 m/z are likewise hypothesized to be flavonoid C-glycosides based on the tandem MS/MS data. This leads to most of the desired masses in Chemotype 2 to be either flavonoid glycosides or sesquiterpenes.

### 3.5.3: *SCXRD analysis of compounds isolated*

X-ray crystallographic data was collected at low temperature (100 K) using a Bruker SMART Apex CCD diffractometer with Mo  $K\alpha$  radiation. Data was refined using SHELXL-2019/1 (Sheldrick, 2019). The X-ray intensity data were measured ( $\lambda = 0.71073 \text{ \AA}$ ).

Compound **13** was previously isolated by Stahl and coworkers in 1972.<sup>34</sup> The crystal was grown in methanol. **13** crystallized in the monoclinic space group  $P2_1/n$  with one molecule in the asymmetric unit. The compound was determined to be 7,8,11,12-Tetrahydro-4,10,11-trimethylcyclodeca[*b*]furan-2(4*H*)-one. The centrosymmetric nature of the space group verifies that this sample is racemic, and the other enantiomer is generated by the inversion center. Table 3.5-6 provides crystallographic information.



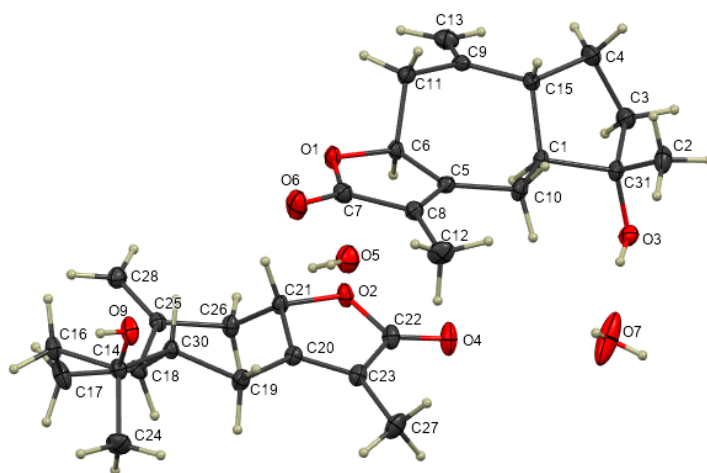
**Figure 3.5-7:** Crystal structure of Compound 13

The integration of the data using a monoclinic unit cell yielded a total of 22828 reflections to a maximum  $\theta$  angle of  $31.00^\circ$  (0.69 Å resolution), of which 4040 were independent (average redundancy 5.650, completeness = 100.0%,  $R_{\text{int}} = 21.97\%$ ,  $R_{\text{sig}} = 9.80\%$ ) and 3505 (86.76%) were greater than  $2\sigma(F_2)$ . The final cell constants are based upon the refinement of the XYZ-centroids of 9913 reflections above  $20\sigma(I)$  with  $4.604^\circ < 2\theta < 64.61^\circ$ . The calculated minimum and maximum transmission coefficients (based on crystal size) are 0.7223 and 0.7464. The final anisotropic full-matrix least-squares

refinement on F2 with 157 variables converged at R1 = 5.91%, for the observed data and wR2 = 16.89% for all data. The goodness-of-fit was 1.060. The largest peak in the final difference electron density synthesis was 0.615 e-/Å<sup>3</sup> and the largest hole was -0.391 e-/Å<sup>3</sup> with an RMS deviation of 0.090 e-/Å<sup>3</sup>.

Compound **14** was previously isolated by Liu and coworkers in 2013.<sup>35</sup> The compound crystallized in P2<sub>1</sub> space group with two molecules in the asymmetric unit connected by hydrogen bonding by two water molecules that co-crystallized. Both were determined to be (1R,4S,5R,8S)-4- hydroxyguaia-7(11),10(15)-dien-12,8-olide. Table 3.5-6 gives crystallographic information.

**Figure 3.5-8:** Crystal structure of compound 14



The integration of the data using a monoclinic unit cell yielded a total of 36594 reflections to a maximum  $\theta$  angle of 31.00° (0.69 Å resolution), of which 8928 were independent (average redundancy 4.099, completeness = 99.9%, R<sub>int</sub> = 1.94%, R<sub>sig</sub> = 1.77%) and 8597 (96.29%) were greater than 2 $\sigma$ (F2). The final cell constants are based

upon the refinement of the XYZ-centroids of reflections above  $20 \sigma(I)$ . The calculated minimum and maximum transmission coefficients (based on crystal size) are 0.7223 and 0.7464. The goodness-of-fit was 1.072. The largest peak in the final difference electron density synthesis was  $0.367 \text{ e}/\text{\AA}^3$  and the largest hole was  $-0.255 \text{ e}/\text{\AA}^3$  with an RMS deviation of  $0.044 \text{ e}/\text{\AA}^3$ .

**Table 3.5-6:** Crystallographic data of compounds

	<b>13</b>	<b>14</b>
<b>Chemical formula</b>	C <sub>15</sub> H <sub>20</sub> O <sub>2</sub>	C <sub>15</sub> H <sub>20</sub> O <sub>3</sub>
<b>fw g/mol</b>	232.31	248.32
<b>Crystal system</b>	monoclinic	monoclinic
<b>Space group</b>	P <sub>2</sub> <sub>1</sub> /n	P <sub>2</sub> <sub>1</sub>
<b><i>a</i> (Å)</b>	7.4075(7)	7.5981(3)
<b><i>b</i> (Å)</b>	16.2013(14)	14.2287(5)
<b><i>c</i> (Å)</b>	10.6142(9)	13.1751(4)
<b><math>\beta</math> (deg)</b>	96.0290(10)	99.4770(10)
<b>Volume (Å<sup>3</sup>)</b>	1266.78(19)	1404.93(9)
<b>Z</b>	4	2
<b>Temperature (K)</b>	100(2)	100(2)
<b>R1 (I&gt;2<math>\sigma</math>(I))</b>	0.0593	0.0337
<b>wR1 (I&gt;2<math>\sigma</math>(I))</b>	0.1619	0.0879
<b>Flack</b>	--	0.05(13)

### 3.6: Chemotype 3

Chemotype 3 consisted of 22 parent samples (SI Table S2-1). The mass list (Table 3.6-1) resembles Chemotype 1, and the MS/MS data show that there are several compounds in common between the chemotypes. Based on tandem MS/MS, the chemotype was expected to consist of methylated chalcones and flavanones. Of the 18 desired masses, 7 were fully characterized, while others were partially characterized or were found in other chemotypes. In addition, some compounds, such as 284.1 g/mol,

were isolated from a variety of pools and retention times but proved to be the same compound.

**Table 3.6-1:** Annotation of chemotype-defining masses for Chemotype 3

Mass	m/z	RT (min)*	Annotation
<b>168.05</b>	169.05	3.54	Not isolated, same compound as CT1
<b>226.15</b>	227.07	1.79, 4.38	Not isolated, same compound as CT1
<b>270.1</b>	271.10	3.32, 5.51, 6.30, 13.33	Flavanone and chalcone, fully isolated
<b>272.1</b>	273.11	6.44	Dihydrochalcone, partially isolated
<b>284.1</b>	285.11	2.80, 5.12, 8.37	Flavanone and chalcone, fully isolated
<b>286.1</b>	287.09	4.33, 8.58	Flavanone, not isolated, possibly same as CT1
<b>300.1</b>	301.11	3.12, 6.41, 8.97	Flavanone, fully isolated
<b>302.1</b>	303.12	6.63	Not isolated
<b>314.1</b>	315.12	4.20, 7.23	Flavanone and chalcone, fully isolated
<b>316.13</b>	317.10	3.44, 4.83, 7.49	Not isolated
<b>318.1</b>	319.22	8.14	Not isolated
<b>420.2</b>	421.20	8.23, 11.23	partially isolated, flavanone
<b>422.2</b>	423.22	8.91, 11.92	Not isolated
<b>450.24</b>	451.21	11.45	Not isolated
<b>470.25</b>	471.19	4.31	Not isolated
<b>472.26</b>	473.27	10.96	Not isolated
<b>520.28</b>	521.29	9.55	Not isolated, possible conjugate
<b>554.16</b>	555.16	6.30, 7.72	Not isolated, possible conjugate

The parent samples in Chemotype 3 were previously separated into two separate chemotypes. Initial isolation efforts used the samples previously known as Chemotype 4 and methods can be found in SI S1.2.

The general isolation procedure began as described in Section 3.3.1 and 3.3.2. The crude extract (1.64 g) was separated by 8 runs on Agilent Infinity HPLC+MS. After a pilot run, the method as described in Table 3.6-2 was used for runs 2-8. Thirty-three pools were created based on UV-Vis and MS analysis.

**Table 3.6-2:** Prep-HPLC method of initial isolations of Chemotype 3

Time (min)	%H <sub>2</sub> O + 0.1%FA	%MeOH +0.1%FA
0	95	5
2	75	25
22	0	100
32	0	100
33	95	5

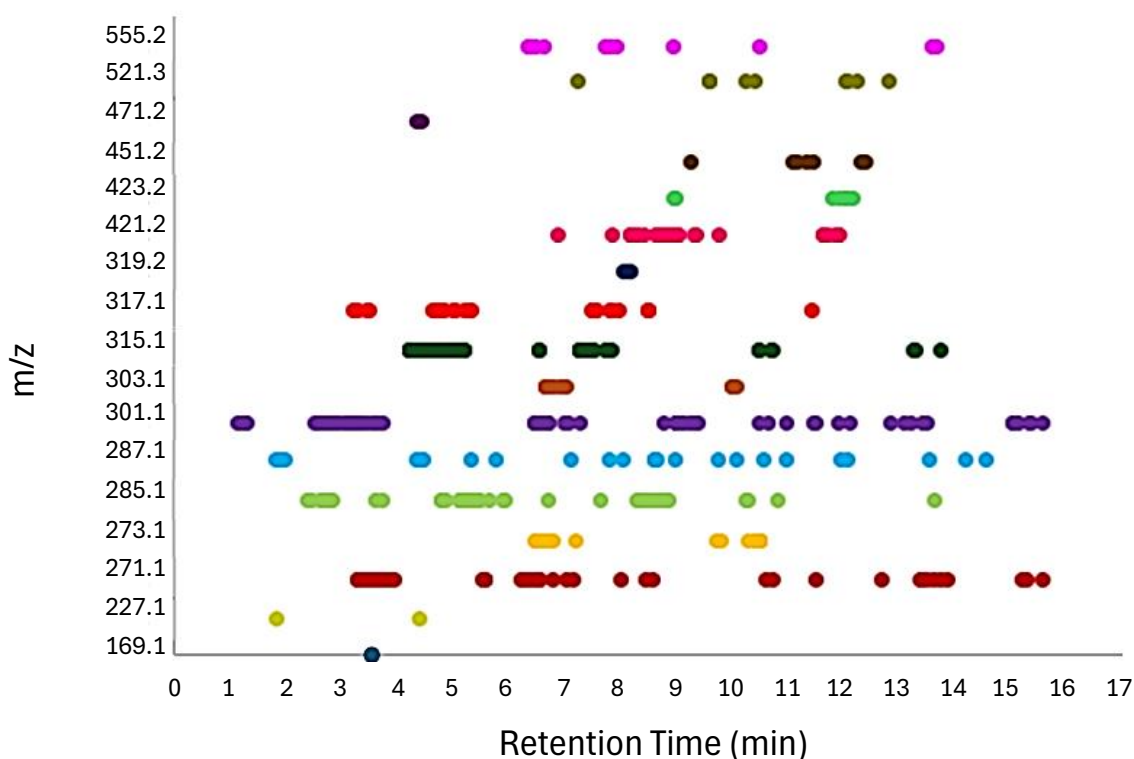
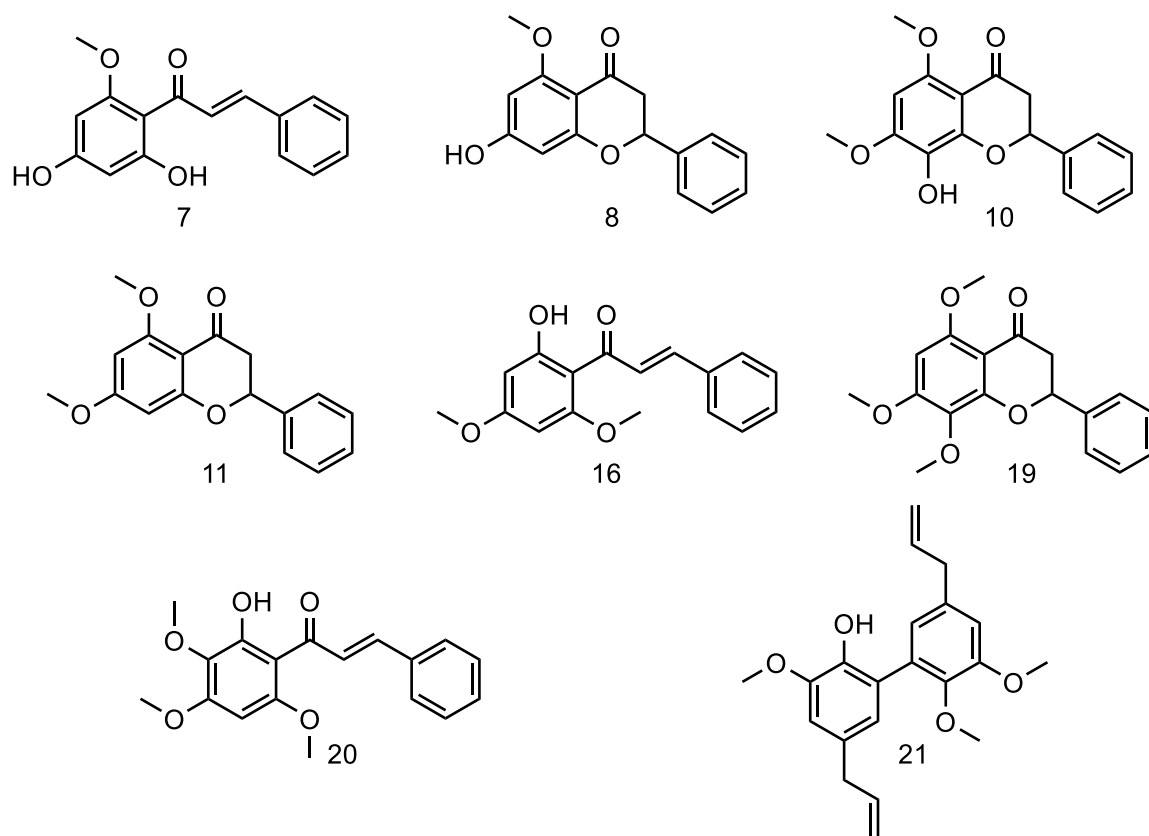
**Figure 3.6-1:** Comparison of CT3 compounds retention times using m/z and RT from tandem MS/MS data

Figure 3.6-1 shows the relationship between the masses and retention times, based on the tandem MS/MS data. As displayed in this figure, there are multiple compounds with the same mass, which correspond to flavanones and chalcones. Based on the fully characterized compounds, as well as the MS/MS and <sup>1</sup>H NMR analysis of partially characterized compounds, the chemotypes consists of mostly methylated flavanones and

chalcones. Scheme 3.6-1 gives the fully characterized compounds, with annotation in Table 3.6-3.



**Scheme 3.6-1:** Isolated compounds from Chemotype 3

**Table 3.6-3:** Annotation of isolated compounds from CT3

Compound	m/z	RT (min) <sup>a</sup>	Pool	Name
<b>7</b>	271	16.4-17.3	18	2',4'-Dihydroxy-6'-methoxychalcone
<b>8</b>	271	--	Yz13 <sup>b</sup>	5-Methoxy-7-hydroxyflavanone
<b>10</b>	301	11.2-11.6	10	8-Hydroxy-5,7-dimethoxyflavanone
<b>11</b>	285	15.4-16.4	17	5,7-Dimethoxyflavanone
<b>16</b>	285	18.7-19.6	21	2'-Hydroxy-4',6'-dimethoxy chalcone
<b>19</b>	315	13.1-14.4	13/14	5,7,8-Trimethoxyflavanone <sup>38</sup>
<b>20</b>	315	17.2-18.2	19	2'-hydroxy-3',4',6'-trimethoxychalcone <sup>39</sup>
<b>21</b>	341	--	Yz14 <sup>b</sup>	Dehydrodieugenol monomethyl ether <sup>40</sup>

<sup>a</sup> Average retention time based on HPLC of POR\_100MeOH\_CT4\_Inf\_Run4

<sup>b</sup> Previously part of Chemotype 4, method used is described in SI S1.2

Many of the compounds fully isolated are the same compounds isolated in Chemotype 1. The presence of these masses on the chemotype-defining mass list for two Chemotypes points to a variation between the chemotypes that is not solely related to the structure of the compounds.

### **3.7: Conclusions and future work**

The variation in metabolomic profile must be annotated to gain a clear picture of biosynthetic relationships. The annotations of the major compounds can be used to determine the class of compounds that have not yet been isolated, using the MS/MS analysis available as well as common  $^1\text{H}$  NMR resonances. An important aspect of this project is the reproducibility of isolation, as the sibling samples can be used to repeat procedures.

While many compounds were isolated and full characterization was used to confirm structure, many more of the chemotype-defining masses remain unknown. Sub-chemotype 4, sub-Chemotypes 3 and sub-Chemotype 5 proved that using sibling samples for isolation gives the same metabolic analysis expected from the parent samples. If a cryptic natural product is found through LC-MS/MS analysis, it is possible to use only individuals containing the cryptic natural product to increase the chances of isolating the desired compound. Several analogs of compound **18** were found, but none were fully isolated. These compounds in particular are important to isolate since they could highlight the variation that influenced the separation of chemotype 2 into the sub-chemotypes. By focusing on the individuals containing these compounds, the amount of material necessary for full characterization could be isolated.

With the initial methods for prep-HPLC determined, further separations will be faster and easier to predict. This could allow for an increase in compound isolation. Using the comparison of  $m/z$  and retention times, such as in Figure 3.6-1, would highlight the pools that contain the desired masses, as well as the presence of isomers. This could prevent the replication of isolated compounds, even between chemotypes.

## Chapter 4: A metabolomics guided discovery of cryptic flavanone sesquiterpene conjugate raduladioxanolide

### 4.1: A highly heritable cryptic compound

The chemical heritability experiment, as described in Chapter 3, observed a series of cryptic compounds that were highly heritable, but only present in a few parents and their offspring. While each compound was found within Chemotype 2, the sub-chemotypes were correlated with a different cryptic compound. The different compounds and their expected chemical formulas are expressed in Table 4.1-1.

**Table 4.1-1:** Cryptic compounds in Chemotype 2

<b>Chemotype 2 Sub- Chemotype</b>	<b>Compound mass</b>	<b>Chemical formula</b>	<b>Difference in Chemical Formula from 530</b>
<b>sCT3</b>	542.2312	$C_{33}H_{34}O_7$	$530 - OH + CH_3 + CH_2$
<b>sCT4</b>	530.1931	$C_{31}H_{30}O_8$	--
<b>sCT5</b>	550.2206	$C_{31}H_{34}O_9$	$530 + H_2O + H_2$

Each compound had similar fractionation patterns, consisting of a flavanone and terpene fragment. The difference between these cryptic compounds defines the separation of the sub-chemotypes within chemotype 2. It was decided to prioritize compound 530.1931 g/mol due to its abundance, although it was only found in three individuals and their



to an 8.75%/min increase of acetonitrile over 4 mins, followed by a 3.75%/min increase of acetonitrile over 16 mins, then held at 100% acetonitrile for 20 mins (Table 4.3-2).

**Table 4.3-1.** HPLC method of Brown Module Sibling Yamazan Run 1

<b>Time (min)</b>	<b>%H<sub>2</sub>O</b>	<b>%ACN</b>
<b>Start</b>	95	5
<b>3</b>	95	5
<b>13</b>	0	100
<b>63</b>	0	100

**Table 4.3-2.** HPLC method of Brown Module Sibling Yamazan Run 5-26

<b>Time (min)</b>	<b>%H<sub>2</sub>O</b>	<b>%ACN</b>
<b>Start</b>	95	5
<b>4</b>	60	40
<b>20</b>	0	100
<b>40</b>	0	100

Runs 1-4 were pooled together and stored, as the fractionation was not the same as the later runs. Fractions from runs 5-21 were pooled together to create 11 master pools based on UV-Vis absorption peaks and retention times, labeled BrMo\_Sib\_Yz\_pool\_#. Runs 22-26 were stored separately, since the fractionation was changed through the saturation of the column. Through LC-MS/MS analysis, it was determined that compound 531 appeared to be in Pools 8 and 9, which were then combined to be separated further on Agilent Infinity prep-HPLC+MS. Despite the large peaks present in the chromatography, the fractions containing 531 m/z were in a valley of the chromatograph. From the original 8 g, the fractions consisted of 680 mg. This pool was further purified using Agilent

Infinity prep-HPLC + MS, using the method described in Table 4.3-3 (C18 21.2 mm x 150 mm). The six runs were pooled together based on UV-Vis absorption peaks and MS.

**Table 4.3-3.** Prep-HPLC of BrMo\_Sib\_Yz\_8/9\_Inf\_Run1-6

<b>Time (min)</b>	<b>%H<sub>2</sub>O</b>	<b>%ACN</b>
<b>Start</b>	60	40
<b>20</b>	0	100
<b>26</b>	0	100
<b>27</b>	60	40

Based on the MS data of the HPLC fractions, compound 531 was found only in BrMo\_Sib\_Yz\_8/9\_Inf\_Pool10, which showed no obvious UV-Vis absorption peaks and amounted to 23 mg. This material was further separated on a preparatory TLC plate (1000 microns silica), using 50/50 hexane/ethyl acetate plus 0.5% formic acid. There were three major bands on the plate; each was scraped, sonicated and extracted with 25 mL of ethyl acetate, and dried under high vacuum. Using <sup>1</sup>H NMR spectroscopy and GC-MS, compound 531 was determined to be in the top band (B3). A mass of 2.9 mg of purified material was isolated.

#### **4.4: Structure determination: raduladioxanolid**

Due to the small amount of material, a Shegemi NMR tube (CDCl<sub>3</sub>) was used to increase the concentration of the sample for NMR analysis. Additional LC-MS/MS and IM analysis proved this sample consisted of multiple isomers, which was confirmed as a ~ 1:1.2 mixtures by ion mobility and <sup>1</sup>H NMR analysis. The chemical formula was calculated to be C<sub>31</sub>H<sub>30</sub>O<sub>8</sub> with 17 degrees of unsaturation. Fractionation in the tandem MS/MS suggested a flavanone component and a terpene component.

The  $^{13}\text{C}$  and  $^1\text{H}$  NMR spectra (Table 4.4-1) contained resonances for two carbonyl carbons ( $\delta_{\text{C}}$  195.96 and 174.22) and a methoxy carbon ( $\delta_{\text{C}}$  55.7,  $\delta_{\text{H}}$  3.80). The carbon at  $\delta_{\text{C}}$  195.96 (C-4') is correlated with a diastereotopic methylene (C-3') [ $\delta_{\text{H}}$  2.78 (m) and 3.06 (m),  $\delta_{\text{C}}$  43.26] through HMBC. Further HMBC analysis shows coupling between H-3' $\alpha/\beta$  and an oxygenated C-2' [ $\delta_{\text{C}}$  78.9,  $\delta_{\text{H}}$  5.31 (t)], as well as an aromatic quaternary carbon C-1'' [ $\delta_{\text{C}}$  130.79]. This corresponds to an O-CH-CH<sub>2</sub>-CO-system in the C ring of a flavanone, with correlation to a benzene ring typical of the B ring.

A singlet at  $\delta_{\text{H}}$  12.02 had no cross peaks in HSQC and was therefore assigned as a phenol. The position downfield suggests hydrogen bonding to the carbonyl, and for it to be a substituent on C-5', which is supported by the HMBC correlations of quaternary C-5', quaternary C-4a', and aromatic C-6' [ $\delta_{\text{C}}$  164.16, 103.13, 95.12 respectively]. Two doublets in an a/b pattern at  $\delta_{\text{H}}$  6.05 and 6.07 correspond to aromatic methines on the A ring of the flavanone (C-8' and C-6' respectively). Both methine contain a cross peak in common with a methoxy CH<sub>3</sub> [ $\delta_{\text{C}}$  55.7,  $\delta_{\text{H}}$  3.80 (s, 3H)], which corresponds to quaternary carbon C-7' at  $\delta_{\text{C}}$  167.98. Overlapping peaks in the aromatic region of the  $^1\text{H}$  NMR spectrum correspond to three protons [ $\delta_{\text{H}}$  6.83-6.95], which suggests a tri-substituted benzene as the B ring of a flavanone. This is supported by the HMBC cross peaks between these aromatic peaks and C-1'', as well as two oxygenated quaternary carbons C-3'' and C-4'' [ $\delta_{\text{C}}$  14.55 and 146.30 respectively]. This accounts for 10 of the 17 degrees of unsaturation.

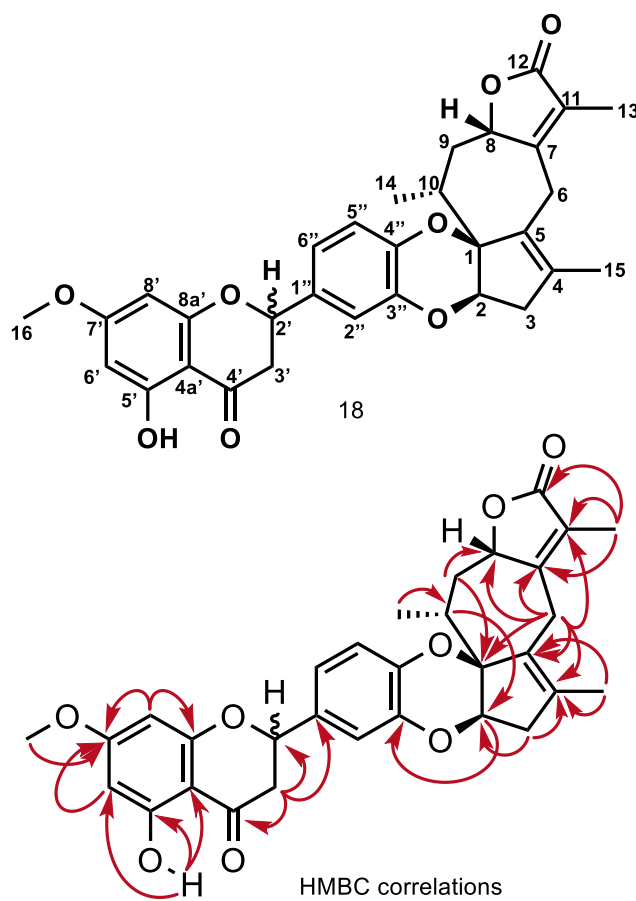
The HMBC shows a cross peak between C-3'' and a proton at  $\delta_{\text{H}}$  4.79, which the HSQC proves is two overlapping methine peaks [ $\delta_{\text{C}}$  73.72 and 82.78]. This was supported by analyzing the  $^1\text{H}$  NMR spectrum in acetone- $d_6$ , which separated the peaks. The remaining carbon resonances include a carbonyl, three methyl groups, three diastereotopic methylenes, a methine, four quaternary carbons and an oxygenated quaternary carbon. This part of the compound was hypothesized to be a sesquiterpene lactone with three rings in a 6-6-5 membered structure. However, similarity in the  $^1\text{H}$  NMR resonances with sesquiterpene americanolide G, particularly with the presence of a methine at  $\delta_{\text{H}}$  4.79 (H-8), suggested that the structure is in a 5-7-5 membered ring structure.<sup>41</sup>

Starting at the lactone, the carbonyl C-12 [ $\delta_{\text{C}}$  174.22] shared a cross-peak with a methyl group H-13 [ $\delta_{\text{C}}$  8.60,  $\delta_{\text{H}}$  1.88]. H-13 is HMBC correlated with two quaternary carbons C-11 and C-7 [ $\delta_{\text{C}}$  120.90 and 160.05 respectively]. Diastereotopic methylene group H-6 $\alpha/\beta$  [ $\delta_{\text{C}}$  22.6,  $\delta_{\text{H}}$  2.91/3.58] correlated with C-7 and C-11 through HMBC. The lack of cross-peaks in COSY demonstrates that this methylene is surrounded by quaternary carbons.

HMBC correlation between diastereotopic methylene H-9 $\alpha/\beta$  [ $\delta_{\text{H}}$  1.39, 2.09] and C-8 [ $\delta_{\text{C}}$  82.78] was supported by the COSY coupling with the methine H-8 [ $\delta_{\text{H}}$  4.79]. COSY coupling between the final methine H-10 [ $\delta_{\text{H}}$  2.36] and one of the protons of the methylene group [ $\delta_{\text{H}}$  1.39], as well as the HMBC correlation with the methyl group C-14 and oxygenated quaternary carbon C-1 [ $\delta_{\text{C}}$  16.64 and 89.19 respectively] support the

hypothesis of the 7-membered ring. H-6 correlates through HMBC with two additional quaternary carbons C-5 and C-4 [ $\delta_C$  139.17 and 131.9 respectively]. H-3 $\alpha/\beta$  [ $\delta_H$  2.50, 2.51  $\delta_C$  39.69] and methyl group H-15 [ $\delta_H$  1.73,  $\delta_C$  14.63] both correlate with C-4 through HMBC. In addition, H-3 $\alpha/\beta$  correlate with an oxygenated C-2 [ $\delta_C$  73.72], the methine connected to the benzene ring of the flavanone. With two oxygenated carbons on the 5-membered ring, as well as two oxygenated carbons on the benzene ring, it is suggested that the oxygens form a bridge between the two sections of the conjugate. This is supported by this final 6-membered ring satisfying the degrees of unsaturation. The final structure is the novel flavanone-sesquiterpene conjugate raduladioxanolide.

**Table 4.4-1:** NMR assignments for isolated compound 18



Position	$\delta_C$ , type	$\delta_H$	HMBC
1	89.19, C		
2	73.72, CH	4.79 (t)	3"
3	39.69, CH <sub>2</sub>	2.51, 2.50 (m)	2, 4
4	131.9, C		
5	139.17, C		
6	22.6, CH <sub>2</sub>	2.91 (d), 3.58 (dd)	1, 4, 5, 7, 8, 11
7	160.05, C		
8	82.78, CH	4.79 (t)	
9	35.83, CH <sub>2</sub>	1.39, 2.09 (m)	1, 8
10	36.16, CH	2.36 (m)	2
11	120.9, C		
12	174.22, C		
13	8.6, CH <sub>3</sub>	1.88 (s)	7, 11, 12
14	16.64, CH <sub>3</sub>	1.21 (dd)	10
15	14.63, CH <sub>3</sub>	1.73 (s)	4, 5
16	55.7, CH <sub>3</sub>	3.80 (s)	7'
1'	O		
2'	78.9, CH	5.31 (m)	
3'	43.26, CH <sub>2</sub>	2.78 (ddd), 3.06 (m)	2', 4', 1"
4'	195.96, C		
4a'	103.13, C		
5'	164.16, C		
6'	95.12, CH	6.07 (d)	7'
7'	167.98, C		
8'	94.26, CH	6.05 (d)	7', 8a'
8a'	162.79, C		
1"	130.79, C		
2"	114.19, CH	6.83-6.95 (m)	1", 3", 4", 5", 6"
3"	140.55, C		
4"	146.3, C		
5"	116.47, CH	6.83-6.95 (m)	1", 2", 3", 4", 6"
6"	118.89, CH	6.83-6.95 (m)	1", 2", 3", 4", 5"

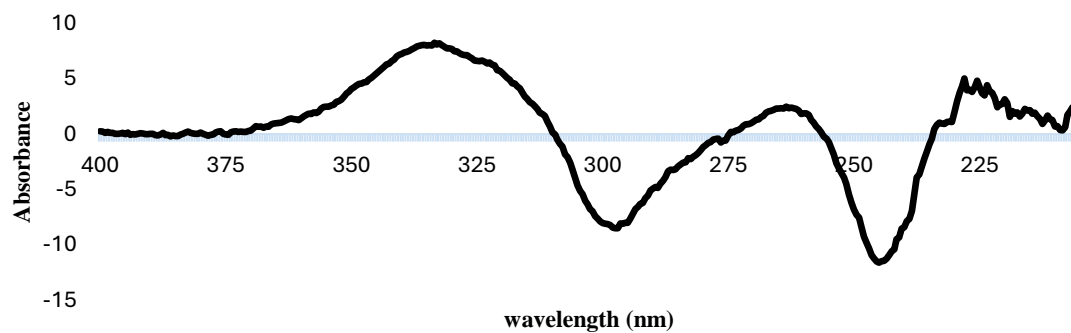


**Figure 4.4-1:** Circular Dichroism Spectrum of Raduladioxanolide 0.625 mmol/mL

The CD spectrum of Figure 4.4-1 supports the presence of chiral centers in the compound. This analysis is currently being used to calculate the configuration of the compound through DFT calculations.

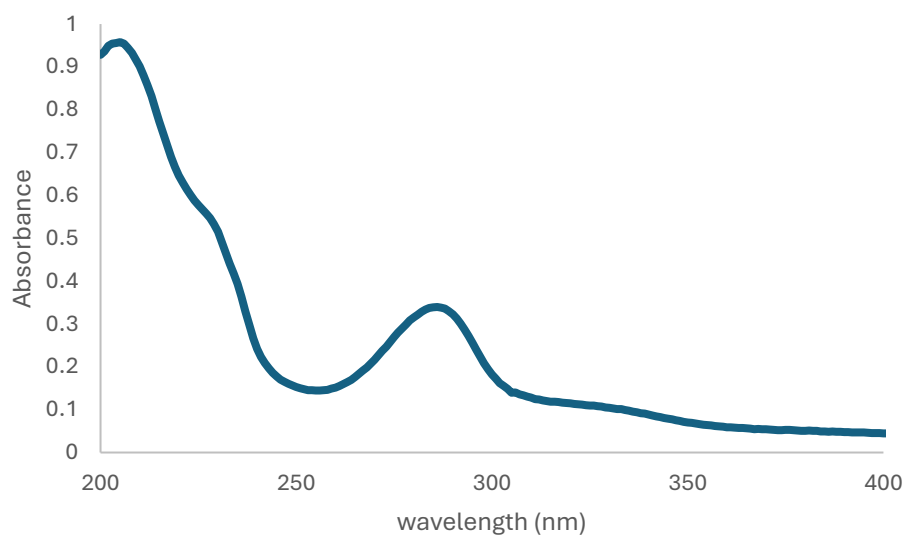
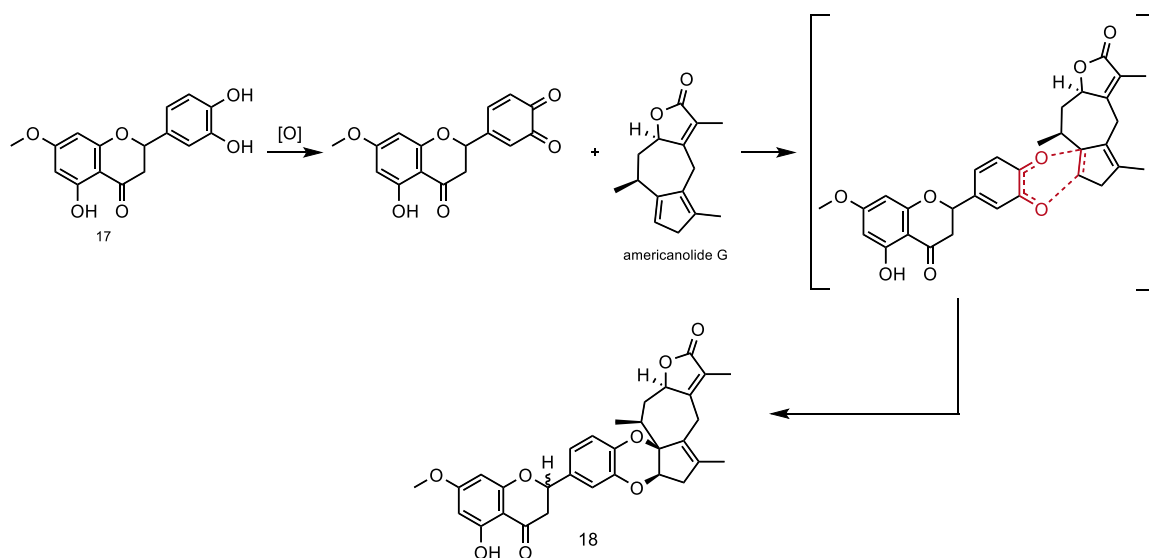


**Figure 4.4-2:** UV-Vis absorbance spectrum of compound 18 in acetonitrile.

The UV-Vis spectrum from 200 nm to 400 nm of isolated compound 18 in acetonitrile has a  $\lambda_{\text{max}}$  of 286 nm (Figure 4.4-2).

#### 4.5: Proposed biosynthetic pathway of raduladioxanolide

Fractionation in tandem MS/MS suggested the conjugation of a flavanone and guaianolide sesquiterpene. The neutral loss of the flavanone moiety was found to be 302.1 m/z. Compound **17** was isolated from same individuals as **18** and is hypothesized to be the biosynthetic precursor, along with a sesquiterpene. Although not isolated, the sesquiterpene moiety is hypothesized to be like americanolide G, which has a similar structure to isolated compounds **13** and **14**.



**Scheme 4.5-1:** Proposed biosynthetic pathway of isolated compound **18**

The proposed biosynthetic pathway given in Scheme 4.5-1 starts with the oxidation of **17** to the orthoquinone of the flavanone. This is followed by a Diels-Alder cycloaddition between the orthoquinone and trisubstituted double bond of the sesquiterpene to produce raduladioxanolide (**18**).

#### 4.6: Conclusions

The untargeted metabolic analysis of the individuals focused on the variation of metabolites. This compound was only observed in three parent individuals, yet it proved to be highly heritable in their offspring. The function of the compound, as well as why a carbon-expensive compound would be continually generated, is still unknown. This isolation demonstrates how an untargeted metabolic analysis can lead to the targeted isolation of cryptic natural products, despite the minor abundance.

The future isolation of the additional cryptic compounds observed in the other sub-chemotypes (Table 4.1-1) will give insight into the variation that led to the separation of chemotype 2 into sub-chemotypes. Compound **18** consisted of two fragments: a flavanone with  $m/z = 303$  and a sesquiterpene with  $m/z = 231$ . Compound  $m/z = 551$  from sCT5 shows a similar fractionation of  $m/z = 303$  and loss of 248.1408, which could be related to Compound **14**, a sesquiterpene with the same  $m/z$  isolated from sCT5. The difference between the sesquiterpene of 248 g/mol and the sesquiterpene of raduladioxanolide (**18**) is that 248 g/mol has one less double bond and has an alcohol. This difference would match the difference in chemical formula between 531  $m/z$  and 551  $m/z$ . The difference in chemical formula between raduladioxanolide and  $m/z = 543$  infers that the unknown compound does not have as many phenol groups, has an additional methyl group, and has an additional methine. The methine could point to the additional of a terminal alkene, as seen in sesquiterpene compound **14**. While the fragments of the conjugates can be hypothesized, the connection between them cannot be

determined through MS analysis. The biosynthetic method could highlight the variation that grouped these compounds into the sub-chemotypes.

## Chapter 5: Using single crystal x-ray diffraction in natural product chemistry

### 5.1: The struggle of absolute configuration

While NMR spectroscopy is a powerful tool in structure determination, the molecular structure cannot always be completely derived from this method. In many cases, the overlap of peaks, especially in the aliphatic region of the spectrum, can convolute the full elucidation of an unknown structure. An example of this limitation is in the isolation and structure determination of a series of alkenylphenols from *Piper sanctifelicis* (*Piper scintillans*). This study describes 10 alkenylphenols compounds to establish the pattern of their allocation within the plant and to observe what their ecological role may be.<sup>42</sup>

The ten compounds were first observed in the GC-MS of ripe infructescence, as seen in Figure 5.1-1. Further isolation using flash column chromatography and preparatory TLC allowed for the isolation of the major components.

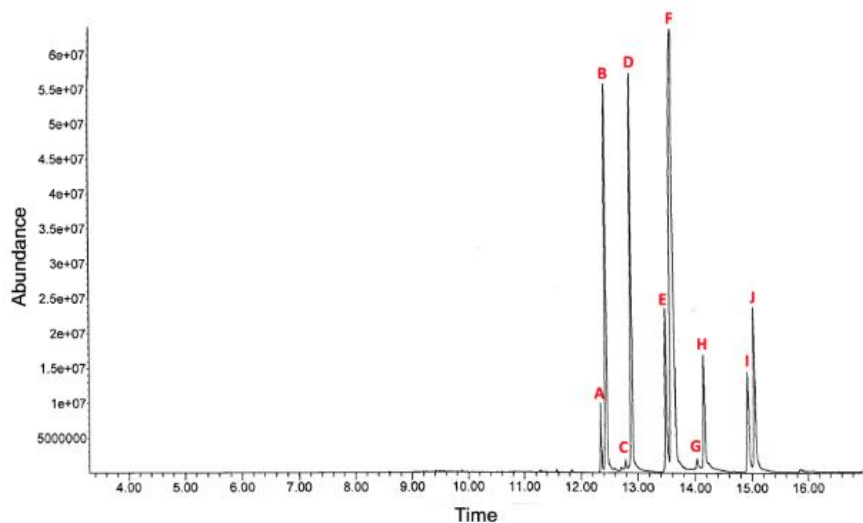
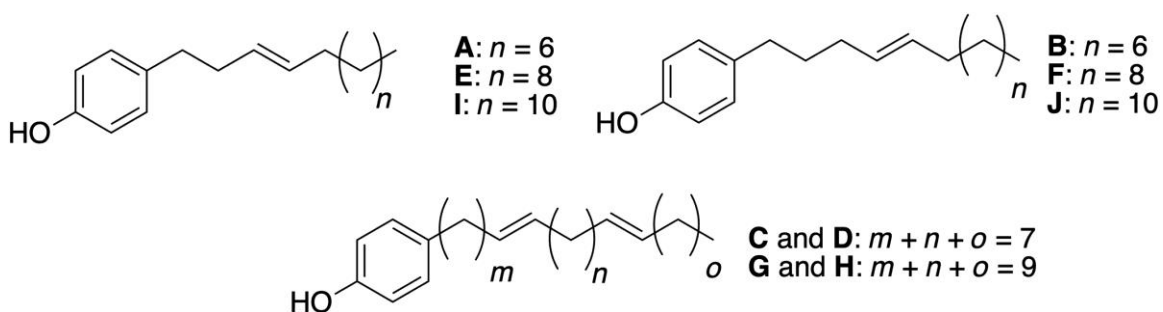


**Figure 5.1-1:** GMCS of metabolites in crude extract of *P. scintillans*

The analysis of the molecular ion of the peaks gave the length of the alkenyl chain, with the compounds differing in the placement of the double bond. The placement of the double bond was tentatively assigned based on EI-MS fractionation and literature reviews, and the structures were assigned as shown in Scheme 5.1-1.



**Scheme 5.1-1:** Isolated compounds from *P. scintillans*. The placement of the double bonds is tentatively assigned with 2D NMR spectroscopy, EI-MS fractionation and literature reviews.

In this case, the placement of the double bond could not be determined through 2D NMR spectroscopy due to the abundance of peaks in the aliphatic region of the spectrum.

Applying methods for x-ray diffraction on a hard to crystallize or oil natural product, such as through the crystalline sponge method or co-crystallization, is required to determine the absolute structure of these compounds.

## 5.2: Crystalline Sponge Method

The crystalline sponge (CS) method provides a route to using SCXRD with non-crystalline compounds without changing the stereochemistry by coordinating with a metal or other heavy atom and requiring magnitudes less material. In this method, a natural product compound on the nanogram to microgram scale is incorporated into a

porous metal-organic framework (MOF), producing an ordered assembly that is analyzed by SCXRD to provide the molecular and absolute structure of the natural product in a single experiment. In 2013, the Fujita group introduced this method for natural products using the MOF  $[(\text{ZnI}_2)_3\text{-(tpt)}_2 \cdot x(\text{cyclohexane})]_n$  where tpt=2,4,6-tris(4-pyridyl)-1,3,5-triazine).<sup>18</sup> The hydrophobic pores of the MOF absorb the guest compound through thermodynamically favored solvent-guest exchange; the guest compounds are ordered within the pores through weak intermolecular interactions, ranging from Van der Waals to hydrogen bonding interactions.<sup>43</sup>

To synthesize the MOF, zinc iodide dissolved in methanol, then carefully layered on top of a mixture of TPT and chloroform. As the layers diffuse together, crystals are grown in various morphologies, with the desired unit cell of monoclinic C. The crystals are then moved to soak in cyclohexane to exchange the incorporated methanol with cyclohexane. The unit cell of  $[(\text{ZnI}_2)_3\text{-(tpt)}_2 \cdot x(\text{cyclohexane})]_n$  (Figure 5.2-1) shows the encapsulated cyclohexane molecule.

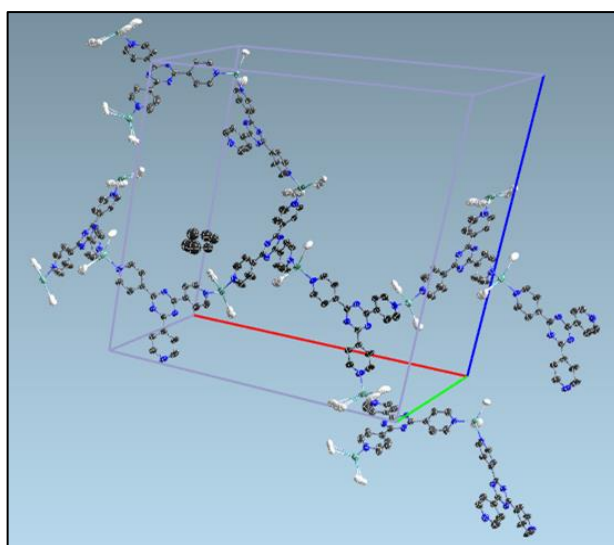


**Figure 5.2-1:** Unit cell of MOF  $[(\text{ZnI}_2)_3\text{-(tpt)}_2 \cdot x(\text{cyclohexane})]_n$

Unfortunately, all attempts at incorporating a natural product as a guest compound were unsuccessful. Changes in solvent used, temperature, surface area available for crystallization, and changes in concentration were attempted. One of the most common issues was the quick degradation of the crystals.<sup>44</sup> Further, the inherent positions disorder around the  $ZnI_2$  units of the MOF, and the presence of multiple disordered solvent molecules complicates the determination of the structure of guest compounds.

In 2019, de Poel and coworkers presented a MOF consisting of lanthanide metals ( $Eu(NO_3)_3 \cdot 6H_2O$ ) linked with carboxylic acid containing ligand  $H_3BTB$  (1,3,5-benzenetri benzoic acid) that was stable in a variety of solvents, including water<sup>45</sup>. In my expansion of this work, several lanthanide salts were used, including dysprosium (III) chloride, gadolinium (III) chloride, terbium (III) nitrate hexahydrate, and europium (III) nitrate hexahydrate. Like the previous crystalline sponge method, a solution of the ligand in dimethylformamide was layered on top of a solution of the lanthanide salt in water.

The  $(\text{Eu}(\text{NO}_3)_3 \cdot 6\text{H}_2\text{O})$  and  $\text{GdCl}_3$  crystals showed the most promise (Figure 5.2-2); however, the incorporation of guest natural products was unsuccessful.

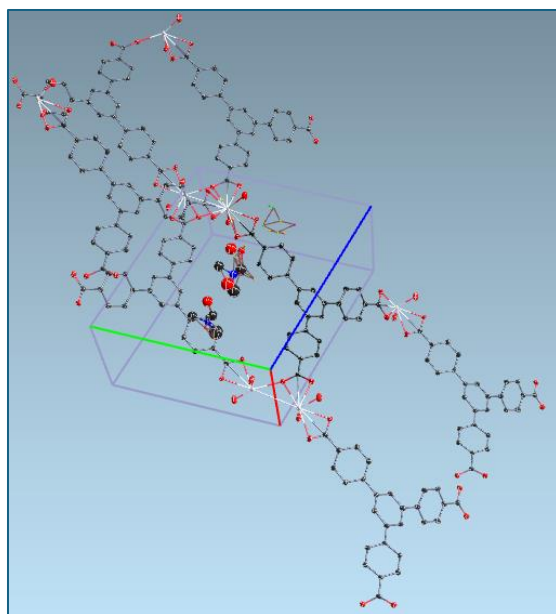
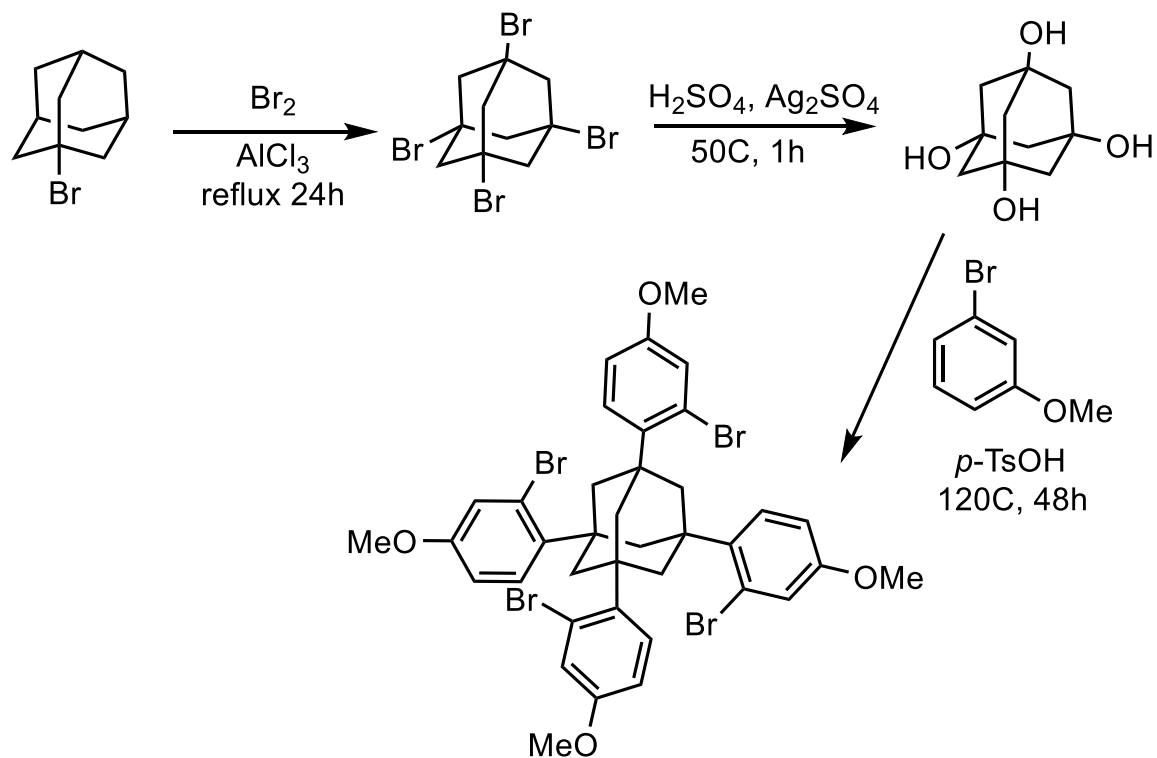


**Figure 5.2-2:** Crystal structure of the unit cell of Eu MOF

### 5.3: Co-crystallization Method

To bypass the issue with guest incorporation, the co-crystallization method introduces the natural product during the crystallization process.<sup>19</sup> The novel compound 1,3,5,7-tetrakis(2-bromo-4-methoxyphenyl)adamantane (TBro) was proven to interact well with saturated hydrocarbons, thus expanding the scope of this method. To create the inclusion complexes, the finely powdered crystalline chaperone is added to the liquid analyte and a crystal grows over several days.<sup>46</sup> Scheme 5.3-1 shows the synthesis of TBro (**25**) from 1-bromoadamantane and bromine.<sup>19,47</sup>



**Scheme 5.3-1:** Synthesis of compound 25

A liquid natural product, (-)(-) $\alpha$ -pinene, was chosen to be used for a proof-of-concept experiment. Pinene was successfully encapsulated by the chaperone, as seen in Figure 5.3-1.

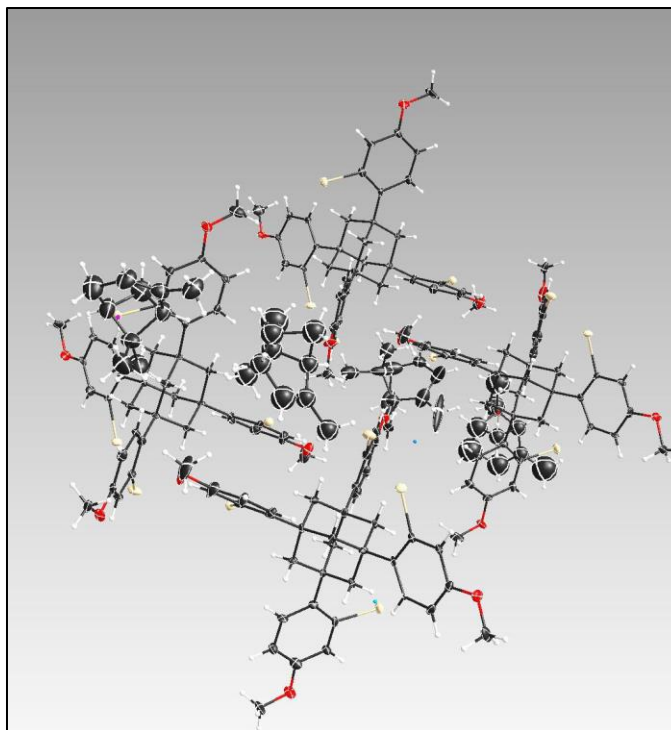
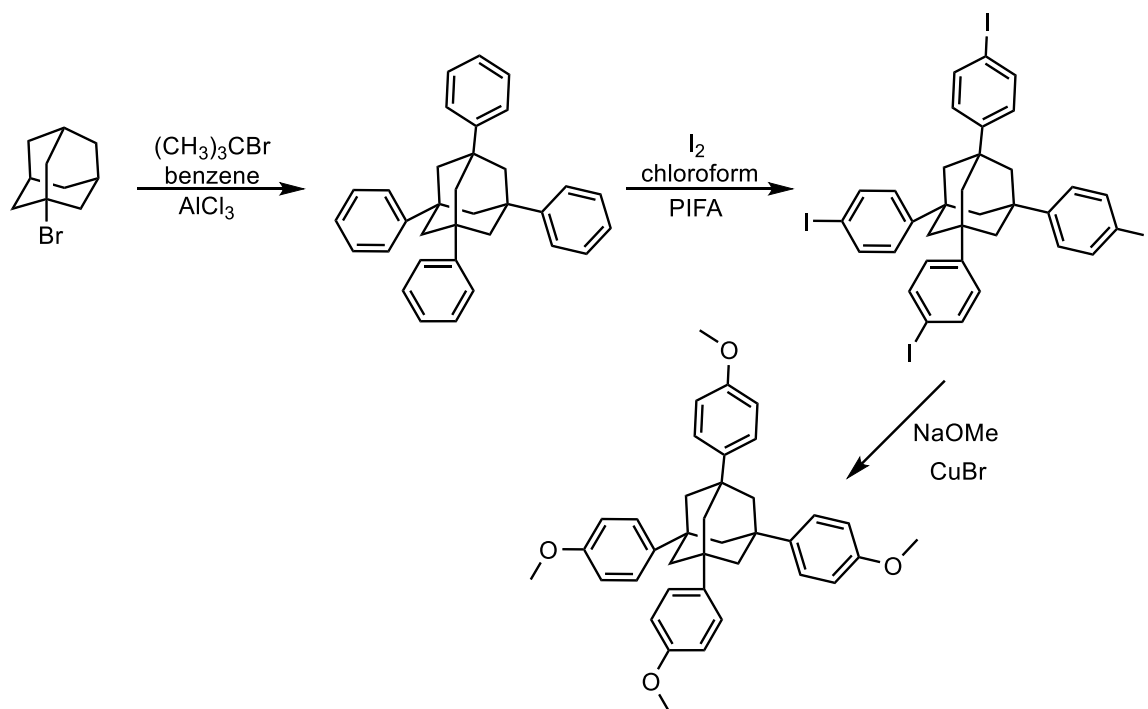


**Figure 5.3-1:** Crystal structure of TBro with pinene guest

However, all attempts to encapsulate a non-liquid guest were unsuccessful; in these attempts, only the solvent was captured. At this point, it was decided to synthesize other analogs that may allow for better guest encapsulation. Following the method described by Zhu and co-workers, 1,3,5,7-tetrakis(4-iodophenyl)adamantane (TIodoA) and 1,3,5,7-tetrakis(4-methoxyphenyl)adamantane (TMeOA) were synthesized (Scheme 5.3-2).<sup>48,49</sup>



### Scheme 5.3-2: Synthesis of TlodoA and TPA

This updated method allows for the direct synthesis of 1,3,5,7-tetraphenyladamantane (TPA) from 1-bromoadamantane at much higher yields. Future works include using Ullmann Coupling to synthesize more analogs from TlodoA, but the issue of TPA solubility has not yet been overcome.<sup>50</sup>

### 5.4: Conclusions

While these methods did not prove fruitful for the non-crystalline natural products attempted, the potential remains. The synthesis of TlodoA provides a starting point for multiple analogs to be created. Using different instrumentation, such as a dual-source XRD, could allow for the observation of guest molecules in smaller crystals. Focusing on the solubility issues of TPA could lead to new adamantane analogs, using a combination of Suzuki and Ullman Coupling.

## References

- (1) Dyer, L. A.; Philbin, C. S.; Ochsenrider, K. M.; Richards, L. A.; Massad, T. J.; Smilanich, A. M.; Forister, M. L.; Parchman, T. L.; Galland, L. M.; Hurtado, P. J.; Espeset, A. E.; Glassmire, A. E.; Harrison, J. G.; Mo, C.; Yoon, S.; Pardikes, N. A.; Muchoney, N. D.; Jahner, J. P.; Slinn, H. L.; Shelef, O.; Dodson, C. D.; Kato, M. J.; Yamaguchi, L. F.; Jeffrey, C. S. Modern Approaches to Study Plant–Insect Interactions in Chemical Ecology. *Nat. Rev. Chem.* **2018**, *2* (6), 50–64. <https://doi.org/10.1038/s41570-018-0009-7>.
- (2) Atanasov, A. G.; Waltenberger, B.; Pferschy-Wenzig, E.-M.; Linder, T.; Wawrosch, C.; Uhrin, P.; Temml, V.; Wang, L.; Schwaiger, S.; Heiss, E. H.; Rollinger, J. M.; Schuster, D.; Breuss, J. M.; Bochkov, V.; Mihovilovic, M. D.; Kopp, B.; Bauer, R.; Dirsch, V. M.; Stuppner, H. Discovery and Resupply of Pharmacologically Active Plant-Derived Natural Products: A Review. *Biotechnol. Adv.* **2015**, *33* (8), 1582–1614. <https://doi.org/10.1016/j.biotechadv.2015.08.001>.
- (3) Hartmann, T. The Lost Origin of Chemical Ecology in the Late 19th Century. *Proc. Natl. Acad. Sci.* **2008**, *105* (12), 4541–4546. <https://doi.org/10.1073/pnas.0709231105>.
- (4) Fraenkel, G. S. The Raison d’Être of Secondary Plant Substances. *Science* **1959**, *129* (3361), 1466–1470.
- (5) Newman, D. J.; Cragg, G. M. Natural Products as Sources of New Drugs over the Nearly Four Decades from 01/1981 to 09/2019. *J. Nat. Prod.* **2020**, *83* (3), 770–803. <https://doi.org/10.1021/acs.jnatprod.9b01285>.
- (6) Uckele, K. A.; Jahner, J. P.; Tepe, E. J.; Richards, L. A.; Dyer, L. A.; Ochsenrider, K. M.; Philbin, C. S.; Kato, M. J.; Yamaguchi, L. F.; Forister, M. L.; Smilanich, A. M.; Dodson, C. D.; Jeffrey, C. S.; Parchman, T. L. Phytochemistry Reflects Different Evolutionary History in Traditional Classes versus Specialized Structural Motifs. *Sci. Rep.* **2021**, *11* (1), 17247. <https://doi.org/10.1038/s41598-021-96431-3>.
- (7) Glassmire, A. E.; Carson, W. P.; Smilanich, A. M.; Richards, L. A.; Jeffrey, C. S.; Dodson, C. D.; Philbin, C. S.; Humberto, G. L.; Dyer, L. A. Multiple and Contrasting Pressures Determine Intraspecific Phytochemical Variation in a Tropical Shrub. *Oecologia* **2023**, *201* (4), 991–1003. <https://doi.org/10.1007/s00442-023-05364-3>.
- (8) Han, E. J.; Lee, S. R.; Townsend, C. A.; Seyedsayamdost, M. R. Targeted Discovery of Cryptic Eneidyne Natural Products via FRET-Coupled High-Throughput Elicitor Screening. *ACS Chem. Biol.* **2023**, *18* (8), 1854–1862. <https://doi.org/10.1021/acscchembio.3c00281>.
- (9) Scherlach, K.; Hertweck, C. Mining and Unearthing Hidden Biosynthetic Potential. *Nat. Commun.* **2021**, *12* (1), 3864. <https://doi.org/10.1038/s41467-021-24133-5>.
- (10) Cannell, R. J. P. *Natural Products Isolation*; Springer Science & Business Media, 1998.
- (11) Sticher, O. Natural Product Isolation. *Nat. Prod. Rep.* **2008**, *25* (3), 517–554. <https://doi.org/10.1039/B700306B>.
- (12) Bumpus, S. B.; Evans, B. S.; Thomas, P. M.; Ntai, I.; Kelleher, N. L. A Proteomics Approach to Discovering Natural Products and Their Biosynthetic Pathways. *Nat. Biotechnol.* **2009**, *27* (10), 951–956. <https://doi.org/10.1038/nbt.1565>.

- (13) Qiu, F.; Imai, A.; McAlpine, J. B.; Lankin, D. C.; Burton, I.; Karakach, T.; Farnsworth, N. R.; Chen, S.-N.; Pauli, G. F. Dereplication, Residual Complexity, and Rational Naming: The Case of the Actaea Triterpenes. *J. Nat. Prod.* **2012**, *75* (3), 432–443. <https://doi.org/10.1021/np200878s>.
- (14) Marston, A.; Hostettmann, K. Modern Separation Methods. *Nat. Prod. Rep.* **1991**, *8* (4), 391–413. <https://doi.org/10.1039/NP9910800391>.
- (15) Chervin, J.; Stierhof, M.; Tong, M. H.; Peace, D.; Hansen, K. Ø.; Urgast, D. S.; Andersen, J. H.; Yu, Y.; Ebel, R.; Kyeremeh, K.; Paget, V.; Cimpan, G.; Wyk, A. V.; Deng, H.; Jaspars, M.; Tabudravu, J. N. Targeted Dereplication of Microbial Natural Products by High-Resolution MS and Predicted LC Retention Time. *J. Nat. Prod.* **2017**, *80* (5), 1370–1377. <https://doi.org/10.1021/acs.jnatprod.6b01035>.
- (16) Kellogg, J. J.; Todd, D. A.; Egan, J. M.; Raja, H. A.; Oberlies, N. H.; Kvalheim, O. M.; Cech, N. B. Biochemometrics for Natural Products Research: Comparison of Data Analysis Approaches and Application to Identification of Bioactive Compounds. *J. Nat. Prod.* **2016**, *79* (2), 376–386. <https://doi.org/10.1021/acs.jnatprod.5b01014>.
- (17) Richards, L. A.; Oliveira, C.; Dyer, L. A.; Rumbaugh, A.; Urbano-Muñoz, F.; Wallace, I. S.; Dodson, C. D.; Jeffrey, C. S. Shedding Light on Chemically Mediated Tri-Trophic Interactions: A 1H-NMR Network Approach to Identify Compound Structural Features and Associated Biological Activity. *Front. Plant Sci.* **2018**, *9*.
- (18) Inokuma, Y.; Yoshioka, S.; Ariyoshi, J.; Arai, T.; Hitora, Y.; Takada, K.; Matsunaga, S.; Rissanen, K.; Fujita, M. X-Ray Analysis on the Nanogram to Microgram Scale Using Porous Complexes. *Nature* **2013**, *495* (7442), 461–466. <https://doi.org/10.1038/nature11990>.
- (19) Krupp, F.; Frey, W.; Richert, C. Absolute Configuration of Small Molecules by Co-Crystallization. *Angew. Chem. Int. Ed.* **2020**, *59* (37), 15875–15879. <https://doi.org/10.1002/anie.202004992>.
- (20) Baumgartner, B.; Erdelmeier, C. A. J.; Wright, A. D.; Rali, T.; Sticher, O. An Antimicrobial Alkaloid from *Ficus Septica*. *Phytochemistry* **1990**, *29* (10), 3327–3330. [https://doi.org/10.1016/0031-9422\(90\)80209-Y](https://doi.org/10.1016/0031-9422(90)80209-Y).
- (21) Dätwyler, P.; Ott-Longoni, R.; Schöpp, E.; Hesse, M. Über Juliprosin, Ein Weiteres Alkaloid Aus *Prosopis juliflora*. DC. 180. Mitteilung Über Organische Naturstoffe. *Helv. Chim. Acta* **1981**, *64* (6), 1959–1963. <https://doi.org/10.1002/hlca.19810640629>.
- (22) Snider, B. B.; Neubert, B. J. Syntheses of Ficuseptine, Juliprosine, and Juliprosopine by Biomimetic Intramolecular Chichibabin Pyridine Syntheses. *Org. Lett.* **2005**, *7* (13), 2715–2718. <https://doi.org/10.1021/ol050931l>.
- (23) Razzaq, A.; Sadia, B.; Raza, A.; Khalid Hameed, M.; Saleem, F. Metabolomics: A Way Forward for Crop Improvement. *Metabolites* **2019**, *9* (12), 303. <https://doi.org/10.3390/metabo9120303>.
- (24) Patel, M. K.; Pandey, S.; Kumar, M.; Haque, M. I.; Pal, S.; Yadav, N. S. Plants Metabolome Study: Emerging Tools and Techniques. *Plants* **2021**, *10* (11), 2409. <https://doi.org/10.3390/plants10112409>.
- (25) Dixon, R. A.; Gang, D. R.; Charlton, A. J.; Fiehn, O.; Kuiper, H. A.; Reynolds, T. L.; Tjeerdema, R. S.; Jeffery, E. H.; German, J. B.; Ridley, W. P.; Seiber, J. N.

- Applications of Metabolomics in Agriculture. *J. Agric. Food Chem.* **2006**, *54* (24), 8984–8994. <https://doi.org/10.1021/jf061218t>.
- (26) Kuhlisch, C.; Pohnert, G. Metabolomics in Chemical Ecology. *Nat. Prod. Rep.* **2015**, *32* (7), 937–955. <https://doi.org/10.1039/C5NP00003C>.
- (27) Kim, H. K.; Choi, Y. H.; Verpoorte, R. NMR-Based Plant Metabolomics: Where Do We Stand, Where Do We Go? *Trends Biotechnol.* **2011**, *29* (6), 267–275. <https://doi.org/10.1016/j.tibtech.2011.02.001>.
- (28) Falcone Ferreyra, M. L.; Rius, S.; Casati, P. Flavonoids: Biosynthesis, Biological Functions, and Biotechnological Applications. *Front. Plant Sci.* **2012**, *3*. <https://doi.org/10.3389/fpls.2012.00222>.
- (29) Chadwick, M.; Trewin, H.; Gawthrop, F.; Wagstaff, C. Sesquiterpenoids Lactones: Benefits to Plants and People. *Int. J. Mol. Sci.* **2013**, *14* (6), 12780–12805. <https://doi.org/10.3390/ijms140612780>.
- (30) Krishna, B. M.; Chaganty, R. B. Cardamonin and Alpinetin from the Seeds of *Alpinia Speciosa*. *Phytochemistry* **1973**, *12* (1), 238. [https://doi.org/10.1016/S0031-9422\(00\)84672-5](https://doi.org/10.1016/S0031-9422(00)84672-5).
- (31) Chantrapromma, K.; Seechamnaturakit, V.; Pakawatchai, C.; Chantrapromma, S.; Chinnakali, K.; Fun, H.-K. 2,3-Dihydro-8-Hydroxy-5,7-Dimethoxy-2-Phenyl-4H-1-Benzopyran-4-One and 3,3,6-Tribromo-2,3-Dihydro-8-Hydroxy-5,7-Dimethoxy-2-Phenyl-4H-1-Benzopyran-4-One. *Acta Crystallogr. C* **1998**, *54* (2), iuc9800001. <https://doi.org/10.1107/S0108270198099843>.
- (32) Narasimhachari, N.; Seshadri, T. R. Insecticidal Properties and Chemical Constitution. *Proc. Indian Acad. Sci. - Sect. A* **1948**, *27* (2), 128. <https://doi.org/10.1007/BF03170884>.
- (33) Rao, K. V.; Seshadri, T. R. A Note on the Constitution of Alpinetin. *Proc. Indian Acad. Sci. - Sect. A* **1946**, *23* (4), 213. <https://doi.org/10.1007/BF03170939>.
- (34) Stahl, E.; Datta, S. N. Neue sesquiterpenoide Inhaltsstoffe der Gundelrebe (*Glechoma hederacea* L.). *Justus Liebigs Ann. Chem.* **1972**, *757* (1), 23–32. <https://doi.org/10.1002/jlac.19727570105>.
- (35) Liu, H.-Y.; Ran, X.-H.; Gong, N.-B.; Ni, W.; Qin, X.-J.; Hou, Y.-Y.; Lü, Y.; Chen, C.-X. Sesquiterpenoids from *Chloranthus Multistachys*. *Phytochemistry* **2013**, *88*, 112–118. <https://doi.org/10.1016/j.phytochem.2012.12.002>.
- (36) Wang, Q.; Cui, W.; Yang, J.; Yang, B. Development of a Concise Synthesis of the Flavonoid Chrysin. *J. Chem. Res.* **2015**, *39* (5), 300–302. <https://doi.org/10.3184/174751915X14307337733513>.
- (37) Morales, G.; Paredes, A.; Sierra, P.; Loyola, L. A. CYTOTOXICITY , SCAVENGING AND LIPID PEROXIDATION - INHIBITING ACTIVITIES OF 5,3',4'-Trihy-Droxy - 7 - Methoxyflavanone ISOLATED FROM HAPLOPAPPUS RIGIDUS. *J. Chil. Chem. Soc.* **2009**, *54* (2), 105–107. <https://doi.org/10.4067/S0717-97072009000200001>.
- (38) Moshi, M.; Joseph, C.; Innocent, E.; Nkunya, M. In Vitro Antibacterial and Antifungal Activities of Extracts and Compounds from *Uvaria Scheffleri*. *Pharm. Biol.* **2004**, *42* (4–5), 269–273. <https://doi.org/10.1080/13880200490511035>.

- (39) Lien, T. P.; Porzel, A.; Schmidt, J.; Van Sung, T.; Adam, G. Chalconoids from *Fissistigma Bracteolatum*. *Phytochemistry* **2000**, *53* (8), 991–995. [https://doi.org/10.1016/S0031-9422\(99\)00570-1](https://doi.org/10.1016/S0031-9422(99)00570-1).
- (40) de Oliveira, C. R.; Ledvina, Z. D.; Leonard, M. D.; Odoh, S. O.; Dodson, C. D.; Jeffrey, C. S. Isolation of New Neolignans and an Unusual Meroterpenoid from Piper Cabagranum. *Front. Nat. Prod.* **2024**, *2*. <https://doi.org/10.3389/fntpr.2023.1332436>.
- (41) Rodríguez, A. D.; Boulanger, A. New Guaiane Metabolites from the Caribbean Gorgonian Coral, Pseudopterogorgia Americana. *J. Nat. Prod.* **1997**, *60* (3), 207–211. <https://doi.org/10.1021/np9605201>.
- (42) Maynard, L. D.; Slinn, H. L.; Glassmire, A. E.; Matarrita-Carranza, B.; Dodson, C. D.; Nguyen, T. T.; Burroughs, M. J.; Dyer, L. A.; Jeffrey, C. S.; Whitehead, S. R. Secondary Metabolites in a Neotropical Shrub: Spatiotemporal Allocation and Role in Fruit Defense and Dispersal. *Ecology* **2020**, *101* (12), e03192. <https://doi.org/10.1002/ecy.3192>.
- (43) Wada, N.; Kersten, R. D.; Iwai, T.; Lee, S.; Sakurai, F.; Kikuchi, T.; Fujita, D.; Fujita, M.; Weng, J.-K. Crystalline-Sponge-Based Structural Analysis of Crude Natural Product Extracts. *Angew. Chem. Int. Ed.* **2018**, *57* (14), 3671–3675. <https://doi.org/10.1002/anie.201713219>.
- (44) Ramadhar, T. R.; Zheng, S.-L.; Chen, Y.-S.; Clardy, J. Analysis of Rapidly Synthesized Guest-Filled Porous Complexes with Synchrotron Radiation: Practical Guidelines for the Crystalline Sponge Method. *Acta Crystallogr. Sect. Found. Adv.* **2015**, *71* (1), 46–58. <https://doi.org/10.1107/S2053273314019573>.
- (45) de Poel, W.; Tinnemans, P.; Duchateau, A. L. L.; Honing, M.; Rutjes, F. P. J. T.; Vlieg, E.; de Gelder, R. The Crystalline Sponge Method in Water. *Chem. – Eur. J.* **2019**, *25* (65), 14999–15003. <https://doi.org/10.1002/chem.201904174>.
- (46) Rami, F.; Nowak, J.; Krupp, F.; Frey, W.; Richert, C. Co-Crystallization of an Organic Solid and a Tetraaryladamantane at Room Temperature. *Beilstein J. Org. Chem.* **2021**, *17* (1), 1476–1480. <https://doi.org/10.3762/bjoc.17.103>.
- (47) Fu, S. Q.; Zhu, D. Y.; Guo, J. W.; Xian, J. X. Novel Sulfonate-Containing Halogen-Free Flame-Retardants: Effect of Ternary and Quaternary Sulfonates Centered on Adamantane on the Properties of Polycarbonate Composites. *RSC Adv.* **2017**, *7* (62), 39270–39278. <https://doi.org/10.1039/C7RA06504C>.
- (48) Reichert, V. R.; Mathias, L. J. Expanded Tetrahedral Molecules from 1,3,5,7-Tetraphenyladamantane. *Macromolecules* **1994**, *27* (24), 7015–7023. <https://doi.org/10.1021/ma00102a002>.
- (49) Müller, M. J.; Ziese, F.; Belz, J.; Hüppe, F.; Gowrisankar, S.; Bernhardt, B.; Schwan, S.; Mollenhauer, D.; Schreiner, P. R.; Volz, K.; Sanna, S.; Chatterjee, S. Octave-Spanning Emission across the Visible Spectrum from Single Crystalline 1,3,5,7-Tetrakis-(p-Methoxyphenyl)Adamantane. *Opt. Mater. Express* **2022**, *12* (9), 3517–3529. <https://doi.org/10.1364/OME.461427>.
- (50) Ma, D.; Cai, Q. N,N-Dimethyl Glycine-Promoted Ullmann Coupling Reaction of Phenols and Aryl Halides. *Org. Lett.* **2003**, *5* (21), 3799–3802. <https://doi.org/10.1021/ol0350947>.

## Supplementary Information Table of Contents and Figures

### Section 1: Methods

S1.1: NMR Analysis.....	77
S1.2: Sample Preparation.....	77
Table S1-1: Sample preparation of 3 major chemotypes.....	77
S1.3: General Isolation Procedures.....	78
S1.4: Isolations used in CT3 (previously CT4).....	78
Table S0-2: HPLC method used for initial separation of crude <i>P. scintillans</i> .....	78
Table S1-3: Updated HPLC method used for initial separation of crude <i>P. scintillans</i> .....	79

### Section 2: Section 2: POR Chemotypes – Parent samples

Table S2-1: Parent Samples separated into Chemotypes.....	79
---	----

### Section 3: NMR Spectra and data

#### S3.1: Chapter 2

Figure S3.1-1: <sup>1</sup> H NMR Spectrum (500 MHz) of 1 in CD <sub>3</sub> OD.....	80
Figure S3.1-2: <sup>1</sup> H NMR Spectrum (400 MHz) of 1 in CD <sub>3</sub> OD.....	81
Figure S3.1-3: <sup>13</sup> C NMR Spectrum (101 MHz) of 1 in CD <sub>3</sub> OD.....	81
Figure S 1.1-1: <sup>1</sup> H- <sup>1</sup> H COSY NMR Spectrum (400 MHz) of 1 in CD <sub>3</sub> OD.....	82
Figure S 1.1-2: HSQC NMR Spectrum (400/101 MHz) of 1 in CD <sub>3</sub> OD.....	83
Figure S 1.1-3: HMBC NMR Spectrum (400/101 MHz) of 1 in CD <sub>3</sub> OD.....	83

Figure S3.1-4: $^1\text{H}$ NMR Spectrum (400 MHz) of 1a in $\text{CD}_3\text{OD}$ .....	83
Figure S3.1-5: $^{13}\text{C}$ NMR Spectrum (101 MHz) of 1a in $\text{CD}_3\text{OD}$ .....	84
Figure S3.1-6: $^1\text{H}$ - $^1\text{H}$ COSY NMR Spectrum (400 MHz) of 1a in $\text{CD}_3\text{OD}$ .....	84
Figure S3.1-7: HSQC NMR Spectrum (400/101 MHz) of 1a in $\text{CD}_3\text{OD}$ .....	85
Figure S3.1-8: HMBC NMR Spectrum (400/101 MHz) of 1a in $\text{CD}_3\text{OD}$ .....	85
Figure S3.2-1: $^1\text{H}$ NMR Spectrum (400 MHz) of 9 in $\text{CD}_3\text{CN}$ .....	89
Figure S3.2-2: $^{13}\text{C}$ NMR Spectrum (101 MHz) of 9 in $\text{CD}_3\text{CN}$ .....	89
Figure S3.2-3: $^1\text{H}$ - $^1\text{H}$ COSY NMR Spectrum (400 MHz) of 9 in $\text{CD}_3\text{CN}$ .....	90
Figure S3.2-4: HSQC NMR Spectrum (400/101 MHz) of 9 in $\text{CD}_3\text{CN}$ .....	90
Figure S3.2-5: HMBC NMR Spectrum (400/101 MHz) of 9 in $\text{CD}_3\text{CN}$ .....	91
Figure S3.3-1: $^1\text{H}$ NMR Spectrum (500 MHz) of 18 in $\text{CDCl}_3$ .....	92
Figure S3.3-2: $^{13}\text{C}$ NMR Spectrum (125 MHz) of 18 in $\text{CDCl}_3$ .....	92
Figure S3.3-3: $^1\text{H}$ - $^1\text{H}$ COSY NMR Spectrum (500 MHz) of 18 in $\text{CDCl}_3$ .....	92
Figure S3.3-4: HSQC NMR Spectrum (500/125 MHz) of 18 in $\text{CDCl}_3$ .....	93
Figure S3.3-5: HMBC NMR Spectrum (500/125 MHz) of 18 in $\text{CDCl}_3$ .....	93

## Section 1: Methods

### S1.1: NMR analysis

All spectra were recorded utilizing a Varian 400 spectrometer (399.78 MHz <sup>1</sup>H frequency, 100.56 MHz <sup>13</sup>C frequency) or Varian 500 spectrometer (499.85 MHz <sup>1</sup>H frequency, 125.70 MHz <sup>13</sup>C frequency). For <sup>1</sup>H NMR experiments, standard instrument parameters were used (PROTON), with adjustments to the number of scans (64 nt for crude samples).

Acquisitions were taken in CD<sub>3</sub>OD, based on sample solubility. 600uL of solvent was used in each sample. If the sample mass was under 3 mg, a Shegemi NMR tube (CD<sub>3</sub>OD) was used.

For purified compounds, additional spectra were acquired: <sup>13</sup>C (nt=5000), <sup>1</sup>H{<sup>1</sup>H} gCOSY (nt=8x128), <sup>1</sup>H{<sup>13</sup>C} gHSQC (nt=32x128) and <sup>1</sup>H{<sup>13</sup>C} gHMBC (nt=64x200).

The software MNova (version 14.3, Mestrelab Research, Santiago de Compostela, Spain) was used for further analysis.

### S1.2: Sample Preparation

The parent samples were pooled based on chemotype (SI Table S2-1). The material was ground, extracted three times with methanol, dried under vacuum, and weighed. This extraction was dry loaded onto a C18 plug and washed with 100% water, 95%water/5%MeOH, and 100%MeOH. The 100% methanol partition was kept as the crude extract for further isolation.

Table S1-1: Sample preparation of three major chemotypes

	<b>Chemotype 1</b>	<b>Chemotype 2</b>	<b>Chemotype 3</b>
<b>Dry sample</b>	158.49 g	56.66 g	39.01 g
<b>100% MeOH sample</b>	2.50 g	1.83 g	1.64 g

### S1.3: General Isolation Procedures

Each chemotype was first separated on Agilent Infinity HPLC + MS, using a pilot run to determine the most efficient method of separation. The first separation steps were completed on a 21.2 mm C18 column (21.2 mm x 150 mm) using gradients of methanol + 0.1% formic acid and water with 0.1% formic acid. Methods were adjusted as needed, based on UV-Vis absorbance and MS analysis.

Secondary isolations were chosen based on compound purity (<sup>1</sup>H NMR, LC-MS/MS, GC-MS), compound behavior on silica TLC, and amount of material. Secondary isolations included Agilent Infinity HPLC 10mm C18 column (10 mm x 250 mm, gradients of acetonitrile + 0.1% formic acid and water with 0.1% formic acid) and Prep-TLC (250 micron – 1000 micron silica, solvent systems of hexane/ethyl acetate +0.5% MeOH). Isolations continued until a pure compound was acquired or the amount of material was too small for further purification.

### S1.4: Isolations used in CT3 (previously CT4)

The dry leaf material was extracted with methanol in three overnight extractions. The resulting crude material was then extracted with hexanes and chloroform, resulting in three fractions: hexane (fraction 3), chloroform (fraction 2) and methanol (fraction 1).

Fraction 2 was run on Yamazan Flash HPLC in normal phase using the following method:

Table S1-2: HPLC method used for initial separation of crude *P. scintillans*

Time (mins)	%Hexane	%ethyl acetate
0	95	5
2	95	5
12	0	100
16	0	100
20	0	100
24	0	100

There was an issue with a leak in solvent the line that resulted in bad separation. Fractions recombined, then extracted with hexane, ethyl acetate, acetone, and methanol. The hexane and ethyl acetate fractions were combined (renamed POR-CT3-CT(4)-Frac2-Hex/EtOAc-Yz-P#).

The acetone and methanol fractions were combined as well.

POR-CT3-CT(4)-Frac2-Hex/EtOAc-Yz (220.3mg) was run in normal phase on Yamazan Flash

HPLC using the following method:

Table S1-3: Updated HPLC method used for initial separation of crude *P. scintillans*

Time (mins)	%Hexane	%ethyl acetate
0	100	0
2	100	0
6	77	13
8	0	100
20	0	100

## Section 2: POR Chemotypes – Parent samples

Table S2-1: Parent Samples separated into Chemotypes

CT1	CT2	CT3	sCT3	sCT5
POR.006	POR.016	POR.009	POR.035	POR.055
POR.007	POR.028	POR.013	POR.063	POR.097
POR.032	POR.029	POR.070		
POR.040	POR.055	POR.071		
POR.042	POR.081	POR.072		
POR.044	POR.082	POR.073		
POR.045	POR.084	POR.077		
POR.048	POR.095	POR.099		
POR.051	POR.097	POR.008		
POR.054	POR.086	POR.012		
POR.059	POR.004	POR.014		
POR.060	POR.017	POR.022		
POR.064	POR.018	POR.065		
POR.085	POR.021	POR.066		
POR.092	POR.026	POR.069		
POR.001	POR.035	POR.075		
POR.005	POR.047	POR.076		

---

POR.010	POR.049	POR.083
POR.027	POR.052	POR.090
POR.030	POR.053	POR.091
POR.033	POR.063	POR.093
POR.036	POR.067	POR.096
POR.037	POR.068	
POR.038	POR.079	
POR.039	POR.080	
POR.041	POR.089	
POR.043	POR.100	
POR.046		
POR.057		
POR.058		
POR.061		
POR.062		

---

### Section 3: NMR Spectra and data

#### S3.1: Chapter 2

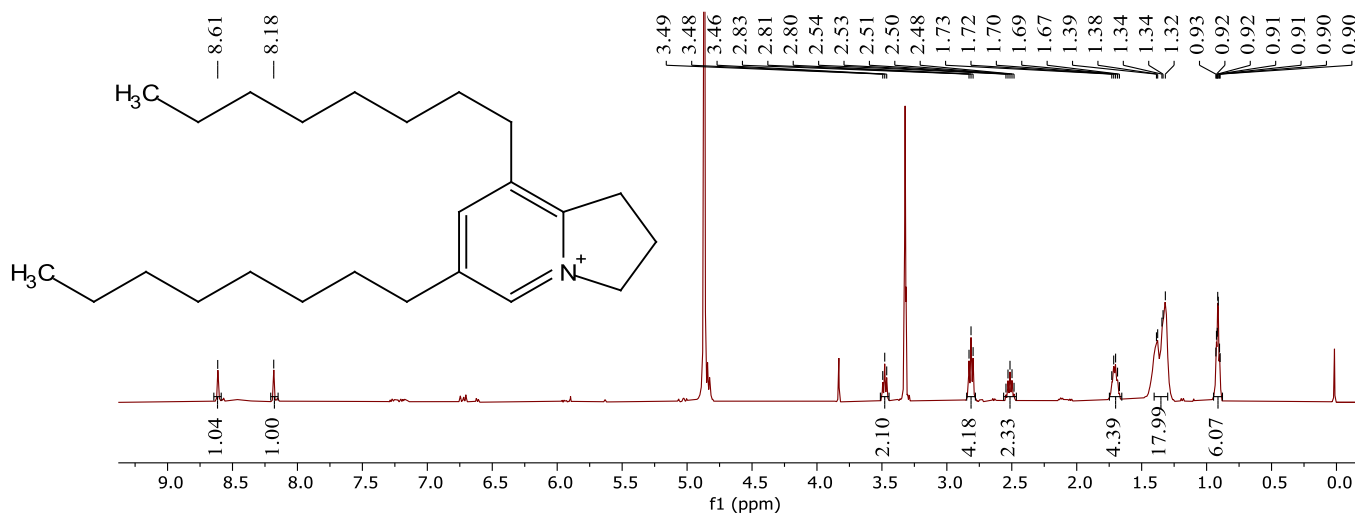
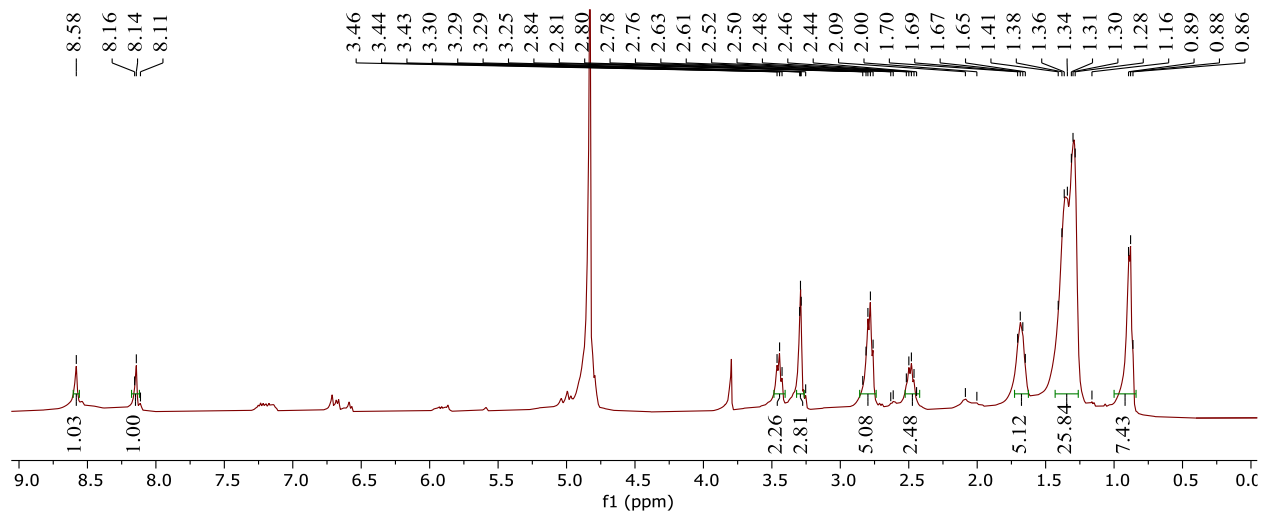
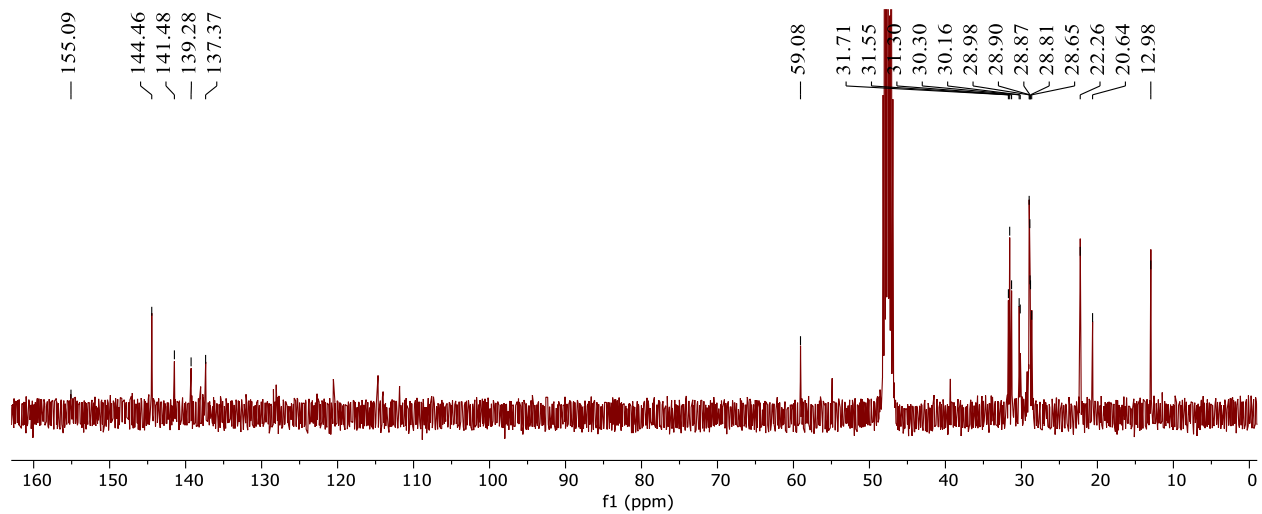


Figure S3.1-1: <sup>1</sup>H NMR Spectrum (500 MHz) of 1 in CD<sub>3</sub>OD

Figure S3.1-2: <sup>1</sup>H NMR Spectrum (400 MHz) of 1 in CD<sub>3</sub>ODFigure S3.1-3: <sup>13</sup>C NMR Spectrum (101 MHz) of 1 in CD<sub>3</sub>OD

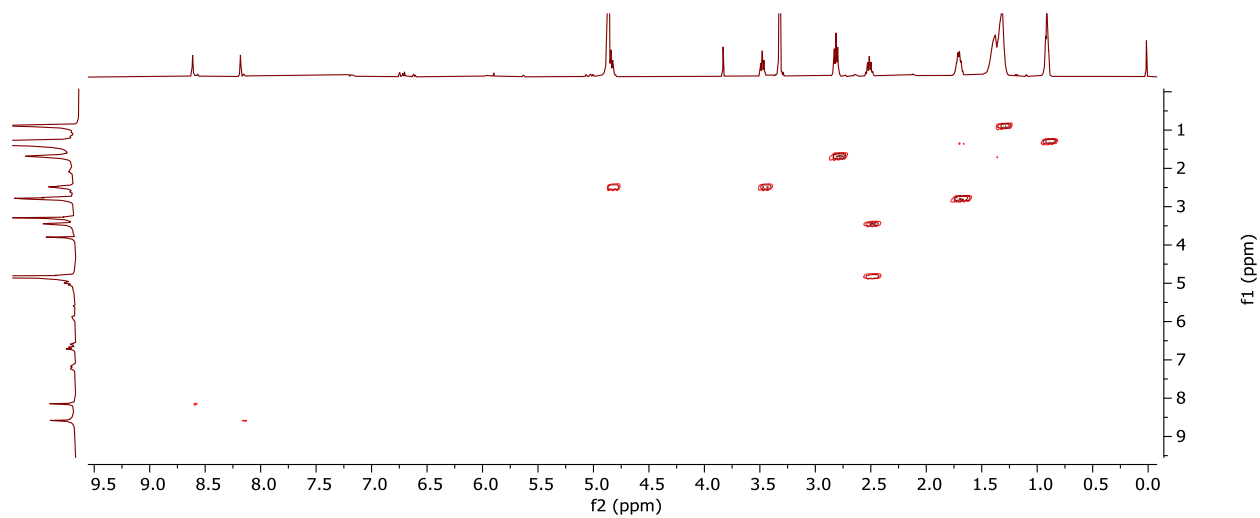


Figure S 3.1-1:  $^1\text{H}$ - $^1\text{H}$  COSY NMR Spectrum (400 MHz) of 1 in  $\text{CD}_3\text{OD}$

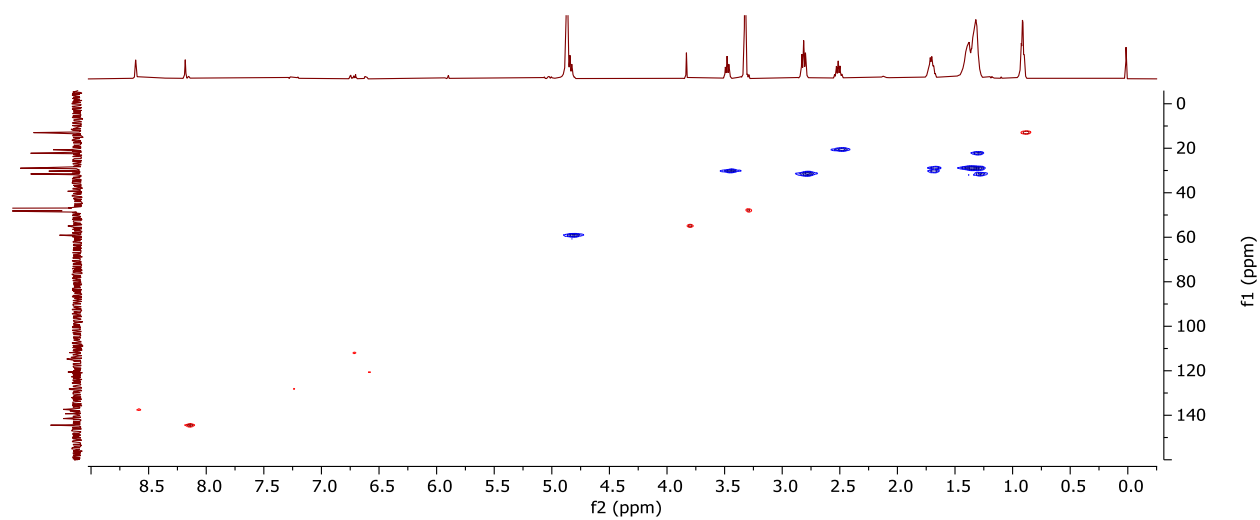
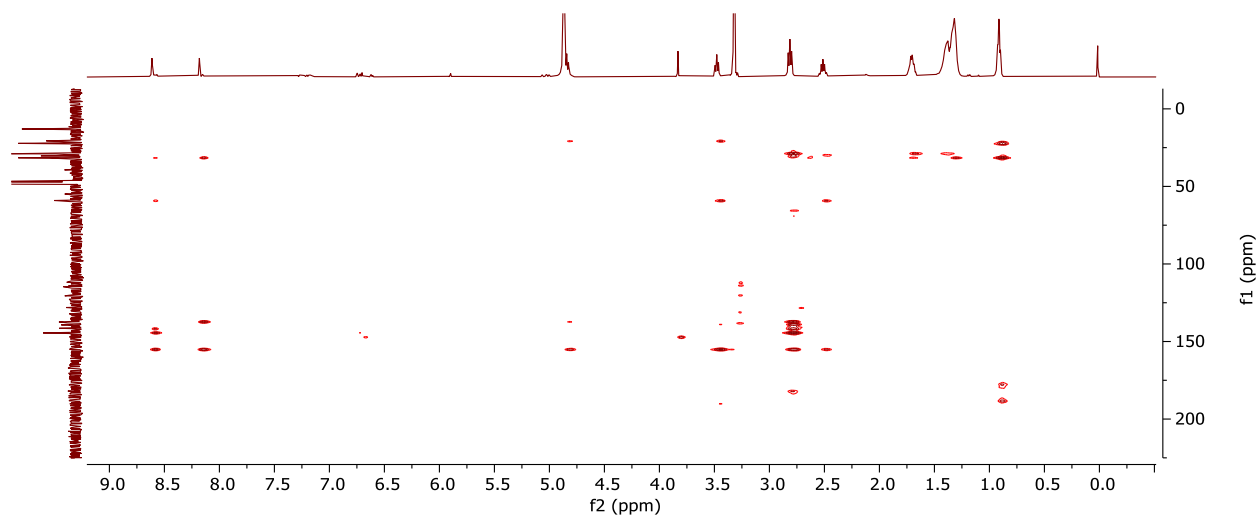
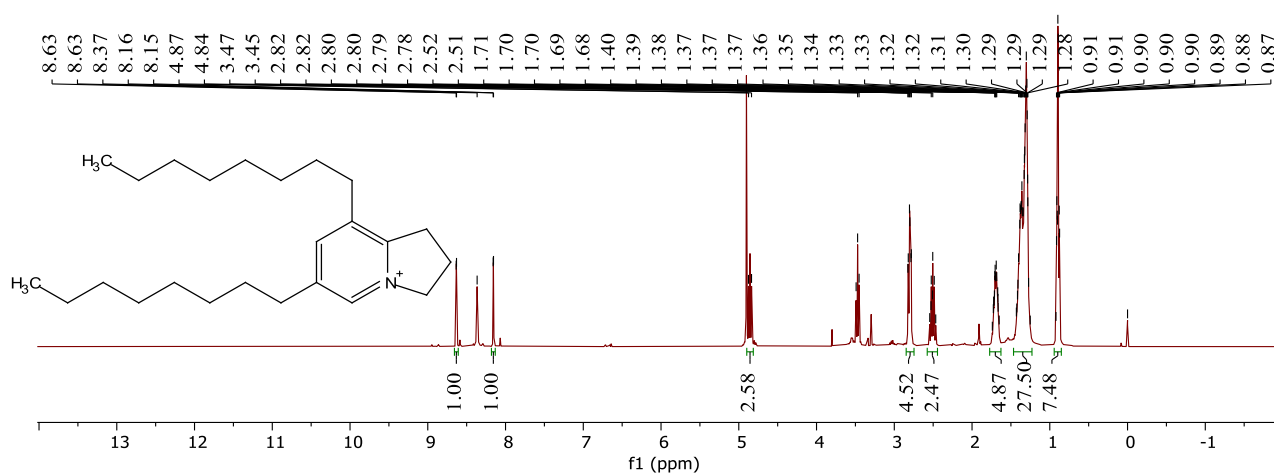


Figure S 3.1-2: HSQC NMR Spectrum (400/101 MHz) of 1 in  $\text{CD}_3\text{OD}$

Figure S 3.1-3: HMBC NMR Spectrum (400/101 MHz) of 1 in CD<sub>3</sub>ODFigure S3.1-4: <sup>1</sup>H NMR Spectrum (400 MHz) of 1a in CD<sub>3</sub>OD

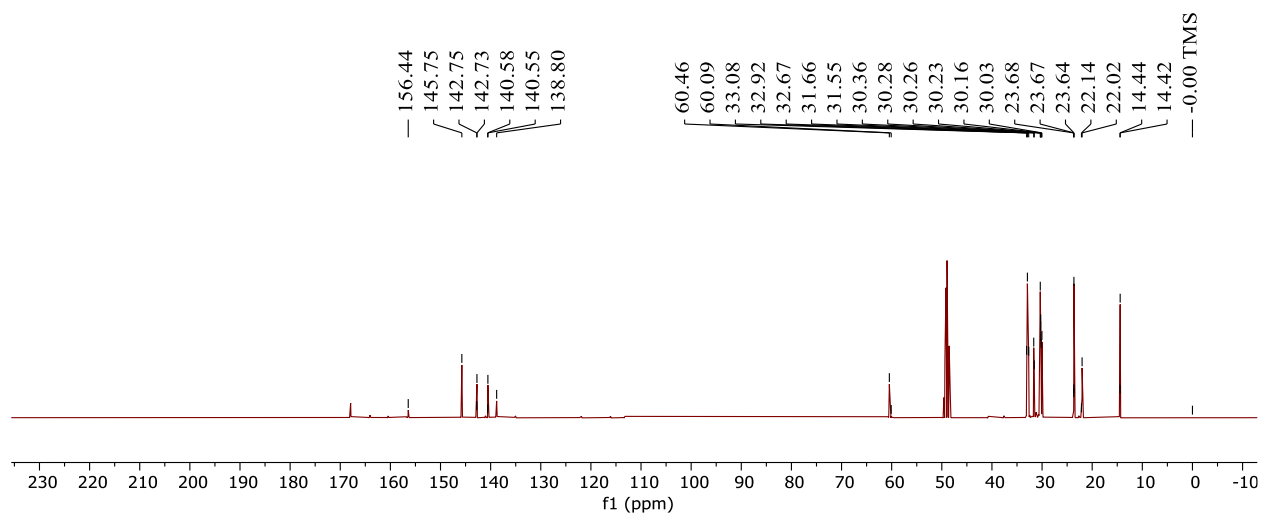


Figure S3.1-5:  $^{13}\text{C}$  NMR Spectrum (101 MHz) of 1a in  $\text{CD}_3\text{OD}$

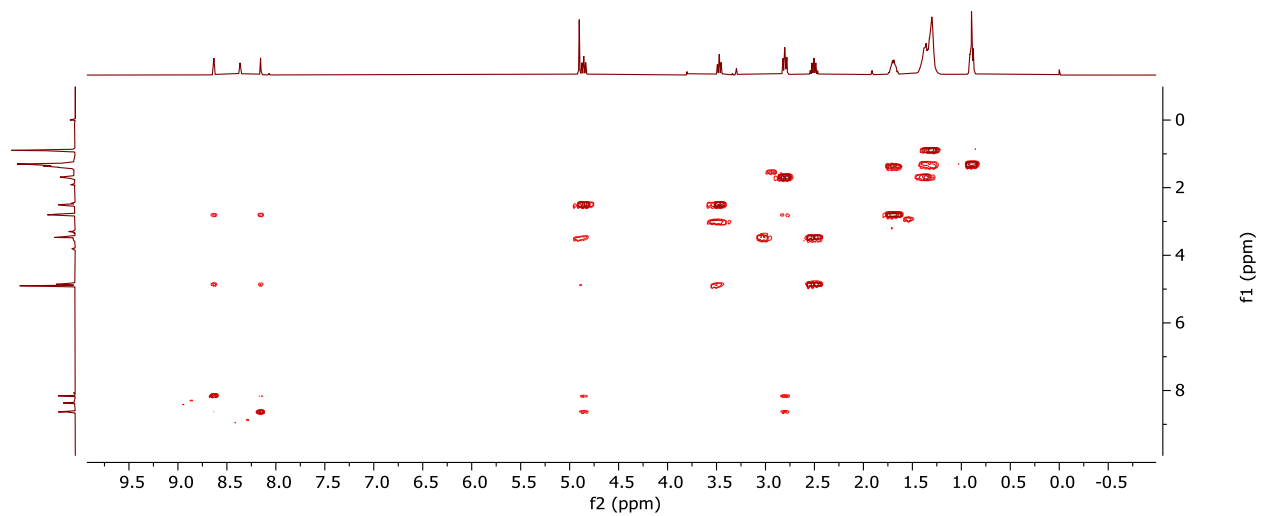


Figure S3.1-6:  $^1\text{H}$ - $^1\text{H}$  COSY NMR Spectrum (400 MHz) of 1a in  $\text{CD}_3\text{OD}$

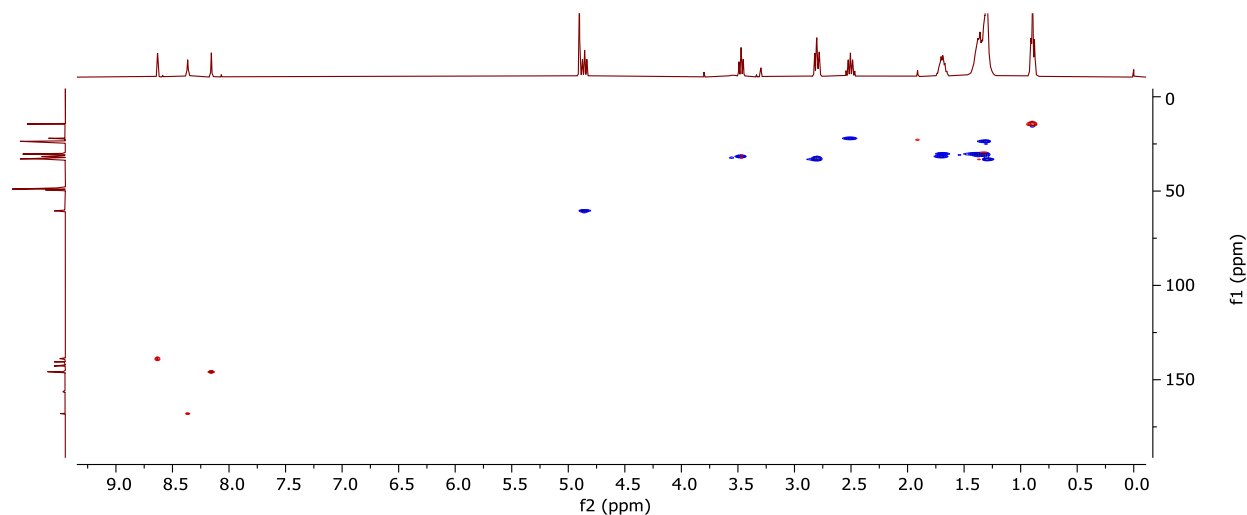


Figure S3.1-7: HSQC NMR Spectrum (400/101 MHz) of 1a in CD<sub>3</sub>OD

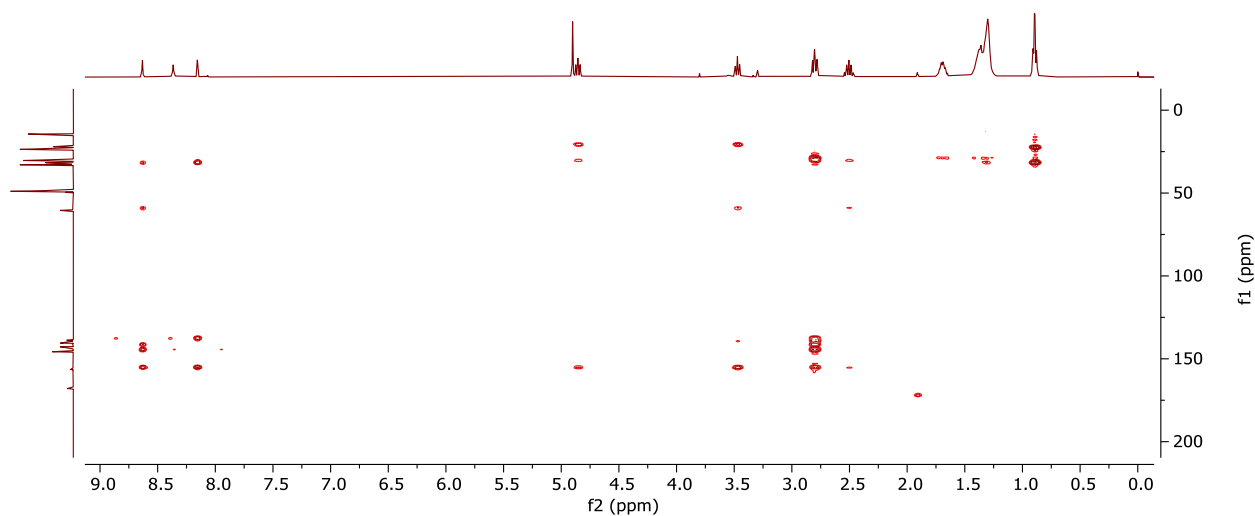


Figure S3.1-8: HMBC NMR Spectrum (400/101 MHz) of 1a in CD<sub>3</sub>OD

### S3.2: Chapter 3

**2',4'-Dihydroxy-6'-methoxychalcone (7):** <sup>1</sup>H NMR (400 MHz, cd<sub>3</sub>od) δ 7.92 (d, J = 15.6 Hz, 1H), 7.69 (d, J = 15.6 Hz, 1H), 7.65 – 7.61 (m, 2H), 7.45 – 7.37 (m, 3H), 6.01 (d, J = 2.2 Hz, 1H), 5.94 (d, J = 2.3 Hz, 1H), 3.93 (s, 3H). <sup>13</sup>C NMR (101 MHz, cd<sub>3</sub>od) δ 192.46, 167.32, 165.43, 163.34, 141.44, 135.51, 129.71, 128.59, 127.85, 127.49, 105.17, 95.66, 91.07, 54.97.

**5-Methoxy-7-hydroxyflavanone (8):**  $^1\text{H}$  NMR (400 MHz, acetone)  $\delta$  7.59 – 7.50 (m, 2H), 7.47 – 7.30 (m, 3H), 6.13 (dd,  $J = 24.2, 2.2$  Hz, 2H), 5.47 (dd,  $J = 12.7, 3.0$  Hz, 1H), 3.80 (s, 3H), 2.94 (dd,  $J = 16.3, 12.7$  Hz, 1H), 2.65 (dd,  $J = 16.3, 3.0$  Hz, 1H).  $^{13}\text{C}$  NMR (101 MHz, acetone)  $\delta$  187.61, 165.53, 163.73, 129.29 (d,  $J = 26.3$  Hz), 127.18, 96.68, 94.21, 79.75, 56.07, 46.47.

**5-Methoxy-7,8-dihydroxyflavanone (9):**  $^1\text{H}$  NMR (400 MHz,  $\text{cd}_3\text{cn}$ )  $\delta$  7.57 – 7.50 (m, 2H), 7.48 – 7.33 (m, 3H), 6.20 (s, 1H), 5.50 (dd,  $J = 12.5, 3.0$  Hz, 1H), 3.75 (s, 3H), 3.07 – 2.91 (m, 1H), 2.69 (dd,  $J = 16.5, 3.0$  Hz, 1H).  $^{13}\text{C}$  NMR (101 MHz,  $\text{cd}_3\text{cn}$ )  $\delta$  188.25, 154.98, 151.46, 151.04, 139.28, 128.51 (d,  $J = 7.7$  Hz), 126.48, 125.87, 105.15, 93.16, 79.47, 55.48, 45.44.

**8-Hydroxy-5,7-dimethoxyflavanone (10):**  $^1\text{H}$  NMR (400 MHz,  $\text{cd}_3\text{od}$ )  $\delta$  7.56 – 7.50 (m, 2H), 7.44 – 7.32 (m, 3H), 6.35 (s, 1H), 5.51 (dd,  $J = 11.7, 3.3$  Hz, 1H), 3.95 (s, 3H), 3.85 (s, 3H), 3.06 (dd,  $J = 16.7, 11.7$  Hz, 1H), 2.82 (dd,  $J = 16.7, 3.3$  Hz, 1H).  $^{13}\text{C}$  NMR (101 MHz,  $\text{cd}_3\text{od}$ )  $\delta$  192.42, 156.43, 155.97, 140.49, 129.63 (d,  $J = 12.8$  Hz), 127.54, 90.90, 80.54, 56.77, 56.45.

**5,7-Dimethoxyflavanone (11):**  $^1\text{H}$  NMR (500 MHz,  $\text{cdcl}_3$ )  $\delta$  7.53 – 7.34 (m, 7H), 6.18 (dd,  $J = 2.3, 0.7$  Hz, 1H), 6.11 (d,  $J = 2.2$  Hz, 1H), 5.43 (dd,  $J = 13.1, 2.9$  Hz, 1H), 3.91 (d,  $J = 0.8$  Hz, 4H), 3.84 (d,  $J = 1.0$  Hz, 3H), 3.04 (ddd,  $J = 16.4, 13.2, 0.8$  Hz, 1H), 2.82 (ddd,  $J = 16.4, 2.9, 0.7$  Hz, 1H).  $^{13}\text{C}$  NMR (101 MHz,  $\text{cdcl}_3$ )  $\delta$  189.25, 165.99, 165.00, 162.30, 138.76, 128.81, 126.13, 106.01, 93.55 (d), 93.20 (d), 79.25 (d), 56.19 (d), 55.62 (d), 45.61.

**5-Hydroxy-7-methoxyflavone (12):**  $^1\text{H}$  NMR (400 MHz,  $\text{cdCl}_3$ )  $\delta$  12.73 (s, 1H), 7.92 – 7.87 (m, 2H), 7.58 – 7.49 (m, 3H), 6.68 (s, 1H), 6.51 (d,  $J = 2.3$  Hz, 1H), 6.39 (d,  $J = 2.3$  Hz, 1H), 3.89 (s, 3H).  $^{13}\text{C}$  NMR (101 MHz,  $\text{cdCl}_3$ )  $\delta$  182.52, 165.64, 162.24, 157.83, 131.84, 131.37, 129.10, 126.32, 105.93, 98.21, 92.72, 55.83.

**7,8,11,11a-Tetrahydro-3,6,10-trimethylcyclodeca[b]furan-2(4H)-one (13):**  $^1\text{H}$  NMR (400 MHz,  $\text{cd}_3\text{od}$ )  $\delta$  5.23 – 5.08 (m, 1H), 4.89 (dt,  $J = 11.8, 3.3, 1.6$  Hz, 1H), 4.38 (dddd,  $J = 11.0, 2.4, 1.6, 0.9$  Hz, 1H), 3.44 (dq,  $J = 15.0, 2.0$  Hz, 1H), 3.14 – 2.98 (m, 2H), 2.33 – 2.19 (m, 3H), 2.18 – 1.99 (m, 2H), 1.96 – 1.86 (m, 1H), 1.85 – 1.82 (m, 3H), 1.82 – 1.75 (m, 2H), 1.65 (t,  $J = 1.7$  Hz, 3H), 1.54 (q,  $J = 1.1$  Hz, 3H).  $^{13}\text{C}$  NMR (101 MHz,  $\text{cd}_3\text{od}$ )  $\delta$  174.68, 164.45 (d), 148.64, 132.63, 132.27, 130.49, 130.14, 125.02, 123.62, 123.47, 83.65 (d), 83.04, 37.99, 27.00 – 26.34 (m), 25.12 (d).

**(1R,4S,5R,8S)-4-hydroxyguaia-7(11),10(15)-dien-12,8-olide (14):**  $^1\text{H}$  NMR (400 MHz,  $\text{cdCl}_3$ )  $\delta$  5.05 – 5.00 (m, 2H), 4.84 – 4.75 (m, 1H), 3.07 (dd,  $J = 12.9, 3.6$  Hz, 1H), 2.89 (ddt,  $J = 18.8, 3.1, 1.5$  Hz, 1H), 2.49 – 2.34 (m, 1H), 2.09 – 1.95 (m, 3H), 1.82 (q,  $J = 1.7$  Hz, 4H), 1.80 (s, 0H), 1.28 (s, 3H).  $^{13}\text{C}$  NMR (101 MHz,  $\text{cdCl}_3$ )  $\delta$  173.90, 163.24, 146.03, 123.70, 111.31, 82.00 (d), 80.70, 52.61, 50.39, 44.15, 41.07, 28.02, 25.51, 23.72, 8.59.

**5-Hydroxy-7-methoxyflavanone (15):**  $^1\text{H}$  NMR (400 MHz, acetone)  $\delta$  7.61 – 7.50 (m, 2H), 7.43 (tt,  $J = 6.5, 1.0$  Hz, 2H), 7.39 – 7.31 (m, 1H), 6.15 (d,  $J = 2.2$  Hz, 1H), 6.10 (d,  $J = 2.2$  Hz, 1H), 5.47 (dd,  $J = 12.7, 3.0$  Hz, 1H), 3.80 (s, 4H), 2.94 (dd,  $J = 16.3, 12.6$  Hz, 1H), 2.65 (dd,  $J = 16.3, 3.0$  Hz, 1H).  $^{13}\text{C}$  NMR (101 MHz, acetone)  $\delta$  187.73, 165.53, 164.94, 163.73, 140.63,

129.42, 129.17, 127.17, 106.13, 96.62 (d,  $J = 7.7$  Hz), 94.13 (d,  $J = 7.9$  Hz), 79.75 (d,  $J = 2.9$  Hz), 56.08 (d,  $J = 6.3$  Hz), 48.25 – 44.38 (m).

**2'-hydroxy-4',6'-dimethoxy chalcone (16):**  $^1\text{H}$  NMR (400 MHz,  $\text{cdCl}_3$ )  $\delta$  14.29 (s, 1H), 7.90 (d,  $J = 15.6$  Hz, 1H), 7.78 (d,  $J = 15.6$  Hz, 1H), 7.65 – 7.56 (m, 3H), 7.41 – 7.39 (m, 3H), 6.11 (d,  $J = 2.4$  Hz, 1H), 5.97 (d,  $J = 2.4$  Hz, 1H), 3.92 (s, 4H), 3.84 (s, 4H).  $^{13}\text{C}$  NMR (101 MHz,  $\text{cdCl}_3$ )  $\delta$  192.78, 168.54 (d), 166.38, 162.64, 142.46, 135.70, 130.19, 129.01, 128.49, 127.66, 106.47 (d), 93.90, 91.41 (d), 56.04 (d), 55.75 (t).

**5,3',4'-trihydroxy-7-methoxy-flavanone (17):**  $^1\text{H}$  NMR (500 MHz, acetone)  $\delta$  12.15 (s, 1H), 7.06 (dq,  $J = 1.8, 0.6$  Hz, 4H), 6.93 – 6.85 (m, 7H), 6.09 – 6.02 (m, 6H), 5.47 – 5.40 (m, 3H), 3.87 (d,  $J = 0.5$  Hz, 11H), 3.18 (ddd,  $J = 17.2, 12.6, 1.0$  Hz, 4H), 2.76 (dd,  $J = 3.1, 0.8$  Hz, 2H).  $^{13}\text{C}$  NMR (126 MHz, acetone)  $\delta$  196.66, 130.61, 118.38, 115.11, 113.81, 93.69, 79.18, 55.35, 42.74.

**5,7,8-Trimethoxyflavanone (19):**  $^1\text{H}$  NMR (400 MHz,  $\text{cd}_3\text{cn}$ )  $\delta$  7.55 – 7.50 (m, 2H), 7.49 – 7.36 (m, 3H), 6.30 (s, 1H), 5.50 (dd,  $J = 12.6, 3.0$  Hz, 1H), 3.92 (s, 3H), 3.86 (s, 3H), 3.69 (t,  $J = 0.5$  Hz, 3H), 3.00 (dd,  $J = 16.5, 12.6$  Hz, 1H), 2.72 (dd,  $J = 16.5, 3.0$  Hz, 1H).  $^{13}\text{C}$  NMR (101 MHz,  $\text{cd}_3\text{cn}$ )  $\delta$  188.42, 161.07, 158.91, 128.53, 126.32, 90.09, 78.99, 60.13, 55.78 (d), 45.08.

**2'-hydroxy-3',4',6'-trimethoxychalcone (20):**  $^1\text{H}$  NMR (400 MHz,  $\text{cd}_3\text{cn}$ )  $\delta$  13.65 (d,  $J = 6.9$  Hz, 1H), 7.94 (d,  $J = 15.6$  Hz, 1H), 7.76 (d,  $J = 15.7$  Hz, 1H), 7.72 – 7.68 (m, 2H), 7.50 – 7.41 (m, 3H), 6.22 (s, 1H), 3.98 (s, 3H), 3.94 (s, 3H), 3.90 (d,  $J = 10.3$  Hz, 2H), 3.71 (d,  $J = 0.9$  Hz,

3H), 3.67 (d,  $J = 0.4$  Hz, 1H).  $^{13}\text{C}$  NMR (101 MHz,  $\text{cd}_3\text{cn}$ )  $\delta$  194.34, 160.05, 159.69, 143.03, 136.26, 131.30, 129.95, 129.38, 128.61, 56.78.

**Dehydrodieugenol monomethyl ether (21):**  $^1\text{H}$  NMR (400 MHz,  $\text{cdcl}_3$ )  $\delta$  6.78 – 6.74 (m, 2H), 6.74 – 6.71 (m, 2H), 6.44 (d,  $J = 1.5$  Hz, 1H), 6.13 – 5.83 (m, 2H), 5.17 – 5.03 (m, 4H), 3.91 (s, 2H), 3.90 (s, 3H), 3.65 (d,  $J = 0.5$  Hz, 3H), 3.38 (dddt,  $J = 9.5, 6.0, 2.2, 0.9$  Hz, 5H).  $^{13}\text{C}$  NMR (101 MHz,  $\text{cdcl}_3$ )  $\delta$  152.71, 148.16, 144.29, 141.59, 137.87, 137.35, 136.57, 132.18, 131.67, 125.63, 123.55, 123.09, 116.24, 115.80, 112.13, 111.12, 61.37 (d), 56.12 (dd), 40.27, 40.08.

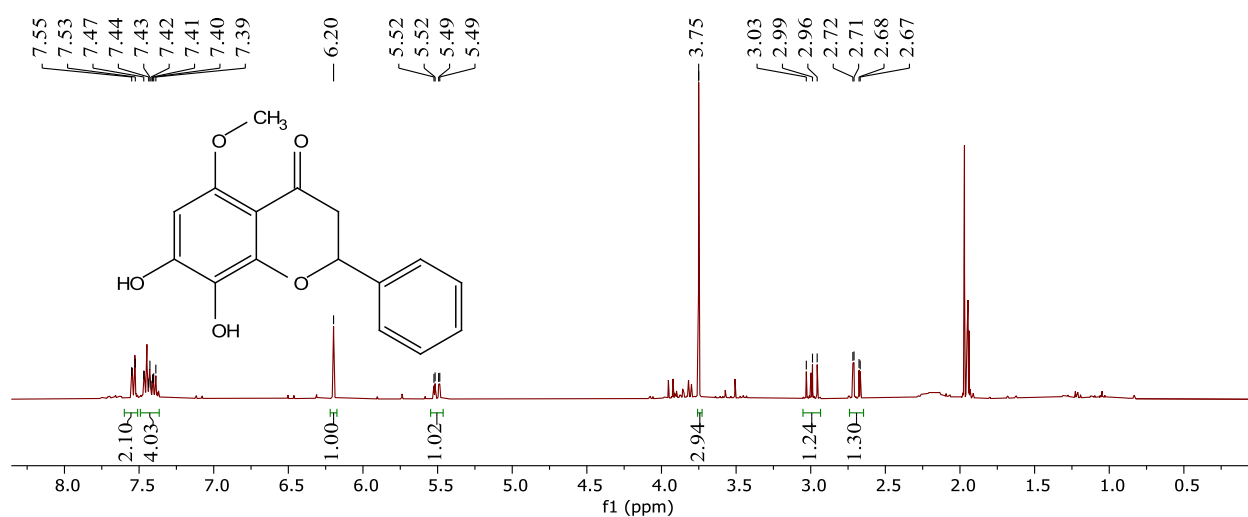


Figure S3.2-1:  $^1\text{H}$  NMR Spectrum (400 MHz) of 9 in  $\text{CD}_3\text{CN}$

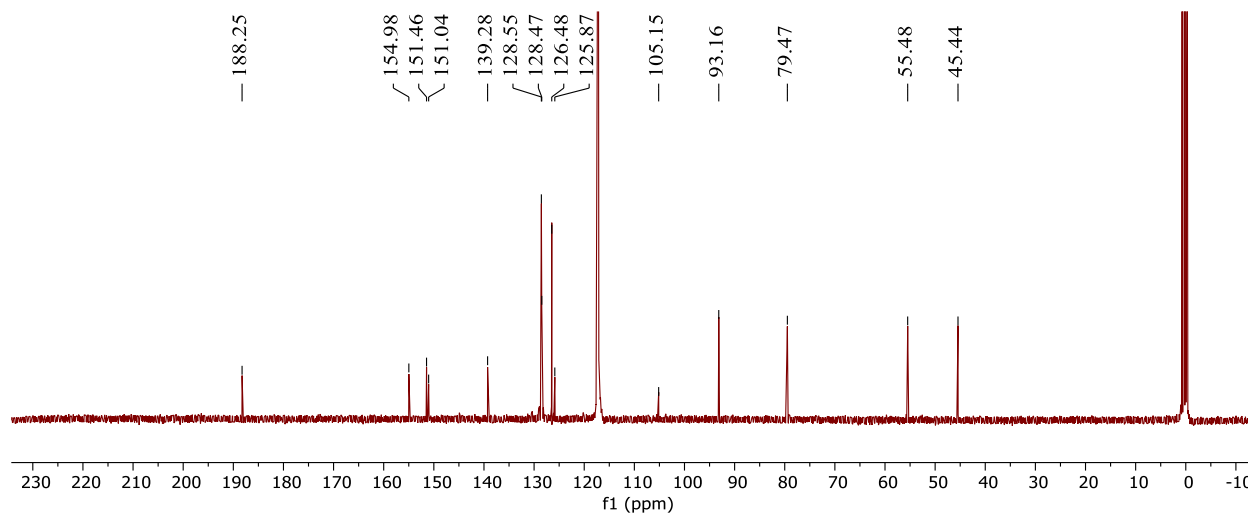


Figure S3.2-2:  $^{13}\text{C}$  NMR Spectrum (101 MHz) of 9 in  $\text{CD}_3\text{CN}$

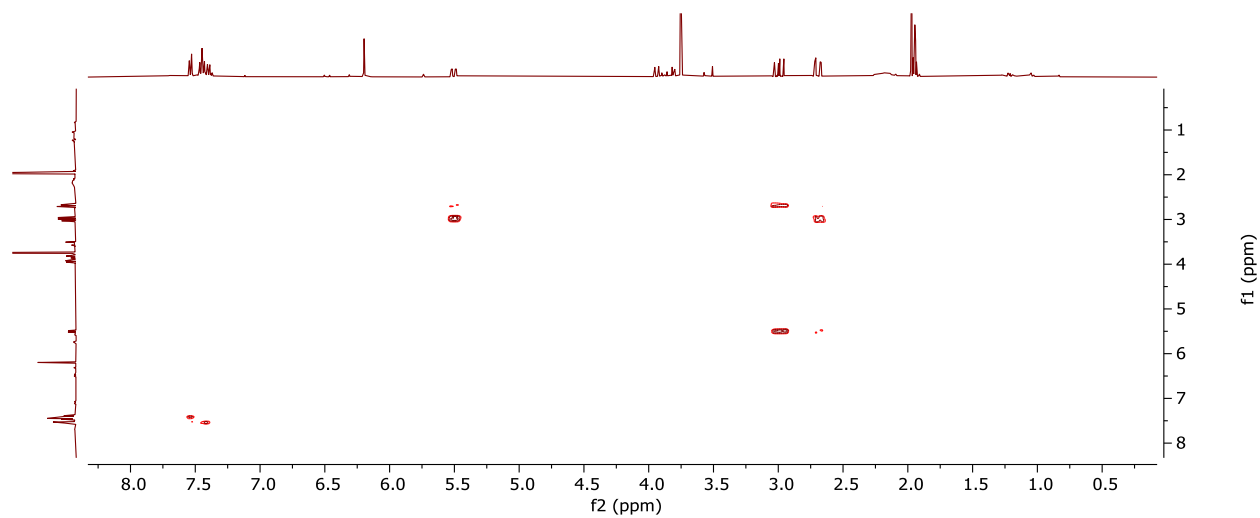


Figure S3.2-3:  $^1\text{H}$ - $^1\text{H}$  COSY NMR Spectrum (400 MHz) of 9 in  $\text{CD}_3\text{CN}$

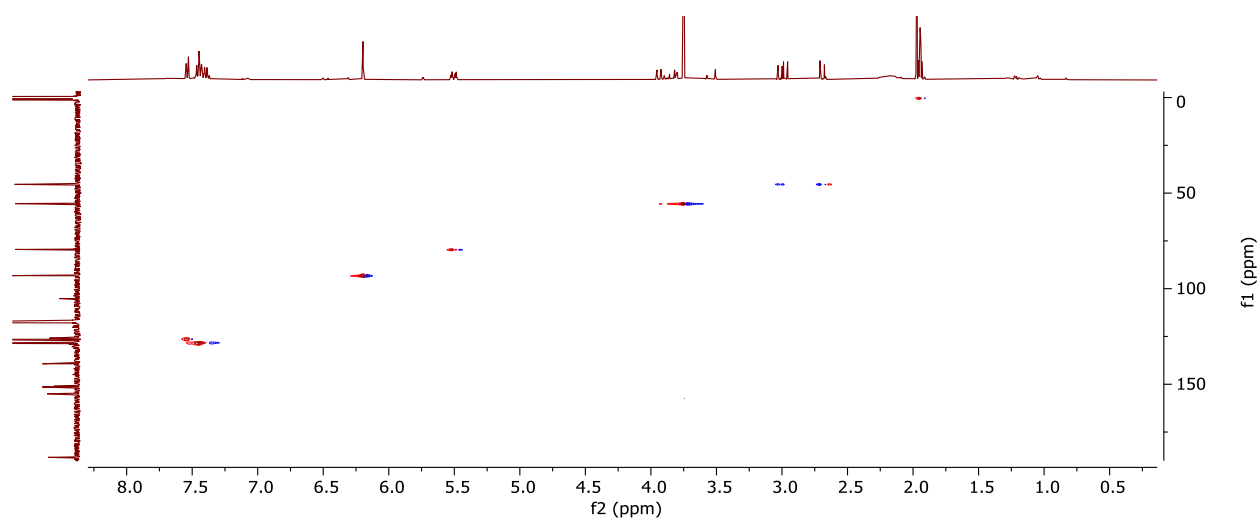


Figure S3.2-4: HSQC NMR Spectrum (400/101 MHz) of 9 in  $\text{CD}_3\text{CN}$

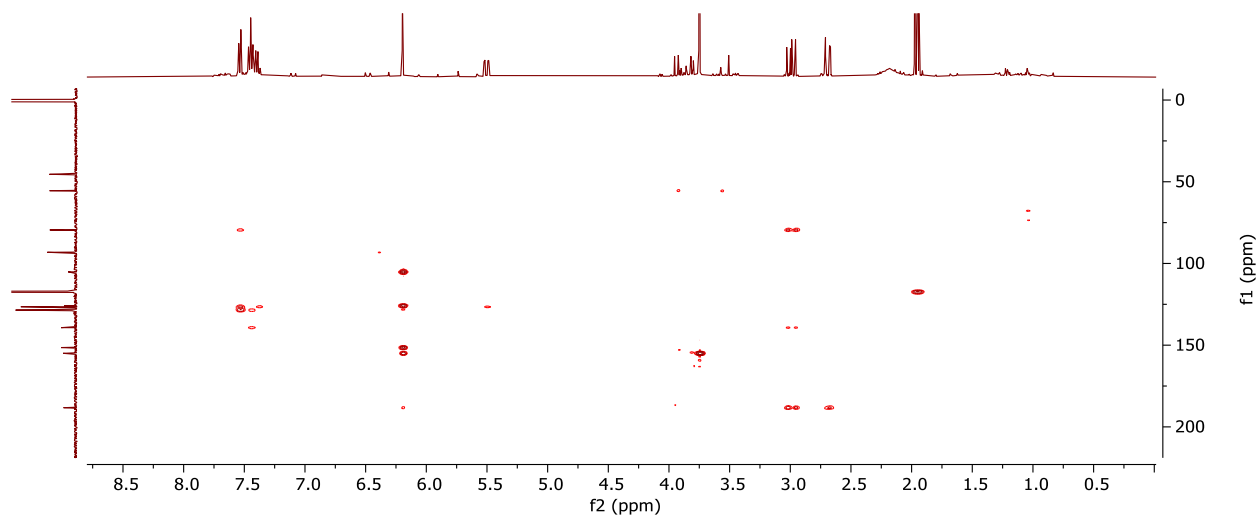


Figure S3.2-5: HMBC NMR Spectrum (400/101 MHz) of 9 in CD<sub>3</sub>CN

### S3.3: Chapter 4

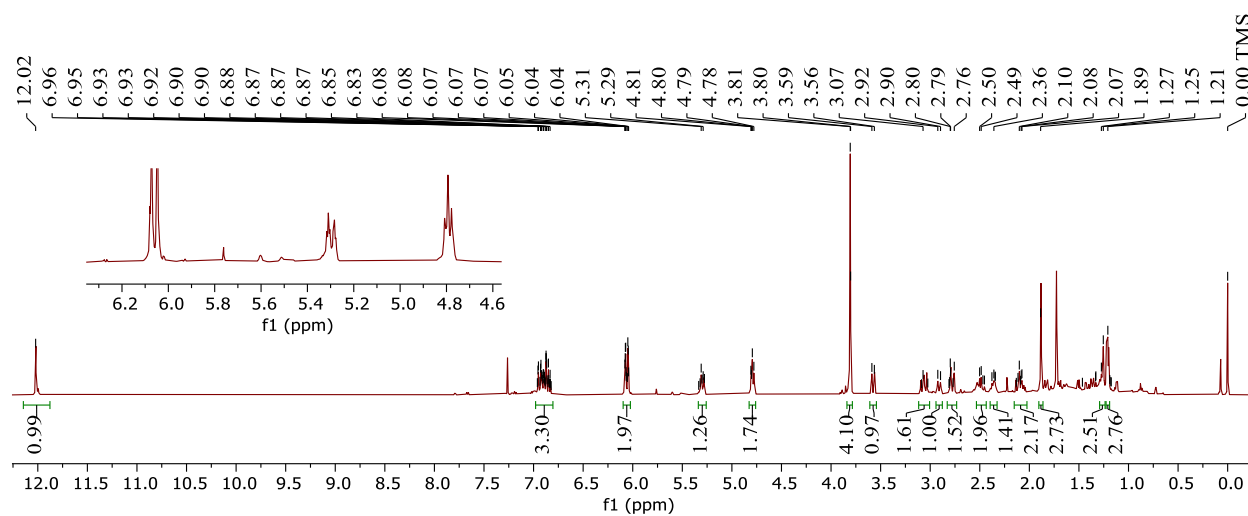
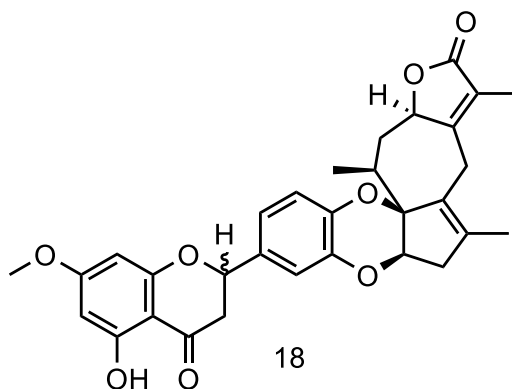
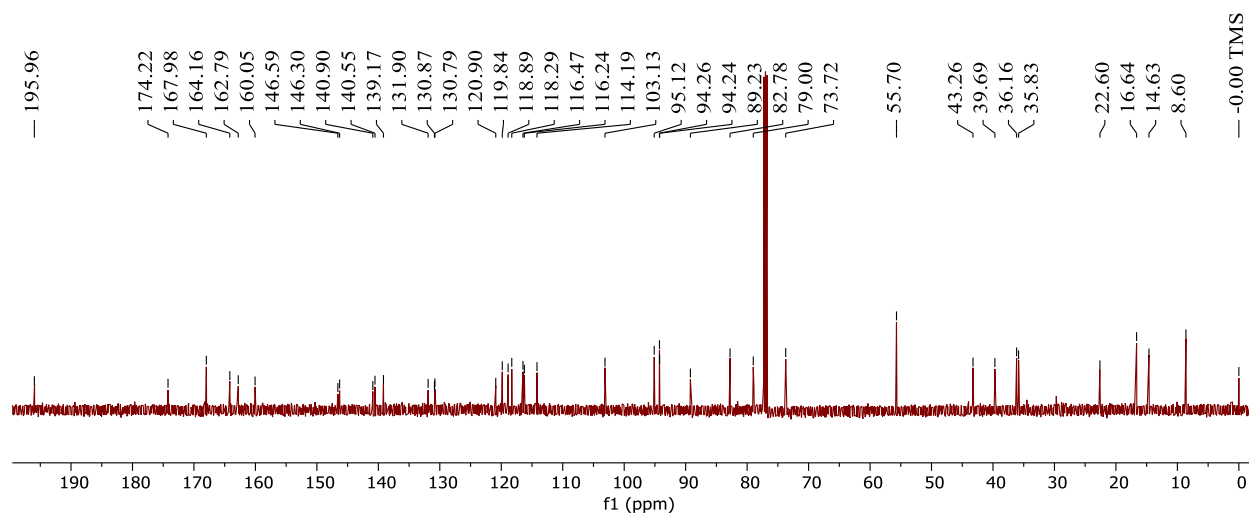
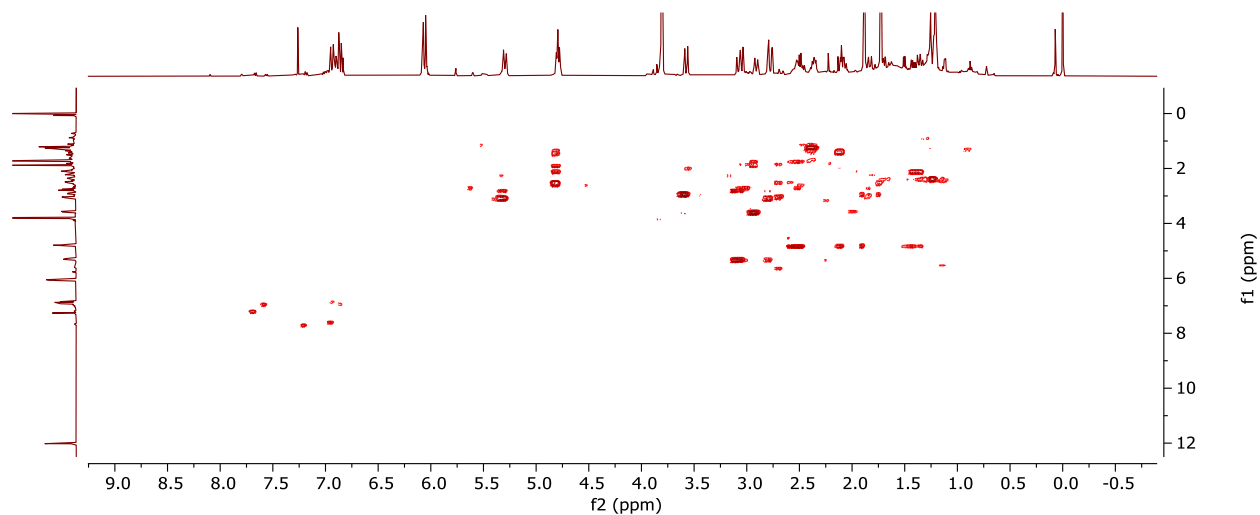


Figure S3.3-1:  $^1\text{H}$  NMR Spectrum (500 MHz) of 18 in  $\text{CDCl}_3$ Figure S3.3-2:  $^{13}\text{C}$  NMR Spectrum (125 MHz) of 18 in  $\text{CDCl}_3$ Figure S3.3-3:  $^1\text{H}$ - $^1\text{H}$  COSY NMR Spectrum (500 MHz) of 18 in  $\text{CDCl}_3$

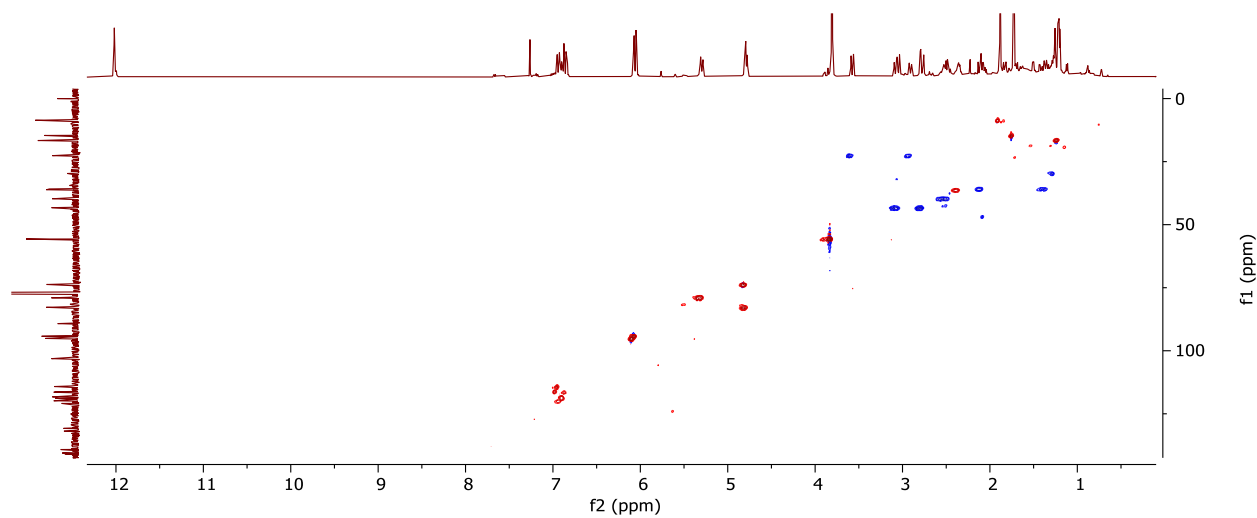


Figure S3.3-4: HSQC NMR Spectrum (500/125 MHz) of 18 in  $\text{CDCl}_3$

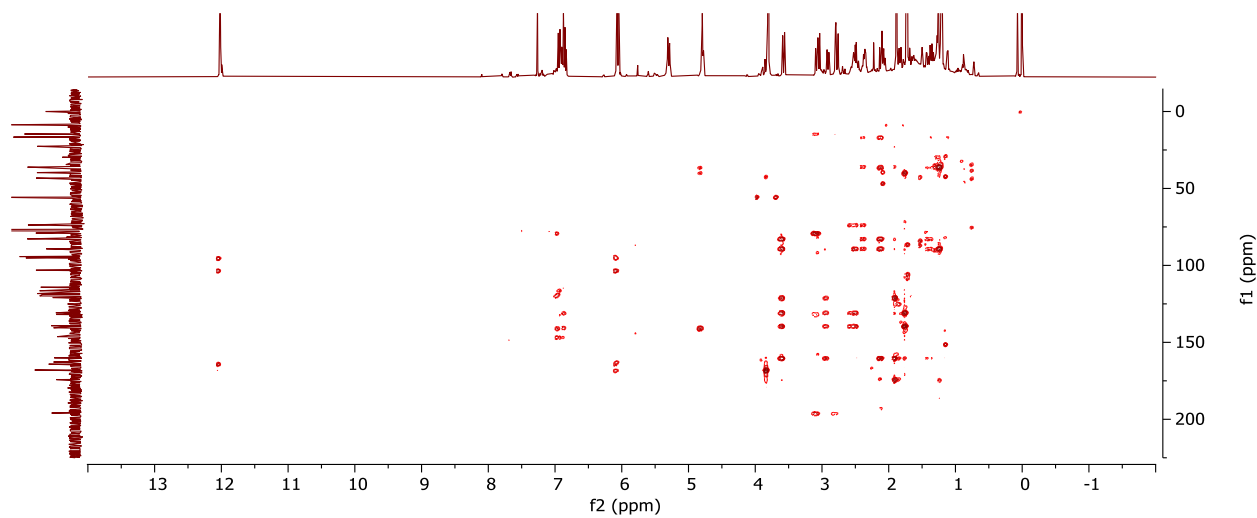


Figure S3.3-5: HMBC NMR Spectrum (500/125 MHz) of 18 in  $\text{CDCl}_3$